Alessandro Casaburo
Pasta-Lab,
Department of Industrial Engineering,
Università degli Studi di Napoli Federico II,
Via Claudio 21,
Napoli 80125, Italy
e-mail: alessandro.casaburo@unina.it

Giuseppe Petrone
Assistant Professor
Pasta-Lab,
Department of Industrial Engineering,
Università degli Studi di Napoli Federico II,
Via Claudio 21,
Napoli 80125, Italy
e-mail: giuseppe.petrone@unina.it

Francesco Franco
Professor
Pasta-Lab,
Department of Industrial Engineering,
Università degli Studi di Napoli Federico II,
Via Claudio 21,
Napoli 80125, Italy
e-mail: francesco.franco@unina.it

Sergio De Rosa
Professor
Pasta-Lab,
Department of Industrial Engineering,
Università degli Studi di Napoli Federico II,
Via Claudio 21,
Napoli 80125, Italy
e-mail: sergio.derosa@unina.it

A Review of Similitude Methods for Structural Engineering

Similitude theory allows engineers, through a set of tools known as similitude methods, to establish the necessary conditions to design a scaled (up or down) model of a full-scale prototype structure. In recent years, to overcome the obstacles associated with full-scale testing, such as cost and setup, research on similitude methods has grown and their application has expanded into many branches of engineering. The aim of this paper is to provide as comprehensive a review as possible about similitude methods applied to structural engineering and their limitations due to size effects, rate sensitivity phenomena, etc. After a brief historical introduction and a more in-depth analysis of the main methods, the paper focuses on similitude applications classified, first, by test article, then by engineering fields. [DOI: 10.1115/1.4043787]

1 Introduction

A fundamental step in the design of a product is experimental testing. While theoretical and numerical approaches are valuable tools, their predictions must be validated by extensive sets of experimental tests before going to production. This way, whether applied to the validation of a simple or complex system, one achieves the desired reliability, performance, and safety. An example given in Ref. [1] may help illustrate the necessary experimental effort: the final static tests of the Lockheed C-141A airlifter required 8 wing tests, 17 fuselage tests, and 7 empennage tests.

Crashworthiness evaluation requires both full-scale and drop tests. Moreover, it may be necessary to repeat some tests due to errors or to focus on unexpected phenomena. Full-scale experimental testing is expensive, in terms of both cost and time and, sometimes, hard to implement; in some cases, the usefulness of acquired data cannot justify the required effort. For these reasons, it is useful to be able to design a model of the original system, viz., a consistently scaled down replica of the full-scale prototype that can be tested at significantly lower cost and with less difficulty. Even if the model is a perfectly scaled-up or down variation of the prototype, it is however another structure, with its own static and dynamic responses that do not coincide with those of the original prototype. As a consequence, the recovery (or reconstruction) of the prototype response is not guaranteed.

Manuscript received April 6, 2018; final manuscript received April 9, 2019; published online June 3, 2019. Editor: Harry Dankowicz.

Holmes and Sliter [2] provide an example of money and time saving when scaled models are used. For a single crash test, the authors estimate savings of between 1/3 and 1/4 the cost of the equivalent full-scale building and testing. The test times are reduced by 1/3 and more if also model fabrication is considered. An entire experimental program, with a mixture of subscale and full-scale models, would thus lead to greater economy in both financial and temporal terms.

Similitude theory provides the conditions to design a scaled (up or down) model of a full-scale prototype and to predict the prototype's structural response from the scaled results. The tools used are known as similitude methods.

In many modern applications, the increasing complexity of engineering systems makes theoretical and numerical analyses insufficient (and entirely unsuitable for very complex structures) for evaluating whether a system's performance meets design requirements. The extensive need for experimental tests, due to the disadvantages of full-scale testing, has resulted in a rapid growth in applications of similitude methods. In fact, such methods are used in a variety of engineering branches (aerospace, naval, civil, and automotive) and applications (free and forced vibrations, impact behavior, seismic response, etc.).

The aim of this paper is to provide a comprehensive review of similitude methods applied to structural engineering. A few related reviews have been already published: the first dates back to the early 2000s [3] and focuses, after an historical review, on the analysis of composite test articles by means of similitude theory applied to the governing equations of plates and shells. Besides being the first review on the topic, the importance of this work lies in the explanation of key terminology related to similitude theory that lacks precise definition, specifically *scaling* (or *scale effects*) and *size effects*. Generally, scale effects describe changes in the response to external causes due to changes in the geometric dimensions of a structure (or a structural component); size effects concern changes of strength and stiffness of the material as a consequence of the physical scaling process. According to Wissmann [4], when a size effect occurs, a physical phenomenon gains importance in a model due to the differences in size of the replica and the prototype. Notwithstanding these definitions, in many articles, the terminology scale effects are used also to refer to effects of size. To avoid any ambiguity, from now on, the terminology size effects will be used exclusively to describe the effects of physical scaling.

A comprehensive review is also provided by Ref. [5]. This combines historical, methodological, and application insights to trace the evolution of similitude theory. Recently, Zhu et al. [6] reviewed vibration problems of plates and shells using similitude theory based on the governing equations and sensitivity analysis. Rosen [7] surveyed the literature in the late 1980s and highlighted commonalities and relationships among all the scientific fields using similitudes. Other more limited reviews are present in the literature, including one on scaling models in marine structures by Vassalos [8] and on scaling techniques applied to the structural response of liquid metal fast breeder reactor vessels to hypothetical core disruptive accident in Cagliostro [9], and the work by Saito and Kuwana [10] on dimensional analysis applied to vibroacoustics.

The idea behind this paper is to give to the reader a new and up-to-date perspective by organizing the discussion around applications categorized in terms of test articles. In this way, all the contributions to a topic scattered across time and fields of study are organized in a new presentation.

Keeping this layout in mind, the paper is organized as follows. First, a short historical review is provided in which some information is given about the first publications and main manuals and books on the topic. Then, similitude theory is defined and a description of the most used methods is given, focusing on their relative advantages and disadvantages. Section 4 is the core of the paper. It is divided into several subsections, each one focused on the application of similitude methods to a particular test article (beams, plates, and cylinders). Section 5 is dedicated to the use of the theory in the study of complex structures across several engineering fields. In Sec. 6, the main points of the paper are summarized, with some final remarks of the authors about ways of employing similitude methods.

At the end of the paper, after the references, an appendix has been added. It contains three reference tables, introduced to give a useful synopsis to interested readers.

2 Short Historical Review

In this section, a brief historical review of similitude methods is provided, following the publication, in chronological order, of the first articles and books that introduced the main similitude methods, still in use today. A brief insight into the development of such methods according to test articles follows. Finally, some papers are discussed which do not fit clearly in this paper but are worthy of mention because of their historical and thematic relevance.

The first reference to similitude theory dates back to the 18th century, as reported in Ref. [6]. In fact, Galilei and Weston [11] stated that size and strength of an object do not decrease in the same ratio: if dimensions decrease, the strength increases. The curious aspect of this statement is that Galileo, in the 18th century, was already facing the problem of size effects. However, the first work in which scientific models based on dimensional analysis are discussed is due to Rayleigh [12]. Although Rayleigh's article aimed to underline the importance of similitude methods, especially in engineering, as discussed in Ref. [13], thirty years had to pass before the publication of another work in which the usefulness of similitude methods is highlighted: the NACA technical report by Goodier and Thomson [14] and the book by Goodier [15]. In these publications, dimensional analysis was applied for the first time with a systematic procedure to simple and complex problems. This resulted in a deep insight on the modeling of materials with nonlinear stress–strain characteristics or plastic behavior, buckling, and/or large deflections.

In the following years, many books were written on the topic. In their review, Simitses et al. [3] cite many works, e.g., Refs. [16–20], in which similitudes and modeling principles are based on dimensional analysis. Kline [21] gives a perspective on deriving similitude conditions with both dimensional analysis and direct use of governing equations. The latter method is accurately treated also in Ref. [22], while a whole chapter of Ref. [23] is dedicated to the former. In Ref. [5], good alternatives to Refs. [21] and [23] are given, such as Refs. [24] and [25]; furthermore, the authors underline that dimensional analysis has driven and justified the writing of several other manuals, such as Refs. [26–28], even though other methods were introduced and successfully applied. A wider modeling interpretation is given in Ref. [29], while Zohuri [30] provides first a perspective on classic dimensional analysis and, then, deepens the topic in Ref. [31], going beyond Buckingham's Π theorem and approaching self-similar solutions.

An overview of similitude methods is reported in Fig. 1. The methods on the vertical axis are dimensional analysis (DA), similitude theory applied to governing equations (STAGE), energy method based on the conservation of energy (EM), asymptotical scaled modal analysis (ASMA), similitude and asymptotic models for structural-acoustic research applications (SAMSARA), empirical similarity method (ESM), and sensitivity analysis (SA). More details on each of these are presented in Sec. 3. The horizontal bars represent the range of years in which each method has been used.

The development and application of similitude methods has not followed a linear path in terms of test articles. Contrary to expectations, the first methods were not applied to simple test articles first and more complicated ones later. For example, in the first relevant application of similitude theory to engineering [14], the authors first provide an extensive theoretical study on general structures (isotropic, composite, linear, and nonlinear). They then proceed to employ dimensional analysis to buckled thin square plates in shear, with and without holes. Many years had to pass to find the first instance in which dimensional analysis was applied to a stiffened panel [32]. Differential equations were used in Ref. [33] to investigate sandwich panels. The first application of similitude theory to a beam is reported in Morton [34] in which the author employs dimensional analysis. Some years later, the first analysis of unstiffened cylinder models is conducted by Hamada and Ramakrishna [35]; oddly, stiffened cylinders were already studied in a previous work by Sato [36] by means of

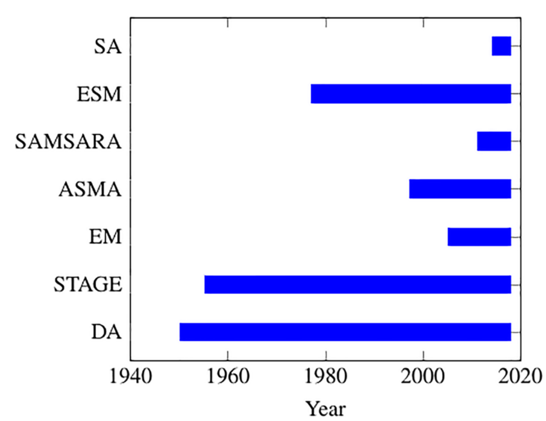

Fig. 1 Time overview of similitude methods

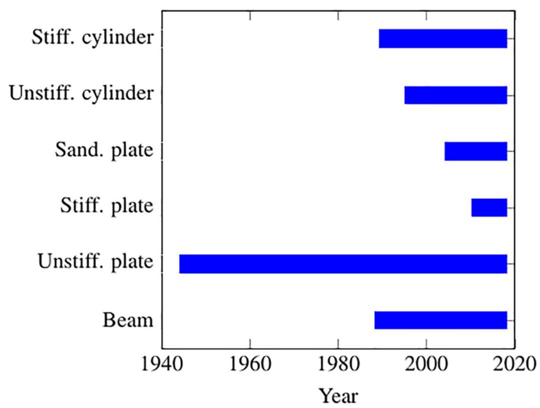

Fig. 2 Time overview of test articles

dimensional analysis. An overview of progress in applying similitude methods to different test articles is shown in Fig. 2. The bars again illustrate the time range in which publications concerned with the corresponding test articles have been published.

A mention to two works with a great historical relevance is needed; both of them are dedicated to similitudes applied to shells.

The first is an analysis executed by Ezra [37]. This is motivated by a peculiar behavior of shells; under certain conditions, they can sustain pressures considerably larger than that which would produce static buckling. On the other hand, when applying a pressure rapidly with a long duration, the structure carries less than it would statically. The author uses dimensional analysis to investigate scale model determination of the buckling of a thin shell structure, with arbitrary shape and subject to an impulsive pressure load with duration not short enough to be considered as a pure impulse, nor long enough to be considered as static pressure. He shows that when the materials of prototype and model are similar, consistent predictions require that the magnitude of the applied pressure must be the same while the duration must be scaled proportionally. If magnitude and duration cannot be controlled, then a complete similitude can be achieved by a suitable choice of a different material for the model.

A second relevant work on the topic is that of Soedel [38]. In this paper, the author derives similitude conditions for free and forced vibrations of shells from Love's equations. Shells are characterized by both in-plane and transverse oscillations; as a consequence, when deriving the exact similitude conditions from the governing equations, the thickness is not independent from the surface geometry. By decoupling the membrane and the bending effects, the author derives two sets of approximate conditions in which the thickness is introduced as a parameter independent of the surface geometry. The choice of the set is dictated by the relative dominance of membrane and bending effects.

Finally, it is worth mentioning that some works by Sterrett consider the topic of similitude and, more generally, model in a wider manner; the epistemological setting of these articles may help to explain the concepts underlying similitude theory.

The application of fundamental laws to scale modeling is the main question in Ref. [39]; the author states that scale modeling must not mediate between an abstract/theoretical world and a phenomenological one, but rather to give insights into phenomena, so that it is possible to tell what happens in a situation that is not directly observable by means of another situation that can be observed.

A direct insight into dimensional analysis and Buckingham's Π theorem applied to both geometrical and physical similitudes is given in Ref. [40]. The usefulness of models is underlined in Ref. [41] in which the author shows how new areas of application and investigative research have been found. The topic is further developed in other articles [42–44].

3 Similitude Methods

Before proceeding to the core of this review, we present a brief introduction to similitude methods. After providing some useful definitions, we quickly describe the main characteristics of each method.

Fundamentally, similitude theory is a branch of engineering sciences which allows to determine the conditions of similitude between two or more systems. The full-scale system is known as *prototype*, while the scaled (up or down) one is the *model*. When a model satisfies the similitude conditions, it is expected to have the same response as the prototype (in a qualitative meaning). This is the reason why such tools are very useful. It is possible to overcome all the problems associated with full-scale testing by designing and investigating a scaled (usually down) model.

Some authors refer to *similitude*, others to *similarity*, thus a remark is necessary about the terminology. In fact, both terms are used interchangeably in the literature although with a slight difference: similarity is closer to the usage in fields of mathematics (for example, self-similarity solutions). An example of such an application is reported by Polsinelli and Levent Kavvas [45] in which Lie scaling methodology is introduced. Such a method performs symmetry analysis of the governing differential equations basing on Lie groups, special structures leading to invariant transformations. An extensive treatise on the topic is given in Ref. [46]. In this paper, we only use the word similitude.

In order to give a brief introduction to similitude methods, it is important to explain two concepts previously introduced, viz., similitude and similitude conditions.

Similitudes can be distinguished according to the parameters taken into account; it is possible to have

(1) *Geometric similitude*, when geometric characteristics are equally scaled.
(2) *Kinematic similitude*, when homologous particles lie at homologous points at homologous times [24]. By recalling the ratio between space and time, it follows that kinematic similitude is achieved, simply, when homologous particles have homologous velocities.
(3) *Dynamic similitude*, when homologous parts of a system are subject to homologous net forces.

A formal definition of kinematic similitude, that also introduces the concept of scale factor, is given by Langhaar [17]:

> The function f' is similar to function f, provided the ratio f'/f is a constant, when the functions are evaluated for homologous points and homologous times. The constant $\lambda = f'/f$ is called the scale factor for the function f.

Baker et al. [24] explain the use of the term homologous in this definition as *corresponding but not necessarily equal values*.

Those listed above are the main types of similitude, but others can be defined. As an example, Baker et al. [24] add constitutive similitude to the list, achieved when there is similitude between the materials stress–strain curves of the prototype and the model, or between the constitutive properties of such materials. However, in general, only geometric, kinematic, and dynamic similitudes are considered, so that it is possible to say that two systems are similar if they share the aforementioned characteristics.

Szucs [22] gives a useful definition of similitude conditions:

> The sufficient and necessary condition of similitude between two systems is that the mathematical model of the one be related by a biunique transformation to that of the other.

So, if X_p and X_m are two vectors of N parameters, respectively, of the prototype and the model, then they are related one to each other in this way

$$X_p = [\Lambda] X_m \quad \text{or} \quad X_m = [\Lambda]^{-1} X_p \tag{1}$$

Table 1 Overview of similitude methods

	Advantages	Disadvantages
DA	Simple Useful when governing equations are not known	Experienced analyzer is needed, with a deep knowledge of the problem Great effort in deriving the conditions Trial-and-error approach, due to the non-uniqueness of nondimensional groups Nondimensional groups may have little physical meaning
STAGE	Similitude conditions are more specific Conditions have physical meaning Scale factors can be applied to both governing equations and solutions	Governing equations must be known Effort in deriving the conditions It cannot be implemented in an algorithm
EM	The procedure is more straightforward than involving the field equations Same level of generality and results of STAGE	Effort in deriving the conditions Problems occur when prototype and model are made of different materials
ASMA	Reduced computational time due to reduced spatial domain Applicable to finite element analysis It can be implemented in an algorithm	It works well only for global response; local information is lost
SAMSARA	Structural response completely achieved for replicas It can be implemented in an algorithm	Structural response partially achieved for avatars
ESM	Transformation matrix is derived empirically	Additional manufacturing and testing
SA	Reduced effort in deriving similitude conditions It can be implemented in an algorithm Similitude-based scaling laws do not need prior knowledge of the structural scaling behavior	It is not based on physical equations Computationally expensive

Note: Table 3 in the Appendix gives the corresponding references related to this table.

where $[\Lambda]$ is the following matrix:

$$[\Lambda] = \begin{bmatrix} \lambda_{x_1} & 0 & \cdots & 0 \\ 0 & \lambda_{x_2} & \cdots & 0 \\ \vdots & \vdots & \ddots & \vdots \\ 0 & 0 & \cdots & \lambda_{x_N} \end{bmatrix} \tag{2}$$

which performs a transformation between the mathematical models for the prototype and scaled model. A diagonal matrix provides the simplest form of transformation.

The diagonal elements of matrix $[\Lambda]$ are known as scale factors of the parameter x_i ($i = 1, 2, \ldots, N$); herein they will be defined as $\lambda_{x_i} = x_{i_m}/x_{i_p}$ (where the subscript m is for model, while p for the prototype), although the other authors use the inverse formulation.

According to the fulfillment of similitude conditions, different models can be defined (and another classification of similitudes can be done):

(1) *True model*: All the conditions are fulfilled. This is referred to as complete similitude.
(2) *Adequate model*: First-order conditions, i.e., the conditions related to the main parameters are fulfilled. This is referred to as first-order similitude.
(3) *Distorted model*: At least one of the first order conditions is not satisfied. This is referred to as partial similitude.

The difference between true and adequate models is of relevance especially when using dimensional analysis. Here, special insight into a problem can be used to reason that some of the conditions are of "second-order" importance.

An interesting example is provided by Harris and Sabnis [26]: in rigid frame problems, axial and shearing forces are of second-order importance relative to bending moments as far as deformations are concerned. Thus, it may be adequate to model the moment of inertia but not the cross-sectional areas of members.

So, it is clear that the difference between true and adequate models relies on the choice of parameters that are accounted for when deriving the similitude conditions. For other methods, such as STAGE or SAMSARA (introduced below), that work according to other principles, such difference is absent and the concepts of true and adequate models can be joined.

When dealing with a scaled model, the main characteristics taken into account are the scaling effects, i.e., the change in response of the structure due to the geometric scaling procedure. In some applications, e.g., impact response, size effects must also be taken into account; they appear as a change in material properties, such as strength and stiffness, due to the scaling procedure. Simitses et al. [3] cite a workshop on the topic (Jackson [47]) in which, while all the presenters agree on the fact that size effect on stiffness is almost nonexistent, they disagree about its influence on strength.

Several similitude methods can be found in the literature. To give an exhaustive explanation of such tools is beyond the aim of this paper; however, it may be helpful to focus briefly on the working principles, advantages, and disadvantages of the main ones. The main aspects, advantages, and disadvantages of each method considered below are summarized in Table 1.

3.1 Dimensional Analysis. Dimensional analysis or, as Coutinho et al. [48] refer to, traditional similarity method, is based on the definition of a set of dimensionless parameters that govern the phenomenon of interest. It relies on the concept of dimensional homogeneity, i.e., an equation which describes a physical phenomenon must have sides with same dimensions. All these concepts are gathered in Buckingham's Π theorem [49]. According to this theorem, let K be the number of fundamental dimensions, required to describe the physical variables, and let $P_1, P_2, \ldots, P_N$ be N physical variables. Suppose that it is possible to relate such variables through the functional relation

$$f_1(P_1, P_2, \ldots, P_N) = 0 \tag{3}$$

Equation (3) may be rewritten in terms of $(N - K)$ dimensionless products, called Π products, as

$$f_2(\Pi_1, \Pi_2, \ldots, \Pi_{N-K}) = 0 \tag{4}$$

Each Π product is a dimensionless product of $K+1$ physical variables so that, without loss of generality

$$\begin{cases} \Pi_1 = f_3(P_1, P_2, \ldots, P_K, P_{K+1}) \\ \Pi_2 = f_4(P_1, P_2, \ldots, P_K, P_{K+2}) \\ \ldots \\ \Pi_{N-K} = f_5(P_1, P_2, \ldots, P_K, P_N) \end{cases} \tag{5}$$

In mechanics, usually $K=3$ and the fundamental dimensions are mass, length, and time: this is called the mass, length, and time (MLT) base. The choice of repeating variables $P_1, P_2, \ldots, P_K$ should be such that they include all K fundamental dimensions, while each dependent variable of interest should appear in just one Π product.

Scale-modeling with dimensional analysis requires that all the dimensionless Π products are scaled in such a way that they are equal for both model and prototype, which means

$$\Pi_j^{(m)} = \Pi_j^{(p)} \tag{6}$$

for $j = 1, 2, \ldots, (N-K)$.

When the condition (6) is fulfilled for each value of j, then complete similitude is achieved; if at least one condition is not satisfied, then the model is distorted. Generally, to simplify the calculations, only first-order conditions are considered, so that the difference between a true and an adequate model is neglected also when using dimensional analysis.

In some applications, dimensional analysis does not directly involve Buckingham's Π theorem. The scaling laws are determined by defining just one scale factor, then expressing the prototype/model ratio of parameters as a power law of such a scale factor. This step requires dimensional consistency, so that the method can be regarded as another version of dimensional analysis.

On the one hand, the described method is simple to use and useful for those systems without a set of governing equations, such as complex or new systems. On the other hand, it is clear that a phenomenologically meaningful choice of the parameters is needed: taking into account a parameter with low or no influence on the phenomenon would complicate the derivation of Π terms unnecessarily, while ignoring an important parameter would lead to an incomplete, and maybe wrong, conclusion. Hence, to use such a method, an experienced analyzer and a deep knowledge of the problem are needed.

Furthermore, Π terms may be not unique, which lead to a trial-and-error approach and to a significative calculation effort. Besides, not all Π terms have physical meaning and, in general, the equations characteristic of the phenomena under observation can be formulated only in an incomplete form. In conclusion, the procedure is not structured, so it cannot be easily implemented into an algorithm.

3.2 Similitude Theory Applied to Governing Equations.

After dimensional analysis, the second and most commonly used method to derive the similitude conditions is similitude theory applied to governing equations (or STAGE, as abbreviated by Coutinho et al. [5]): Kline [21] was the first to introduce this method.

Similitude theory applied to governing equations is applied directly to the field equations of the system, including boundary and initial conditions, which characterize the system in terms of its variables and parameters. Because similar models are governed by an equivalent set of field equations and conditions, similitude conditions may be derived by defining the scale factors and comparing the equations of both prototype and model. This is a direct consequence of invariance as defined by Szucs [22] and expressed by Eq. (1). The derived conditions relate geometric (length, width, thickness, etc.), structural (assembly), excitation (force amplitude, force phase, excitation frequency, etc.), and material properties (Young's modulus, Poisson's ratio, mass density, etc.) of the system to its response. When all of them are satisfied, then complete similitude is achieved; otherwise, if at least one of such conditions is not fulfilled, the similitude is at best partial.

For example, consider an isotropic plate with uniform cross section and subject to a uniform transverse load q [1]. Its governing differential equation is

$$\frac{d^4w}{dx^4} + 2\frac{d^4w}{dx^2dy^2} + \frac{d^4w}{dy^4} = \frac{q}{D} \tag{7}$$

wherein w is the displacement in the direction orthogonal to the xy plane (where the plate lies) and D is the bending stiffness.

For model and prototype, we then obtain

$$\frac{d^4w_m}{dx_m{}^4} + 2\frac{d^4w_m}{dx_m{}^2dy_m{}^2} + \frac{d^4w_m}{dy_m{}^4} = \frac{q_m}{D_m} \tag{8}$$

and

$$\frac{d^4w_p}{dx_p{}^4} + 2\frac{d^4w_p}{dx_p{}^2dy_p{}^2} + \frac{d^4w_p}{dy_p{}^4} = \frac{q_p}{D_p} \tag{9}$$

respectively. The prototype Eq. (9) can now be rewritten in terms of scale factors and model parameters

$$\left(\frac{\lambda_w}{\lambda_x{}^4}\right)\frac{d^4w_m}{dx_m{}^4} + 2\left(\frac{\lambda_w}{\lambda_x{}^2\lambda_y{}^2}\right)\frac{d^4w_m}{dx_m{}^2dy_m{}^2} + \left(\frac{\lambda_w}{\lambda_y{}^4}\right)\frac{d^4w_m}{dy_m{}^4} = \left(\frac{\lambda_q}{\lambda_D}\right)\frac{q_m}{D_m} \tag{10}$$

Equations (7) and (10) are the same if the terms in parenthesis in the last equation are all equal, that is

$$\frac{\lambda_w}{\lambda_x{}^4} = \frac{\lambda_w}{\lambda_x{}^2\lambda_y{}^2} = \frac{\lambda_w}{\lambda_y{}^4} = \frac{\lambda_q}{\lambda_D} \tag{11}$$

Complete similitude is achieved when Eq. (11) is totally satisfied, which leads to the similitude condition $\lambda_x = \lambda_y$. In this case, the orthogonal deflection scale factor λ_w has three equivalent expressions

$$\lambda_w = \frac{\lambda_q\lambda_x{}^4}{\lambda_D} \tag{12}$$

$$\lambda_w = \frac{\lambda_q\lambda_x{}^2\lambda_y{}^2}{\lambda_D} \tag{13}$$

$$\lambda_w = \frac{\lambda_q\lambda_y{}^4}{\lambda_D} \tag{14}$$

Any of Eqs. (12)–(14) ensures a perfect prediction of prototype behavior. Instead, if $\lambda_x \neq \lambda_y$, then the similitude is partial: each of the conditions (12)–(14) yields different results and it is not ensured that any of them provides good predictions. Notably, in this application, the procedure must be completed by also considering the boundary conditions.

When using STAGE, the similitude conditions can be derived by introducing the scale factors into the solutions (exact or approximate) of the equations [1] or into the equations, in dimensional [50] and nondimensional [51] form. In the latter case, the scale factors that appear in the scaling laws, derived from the governing equations for the prototype and the model, are called *explicit scale factors*. The factors that disappear in the scaling laws but relate to the boundary conditions and the excitation mechanisms are called *implicit scale factors* and must be suitably defined in order to obtain a complete set of similitude conditions and, thus, the complete similitude. For example, in Wu [52], which investigates the scaled models of an elastically restrained flat plate under dynamic load, the explicit scale factors are those for the length, width, thickness, and displacement. The implicit scale factors are those for translational and rotational springs, excitation frequency, moving-load speed, damping ratios, and natural frequencies. Until now, no one has investigated partial similitudes in which the distortions are introduced by changing the boundary conditions between prototype and model.

An advantage of such method is that it allows to derive a set of conditions more specific than those obtained through dimensional analysis, because they are equation driven, which means that the relationships are forced by the governing equation. This implies that they have a physical meaning and that the procedure is more structured with respect to the one used in DA, but it lacks of a standard action sequence, so also STAGE cannot be implemented in an algorithm. Furthermore, the range of applications is limited to those systems with at least a set of governing equations and the derivation of similitude conditions still requires a certain calculation effort.

3.3 Energy Methods.

Besides the classic approaches previously mentioned, alternative methods have been proposed; two of them are based on an energy approach. One exploits the principle of conservation of energy and is introduced in Ref. [53]; the other is known as ASMA [54].

3.3.1 *Energy Method Based on the Principle of Conservation of Energy.*

The EM method [53] is based on the principle of conservation of energy, which states that if there is no energy loss (in terms of heat and chemical reactions), the strain energy U stored in the structure is equal to the sum of kinetic energy T and the work made by external forces W. By letting X_i, Y_j, Z_k denote the complete sets of properties (containing geometric ones, material ones, etc.) related to each type of energy, then the principle can be written as

$$U(X_i) = W(Y_j) + T(Z_k) \tag{15}$$

Because the energy equation given by the principle includes the structural domain, the applied loads, and the boundary conditions, the system is considered as a whole and there is no need to determine the explicit and implicit scale factors separately.

To derive the similitude conditions, all the considered energies are scaled simultaneously, so that a scaled energy equation is obtained; by doing so, the prototype Eq. (12) becomes

$$U(X_{i_m}\lambda_i) - W(Y_{j_m}\lambda_j) - T(Z_{k_m}\lambda_k) = 0 \tag{16}$$

In order to achieve a complete similitude, it is necessary that the equations must be rewritten in the following form:

$$\phi(\lambda_i)U(X_{i_m}) - \chi(\lambda_j)W(Y_{j_m}) + \Phi(\lambda_k)T(Z_{k_m}) = 0 \tag{17}$$

where $\phi(\lambda_i)$, $\chi(\lambda_j)$, and $\Phi(\lambda_k)$ are functional relationships among scale factors.

Complete similitude is achieved when the principle of conservation of energy is satisfied, which means that, for the model, $U(X_{i_m}) - W(Y_{j_m}) - T(Z_{k_m}) = 0$ and, by comparing with Eq. (17), $\phi(\lambda_i) = \chi(\lambda_j) = \Phi(\lambda_k)$.

The EM method is more straightforward than STAGE because it provides the scaling factors for structural behavior even when the structure is made of several components, while keeping the same level of generality and obtaining the same conditions. Again, a certain calculation effort is required, especially for complex systems. Furthermore, problems may occur when prototype and model are made of different materials.

3.3.2 *Asymptotical Scaled Modal Analysis.*

The finite element method is the best numerical tool for structural analysis but its computational cost becomes prohibitive as frequency increases, because the spatial mesh is frequency dependent: the higher the frequency range of the analysis, the smaller the mesh dimension. Because the Nyquist sampling theorem must be considered, with sampling rate at least twice the value of the highest frequency in the system response, the computational time increases considerably. The ASMA was conceived to reduce the spatial extent in order to save time during simulations.

A first definition of the method [55] is based on statistical energy analysis (SEA) and aims to define a scaled finite element model which can represent the energy exchange for increasing excitation frequency. The main idea is to reduce the extension of the spatial dimensions not involved in energy transmission, so that the original finite element mesh can be maintained, and, at the same time, to increase artificially the damping level in order to keep the same energy level of the prototype. ASMA is then formally justified without invoking SEA [54] but using the energy distribution analysis (EDA, Mace [56]), which defines the way the scaled model can represent the mean response. All the linear dimensions g not involved in the structural energy transmission are scaled down with a scale factor $\sigma < 1$, so that the scaled dimension is $\bar{g} = g\sigma$. Because this procedure would move mode shapes and natural frequencies to higher frequency, in order to keep the same energy level, damping has to be increased with a certain scale factor ε, so that $\bar{\eta} = \eta\varepsilon$. Boundary conditions and material of the model are the same as for the prototype so that mode shapes are retained.

Combining the reduction of the degrees-of-freedom and eigenvalues to be extracted during the dynamic problem solution, there are several possibilities of computational time saving:

(1) Same number of degrees of freedom and eigensolutions: There is not a direct computational advantage but ASMA can represent the response at higher frequencies.
(2) Same number of degrees of freedom, but reduced number of eigensolutions: The dynamic response is obtained at least in the same frequency range and a certain computational advantage is acquired.
(3) Reduced number of degrees of freedom and eigensolutions: The number is tailored to acquire the dynamic response correctly in the same frequency range with an appreciable computational advantage.

The method is applicable to finite element analysis and it can be implemented in an algorithm. Being based on modal expansions, ASMA can be applied to any structural operator for which the real or complex modal base is known (natural frequencies, mode shapes, and damping). Furthermore, it does not require a reference solution, i.e., there is no need to analyze first the prototype. Finally, it can be applied to every finite element solver. On the other hand, the response is meaningful only for the global frequency response: local information is lost due to the artificially increased value of damping. Furthermore, the response is perfectly replicated if it is averaged on both excitation and acquisition points.

In conclusion, ASMA can be seen as a modulator of the original modal base that allows the analysis of the response of the selected structural operator in the frequency domain where the response is meaningful.

3.4 Similitude and Asymptotic Models for Structural-Acoustic Research Applications.

In order to enlarge the number of parameters, to achieve a complete similitude, and to investigate the possibility to define similitude conditions for acoustic-structural systems, a new method used in combination with EDA was proposed in De Rosa et al. [57]. This is a generalization of the modal approach used in the ASMA method to establish the scaling laws. The method is then successively formalized in Ref. [58] and referred to as SAMSARA.

To reproduce the dynamic response by means of a similitude, it is necessary to satisfy some conditions:

(1) Material does not change, because any change modifies the distribution of natural frequencies.
(2) The boundary conditions do not change.
(3) The excitation is a concentrated harmonic force and it acts at the same dimensionless (homologous) location.
(4) The structural damping is such that the system response can be obtained by using the real mode shapes and the undamped natural frequencies. More complicated models, based on complex mode shapes, do not add further contributions to theory development and results.

The main reason behind these assumptions is to limit the changes of the modal base when the similitude is applied. These conditions are not limitations of SAMSARA but points to be explored in further developments of the method.

When using SAMSARA, if the structure is geometrically scaled in all the dimensions, the model is called *replica*. Instead, a distorted model is called *avatar*. To obtain a replica, similitude conditions must be necessarily satisfied, but the scaling procedure involves also other scale factors that do not appear directly into the scaling conditions. For example, when scaling a plate, a replica is obtained by varying length, width, and thickness of the panel, while by satisfying only the similitude condition (involving just the length or the width) leads to a *proportional sides* model [59].

When a complete similitude is under investigation, the prototype mode shapes appear at different natural frequencies in the model (higher frequencies if the model is scaled down). After the excitation, the energy spreads in a model according to a certain succession of modes with perturbed natural frequencies. By applying a remodulation, such succession of modes can be brought back to prototype ones. In this way, the response of the structure is reconstructed.

Figures 3–6 may clarify the concept of remodulation by comparing the natural frequencies and frequency response functions (FRFs) of orthogonally and longitudinally stiffened cylinders in similitude. Three test articles are compared: the prototype (labeled with A), the replica, and an avatar (labeled with A1). The geometric dimensions subjected to scaling are length, diameter, skin thickness, stringer section, and rib section.

Figure 3 shows the natural frequencies of the prototype cylinder and its replica, before and after remodulation. There are a number of features that are worth noting. Before remodulation, the natural frequencies of replica shift to higher frequencies because of the reduction in size of the cylinder. The remodulation process leads to the overlap on the bisector of both prototype and replica frequencies. The natural frequencies of cylinder A are perfectly

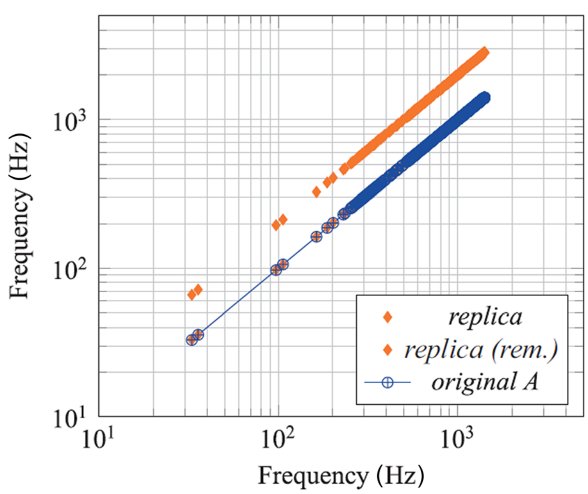

Fig. 3 Natural frequencies of replica and cylinder A before and after remodulation. (Reproduced with permission from Petrone et al. [60]. Copyright by Sage.)

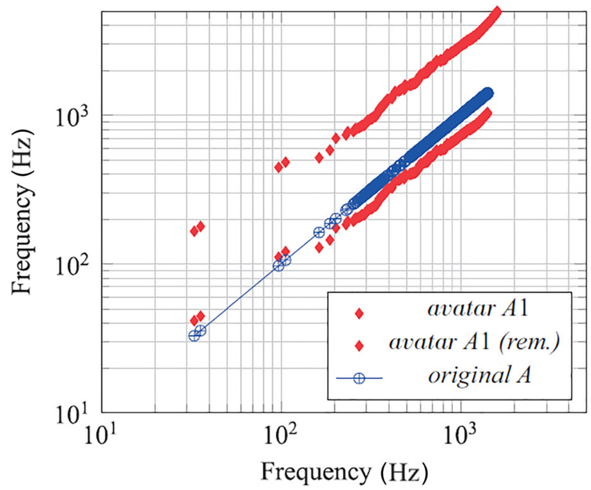

Fig. 4 Natural frequencies of avatar A1 and cylinder A before and after remodulation. (Reproduced with permission from Petrone et al. [60]. Copyright by Sage.)

predicted from the replica because all the geometric dimensions of the prototype have been halved, automatically satisfying the similitude conditions.

Avatar A1 scales down only the length and the diameter. The similitude conditions are not fulfilled, thus the natural frequencies are not located on the bisector after the remodulation process (Fig. 4). Typically, the greater the distortion, the wider the distance between the natural frequencies of the prototype and the remodulated ones of the avatar.

Similar observations can be made for the FRF of the cylinders. Figure 5 shows the forced response of both prototype and replica. In this case, the shift in frequency is more clear (Fig. 5(*a*)): the number of modes of both the test articles is the same, but the poles of the replica move to higher frequency covering, as a consequence, a wider frequency range. After remodulation, the responses perfectly match, despite some slight errors in amplitude, noticeable at high frequency (Fig. 5(*b*)).

When considering the avatar (Fig. 6), the remodulated response (Fig. 6(*b*)) does not fit at all the prototype response.

A characteristic of the method is that it directly involves modal parameters, which means that their scale factors are defined; this being the main novelty of the approach. Different from ASMA, which provides only the mean response, SAMSARA is able to furnish the local one. It can be also implemented in an algorithm. The method allows the solution of both replicas and avatars.

3.5 Empirical Similarity Method. In the field of rapid prototyping, dimensional analysis is typically used, but it has some issues related to the difference in material properties between prototype and model, sensitivity to distortions, too restrictive use of information, and dependence of cost and time on geometrical complexity. For these reasons, Cho and Wood [61] proposed the ESM. This is based on the testing of a specimen pair: one specimen with simple geometric features fabricated through rapid prototyping (prototype specimen) and the other fabricated through the actual production process (product specimen). By measuring the state vectors of this pair and the scaled structure obtained through rapid prototyping, a state transformation is derived. In such transformation, the usual scale factors are replaced by weighting factors.

The empirical transformation matrix can be considered as an advantage, but the fact that additional specimen pairs are needed leads to additional manufacturing and testing.

3.6 Sensitivity Analysis. Recently, SA has been applied to similitude theory. SA can be defined as the study of how

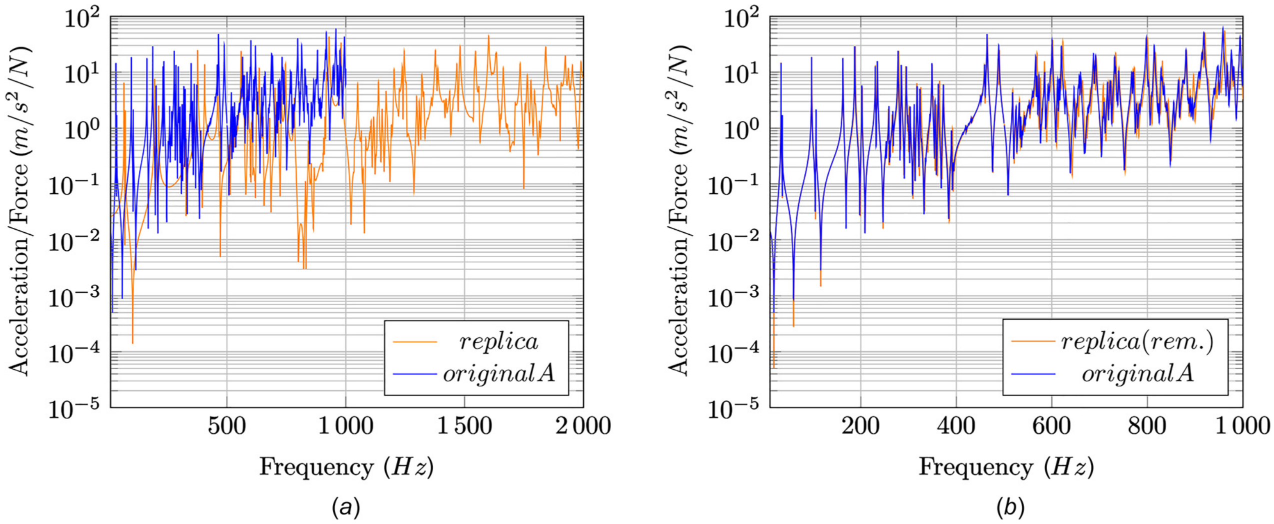

Fig. 5 Forced response of replica and cylinder A before (*a*) and after (*b*) remodulation. (Reproduced with permission from Petrone et al. [60]. Copyright by Sage.)

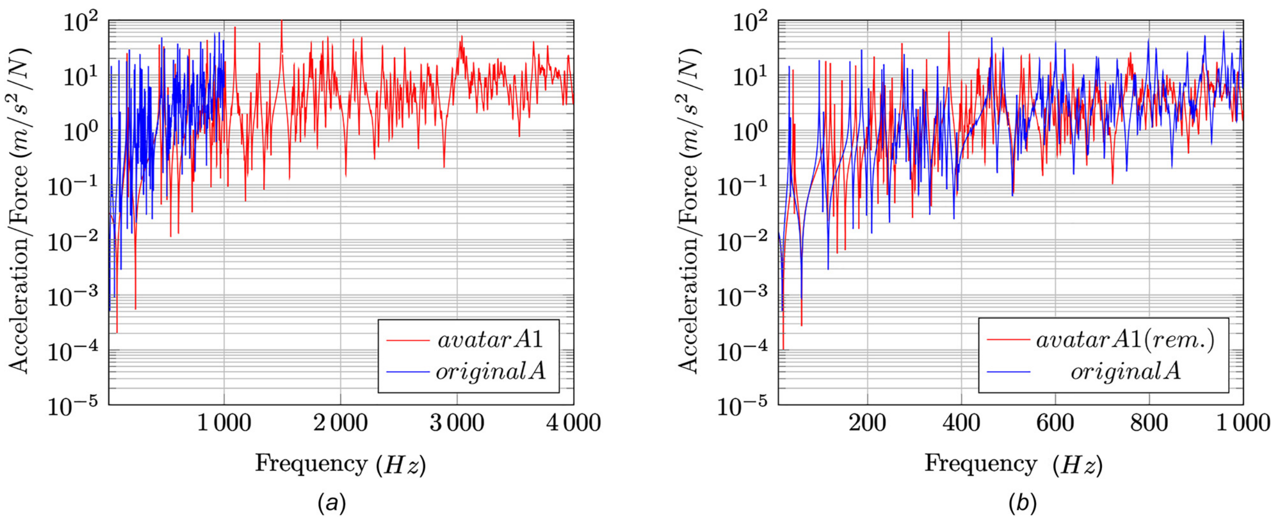

Fig. 6 Forced response of avatar A1 and cylinder A before (*a*) and after (*b*) remodulation. (Reproduced with permission from Petrone et al. [60]. Copyright by Sage.)

uncertainty in the output of a system can be associated with uncertainties in the input of the system. When the global behavior is of interest, then global sensitivity analysis (GSA) is applied. When the response is studied at a particular point of the parameter space with a differential approach, then local sensitivity analysis (LSA) is applied.

Luo et al. [62] employ sensitivity analysis to derive the similitude conditions for distorted models. The authors enunciate four principles to get distorted laws. They are

(1) *Principle 1*: In distorted scaling laws, if parameter j is directly reflected in the governing equation, the index k of the scaling factor λ_j^k can be directly determined from the governing equation.
(2) *Principle 2*: In the sensitivity analysis, if sensitivity's absolute values satisfy $|\Phi_a| > |\Phi_b|$ in distorted scaling laws, the index relation of scaling factors λ_a^α and λ_b^β is $|\alpha| > |\beta|$. Here, Φ_a and Φ_b are the sensitivities (i.e., the change rates) of the natural frequency with respect to geometrical parameters a and b.
(3) *Principle 3*: If $\Phi_j > 0$, λ_j is positively proportional to λ_ω (the scale factor of the natural frequencies) in the distorted scaling law; conversely, λ_j is inversely proportional to λ_ω if sensitivity $\Phi_j < 0$.
(4) *Additional principle*: In the distorted scaling law, the index ratio $\alpha : \beta$ of scaling factors λ_a^α and λ_b^β is approximate to the ratio of the sensitivity $\alpha : \beta \approx \Phi_a : \Phi_b$.

The principles 1–3 help to derive approximate distorted scaling laws, i.e., scaling laws for distorted models that return a high percentage of error between the natural frequency of the distorted model and the predicted natural frequency. The additional principle is used to derive accurate distorted scaling laws, returning an error lower than approximate laws (typically within 5%).

A statistical application of GSA is given in Ref. [63], where the authors employ, first, a 2^k ($k = 3$ in this case) full factorial design to study the effects on the response of the structure to changes in input parameters, then derive sensitivity-based scaling laws through a multiple quadratic regression.

Local sensitivity analysis is then applied by Adams et al. [64]. Let X_j be the design parameter of the system (geometry, material, etc.) and Y_k its response (e.g., natural frequencies or vibration velocities). The model kth response $Y_k^{(m)}$ can be written as the product of the prototype response $Y_k^{(p)}$ and N linearly independent scale factors λ_{X_j}, each one weighed by an unknown power $\alpha_{j,k}$

$$Y_k^{(m)} = Y_k^{(p)} \prod_{i=1}^{N} (\lambda_{X_j})^{\alpha_{j,k}} \tag{18}$$

The approach is directly deduced from Buckingham's Π theorem. According to this theorem, dimensional analysis can be used to derive the weighting terms $\alpha_{j,k}$. The novelty of the method proposed by Adams et al. relies on the application of sensitivity analysis to derive these exponents as

$$\alpha_{j,k} \approx \frac{\ln\left(Y_k^{(+)}\right) - \ln\left(Y_k^{(-)}\right)}{\ln\left(\lambda_{X_j}^{(+)}\right) - \ln\left(\lambda_{X_j}^{(-)}\right)} \tag{19}$$

where the symbols (+) and (–) indicate the scaling up and down, respectively.

Therefore, there is no need to derive dimensionless groups, as in dimensional analysis, or to compare the equations of prototype and model, as in STAGE or SAMSARA. By just knowing the scale factors and the responses, Eqs. (18) and (19) allow to implement SA in an algorithm so that the sensitivity-based scaling laws can be derived without having a priori knowledge of the scaling behavior and with minimum effort. However, both GSA and LSA lack of a physical insight into the problem that may lead one to overlook some important phenomena. Furthermore, too complex systems may lead to prohibitive computational costs and inefficient procedure.

3.7 Methods Summary. A brief introduction to similitude methods has been provided. Up to now, despite the increasing complexity of modern applications and the emerging methods, dimensional analysis and STAGE are still the most used ones.

According to dimensional analysis, similitude conditions are derived by defining sets of nondimensional ratios through the investigation of the reference parameters. It is not based on the knowledge of the governing equations, which makes such a method employable in a wide spectrum of applications, even very complex ones, although a great amount of manual calculation may be needed. For example, dimensional analysis is used a lot in fluid dynamics in order to find the nondimensional numbers representing the main characteristics of a fluid (Mach number, Reynolds number, Peclet number, etc.) by comparing dimensional groups with their own physical meaning.

Dimensional analysis is a very useful tool when the analyzer has a very good knowledge of the problem or when the governing equations are unknown or too complex to be solved analytically or numerically. As the choice of parameters is up to the analyzer, it can be exploited in order to understand the influence of a particular parameter on the phenomenon under observation.

The second most used method is STAGE, based on the definition of scale factors successively substituted into the governing equations in order to derive the similitude conditions. On the one hand, this requires knowing the field equations; on the other hand, the conditions obtained are more specific and the method itself lacks the trial-and-error approach typical of dimensional analysis. In general, when the governing equations are known, it is better to employ STAGE than DA.

Conservation of energy is the foundation of the energy method introduced by Kasivitamnuay and Singhatanadgid [53]. Once the strain energy, the kinetic energy, and the work of the (possibly multicomponent) structure have been evaluated, the scaling conditions are derived keeping the same results and level of generality of STAGE. The procedure is more straightforward than STAGE but still affected by a certain effort when dealing with complex structures.

Asymptotical scaled modal analysis and SAMSARA are the first methods that address similitude theory toward an automatic procedure, because both of them can be implemented in an algorithm.

Because computational costs can sometimes be prohibitive, ASMA was introduced in order to reduce them by scaling down the spatial domain by means of a scale factor. Since the energy level must be kept, an artificial, increased damping was introduced limiting the analysis to the global frequency response. In other words, ASMA can be expected to produce a good level of accuracy only for the mean response of a structure. Such characteristics make the method suitable for computationally expensive analyses where the analyzer is interested only in the mean response or in the response at high frequency range. Furthermore, ASMA is useful in evaluating how SEA energy influence coefficients (both direct and indirect) are affected by changes in the modal overlap factor.

Similitude and asymptotic models for structural-acoustic research applications exploit scale factors, just like STAGE. Since it is based on a generalization of the modal approach, modal parameters are also involved in the scaling procedure. Different from ASMA, SAMSARA provides the local response (from which, with multiple acquisition, the mean response can be reconstructed). SAMSARA is very useful when studying structural dynamics and acoustic-structural systems.

Empirical similarity method is a method used in rapid prototyping applications. It derives a state transformation between a specimen pair and the scaled structure obtained through rapid prototyping. It was introduced in order to overcome the problems of dimensional analysis applied to rapid prototyping, such as differences in material properties and sensitivity to distortions. Additional manufacturing is the main disadvantage of this method.

Sensitivity analysis is another step toward an automatic approach, especially in terms of scaling laws derivation, because this method can also be implemented in an algorithm. SA is divided into global and local sensitivity analyses, according to the purpose. Its automatic nature allows to derive the sensitivity-based scaling laws without knowing the scaling behavior of the system but, at the same time, it is not based on physical relationships. It is also computationally expensive.

4 Applications of Similitude Methods

Similitude theory has been widely applied in many engineering branches, to both complex and simple structures. Elementary structures such as beams, plates, and cylinders may occur as stand-alone simple systems or form the basic structural components of more complex ones (for example, pressure vessels [65,66]). The purpose of this section is to review the applications of similitude theory to such structures.

During the writing of this review, it has been noticed that similitude theory applications concern some particular structural fields, such as static and dynamic behavior, impact response, and damage.

Dynamic response focuses on identifying the natural frequencies and the mode shapes of a structure, since this information is fundamental for analyzing fluid-structure interactions, vibroacoustic phenomena, etc. An application example is the interaction of a structure with a turbulent boundary layer. It is an important source of vibration and noise; the stochastic pressure distribution associated with the turbulence excites significantly the structural response and the radiated acoustic power. For these fluid-structure interaction problems, there are some computational problems related to the fact that solutions are typically lost above the structural/aerodynamic coincidence frequency, even if the mesh is built to simulate very small structural wavelengths.

Prediction capability at each frequency range at acceptable computational costs is another issue associated with dynamic response. Up to now, different methods have been used to investigate problems at low and high frequency ranges.

A characteristic type of dynamic response of particular engineering interest is that associated with impacts. Here, large, short-duration forces may produce damage that can affect the load carrying capacities of a structure. There are several examples in which the resistance of structures to penetration or perforation has primary importance: design of a structure to resist wall perforation by a high velocity projectile, containment of fragments or projectiles generated by possible accidents in nuclear reactors, the threat of the so-called wind-generated missiles, containment of fragments generated in aircraft turbine engine disintegration, bird impacts on aircraft, etc.

For metals, such damage involves plastic deformation and wear in the contact zone, while it takes the form of fiber failure, matrix cracking, and delaminations for composites. Things get further complicated when distinguishing between structures that localize damage and those for which damage can be more widespread. In structures with significant flexibility, multiple collisions may happen and a large amount of energy is released in terms of vibrations. For rigid bodies, impactor and body vibrations are negligible and deformations are confined to the vicinity of the contact region.

From these observations, it follows that impact problems are complex to study and it is easy to imagine that they involve many phenomena that must be accounted for, including inertial effects, material response to varying strain-rate and thermal loading, and material failure and stability. In particular, dependence on strain-rate is a challenge to the scaling procedure. Because of such dependence, the material increases its resistance as the impact load is applied. The model/prototype ratio of dynamic stress, representing how the static flow stress changes when there is a varying strain-rate, is no longer invariant. In similitude terms, this translates into distortions because strain-rate phenomena do not support scaling, at least not with the usual, geometric scaling procedures.

In addition to dynamic response, similitude methods are commonly applied to study the static response, often loading test articles until failure. It is known that size effects have a strong influence on failure mechanisms and the ultimate strength of a structure. These effects cannot be explained by statistical models or fracture mechanics theories. For this reason, experimental tests are very useful for understanding the limits of validity of similitudes.

Significant attention has been dedicated to composite materials, since they emerged more than sixty years ago, as an interesting and useful alternative to the classic, isotropic engineering materials, thanks to their lightness and resistance capabilities. In aeronautics, for example, where both stiffness-to-weight and strength-to-weight properties are important, composite materials are used for load-bearing aircraft structures such as the upper fuselage of the A380 Airbus [67].

Compared to isotropic materials, such as metal, composite materials exhibit nontrivial interactions between micro- and macrostructural properties. It is sufficient to think of the several ways in which a composite material undergoes damage (fiber fracture, delamination, and matrix cracking), or the emergence of size effects. These are all phenomena that start at the microscopic scale and then evolve, eventually, to the macroscopic level of the laminate.

Although these considerations suggest that a microstructure scaling should accompany scaling of a macroscopic test article, this operation is never executed due to its great practical complexity. Instead, only the macrostructure is considered when similitude conditions are derived. This approach leads to some obstacles, as the descriptions of notch and strain-rate sensitivity, for example, are strongly dependent on the microscopic characteristics of a composite material. Notably, notch sensitivity is strong in quasi-isotropic laminates, but weak in unidirectional laminates subject to traction in the fiber direction. Strain-rate sensitivity depends on fiber and matrix materials; glass and Kevlar fibers are rate-sensitive, as is epoxy resin matrix, while carbon fibers are not rate-sensitive. Furthermore, the degree of sensitivity depends on the lay-up and the rate of loading may affect the damage mechanisms. The interaction among all these factors may easily lead to scaling conflicts, thus scaling a composite laminate is an operation to perform with extreme care; testing is required to establish guidelines and to highlight size effects that are not modeled by any scaling procedure.

The use of composite materials is limited by their susceptibility to impact damage that can reduce the compressive strength even if such damage is not visible. The characterization of impact phenomena is necessary because the response of composites is complex, involving localized out-of-plane loading, possible strain-rate effects, and the interaction of several failure modes.

Many articles [33,68–87] showed that stacking sequence is a key parameter in scaling composite materials. There are three scaling approaches, namely ply level scaling (Fig. 7(*a*)), sublaminate scaling (Fig. 7(*b*)), and general reduction of the number of plies. Ply level scaling consists in adjusting the number of plies in a group having the same orientation; thickness is scaled and the stacking sequence is kept. In sublaminate-level scaling, basic sublaminates, stacked together, are introduced so that thicker laminates are formed.

The choice of the scaling strategy has significant consequences on the response of the composite specimen. This choice is studied in many works [68–72] in which it is demonstrated that ply level scaling applied only to the thickness or to all the geometric dimensions (also known as one- and three-dimensional scaling, respectively) leads to a decreasing tensile strength with increasing size. Such behavior is due to the increased severity of edge delamination and debonding, creating stress concentrations that lower the strength of hybrid materials. Instead, two-dimensional ply level scaling, i.e., area scaling, exhibits an increased tensile strength for larger samples. In this case, delamination affects smaller specimens because the relative width of the delaminated zone is greater. The severity variability of delamination is due to Poisson's ratio mismatches between the materials. Sublaminate-level scaling affects area scaling significantly. In fact, it reduces the tendency of smaller models to fail earlier.

The effects of both ply- and sublaminate-level scaling on fiber metal laminates (FMLs) specimens are shown in Fig. 8. Figure 8(*a*) illustrates the failure strength and ply level scaled specimens exhibit a pronounced size effect: in fact, the strength increases steadily from the 1/4 scale sample to the full-size geometry. Figure 8(*b*) shows the tensile strain to failure. No size effect is observed in the ply level scaled FMLs, with the strain being approximately 20% in all sample sizes. This result is quite surprising, because size effects were noticed in the strength data of these models. Neither sublaminate-level scaled models exhibit a noticeable size effect in strain, keeping an average value of 22%.

This section is organized in Secs. 4.1–4.4, one for each structure type; the test articles are then presented in terms of applications, highlighting the commonalities in results and the novelties of the applied methods. At the end of the section, the main points are presented. The contents of the following sections are summarized in Table 2: the rows show, on the left, the test article, on the right the method, the columns separate the applications in terms of used procedures (theoretical and experimental) and each box is

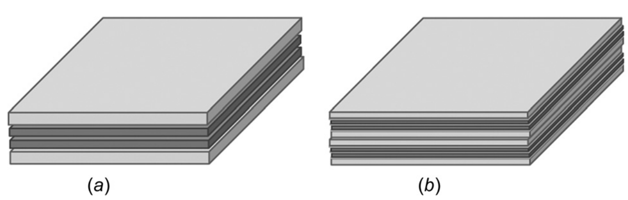

Fig. 7 Schematic of two techniques: ply-level (*a*) and sublaminate-level (*b*) scaling. (Reproduced with permission from Carrillo and Cantwell [68]. Copyright by Sage.)

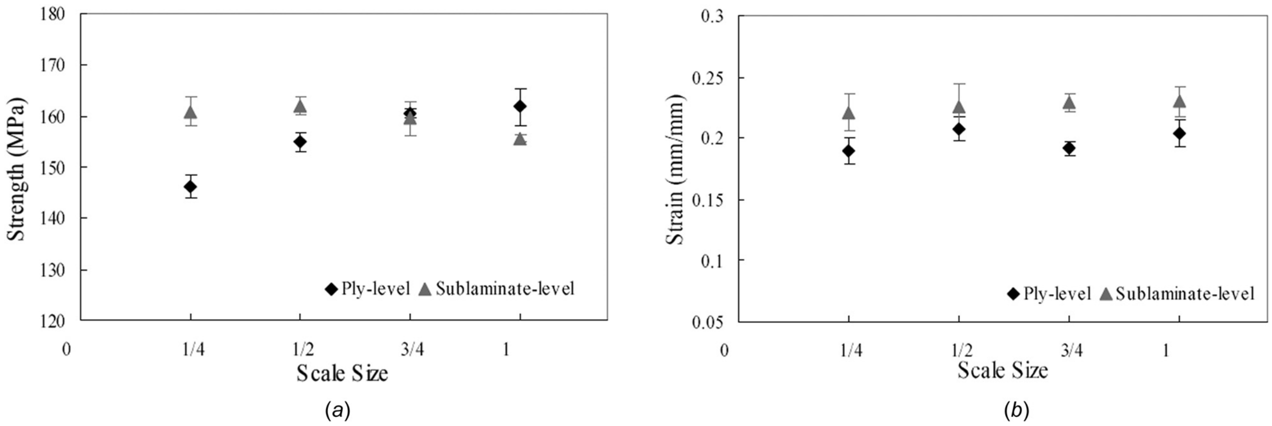

Fig. 8 The effect of scale size on the tensile strength (*a*) and on the strain at failure (*b*) for both ply- and sublaminate-level FMLs. (Reproduced with permission from Carrillo and Cantwell [68]. Copyright by Sage.)

Table 2 Overview of test articles, procedures, methodologies, and materials used in similitude methods

	Analytical/numerical	Experimental	Method
Beam	Aluminum	Aluminum	ASMA
	Aluminum, brass, composite, magnesium alloy, steel, titanium, tungsten alloy	Composite, steel	DA
	Aluminum, steel	—	EM
Unstiffened plate	Aluminum, composite	Aluminum	ASMA
	Aluminum, composite, steel	Aluminum, composite, polyvinyl chloride, steel	DA
	Aluminum, steel	—	EM
	Aluminum	Aluminum	SAMSARA
	Steel	—	SA
	Aluminum, composite, magnesium alloy	Composite	STAGE
	Aluminum, steel	Aluminum, steel	STAGE + SA
Stiffened plate	Steel	Steel	DA
	Aluminum	—	STAGE
Sandwich plate	—	Composite + PMI (polymethacrylimide)	DA
	TC4 titanium alloy + general rubber	—	STAGE
Unstiffened cylinder	Steel	Aluminum, composite, concrete, steel	DA
	Aluminum	—	SAMSARA
	Steel	Steel	STAGE
	Aluminum	—	STAGE + SA
Stiffened cylinder	Composite	—	EM
	Aluminum	—	SAMSARA
	Aluminum, steel	Aluminum, steel	STAGE

Note: Table 4 in the Appendix gives the corresponding references related to this table.

filled with the material. Only the most relevant works are discussed in detail. The complete list is provided in Tables 3 and 4 in the Appendix in which the references for both methods and test articles are indicated.

4.1 Beams. Beams and bars are structures that constitute the main elements of frames, as well as subcomponents of more complex systems, e.g., stiffeners in a stiffened cylinder or spar caps and shear webs in wind turbine blades. Similitude methods have been applied to beams to study static and dynamic behavior, failure, and impact response.

4.1.1 Failure Analysis. An important contribution to similitude theory applied to beams is presented in Jackson and Fasanella [88] and Jackson [89]; in these works, the authors conduct extensive experimental and numerical tests to investigate the behavior to failure of composite beams. In particular, they subject six scaled models of a graphite-epoxy composite beam with unidirectional, angle- and cross-ply, quasi-isotropic stacking sequences, from 1/6 to full-scale, to both static and dynamic (impulsive) eccentric axial compression. The choice of the test article is based on the possibility of achieving large bending deflections promoting global failure away from the supported ends.

By scaling the prototype with dimensional analysis, the reported results highlighted many important characteristics of scaled models, especially in terms of size effects, that reoccur in several subsequent works. A summary of the main experimental results is given as follows:

(1) In static tests, the scaled load and strain responses depend on the laminate stacking sequence and on the number of 0 deg plies in the laminate. For unidirectional and cross-ply laminates, the responses scale well even for large deflections and rotations; in other words, such laminates do not exhibit size effects. In contrast, the responses of angle-ply and quasi-isotropic laminates deviate from those predicted with similitude theory because of damage which alters the beam stiffness.
(2) In static tests, all laminates exhibit a significant size effect in strength: normalized loads, end displacements, and strains at failure increase as the size of the beam decreases, especially for cross-ply beams. For dynamic tests, quasi-isotropic small models are more severely damaged.

(3) The scaled model predictions for dynamic tests are good for unidirectional laminates, but inconsistent for cross-, angle-ply, and quasi-isotropic ones, again mainly due to the size effects.
(4) In both static and dynamic tests, failure modes are the same for the same stacking sequence, independent of specimen scale. In static tests, only the scaled models of cross-ply beams exhibited size effect in failure mechanism (fiber fracture was not present in the larger models).
(5) Static and dynamic test data from beams of the same laminate family and scaled size indicate similar load and strain responses; the dynamic response oscillates about the static response for all the laminate types. With the exception of cross-ply laminates, the failure locations due to both static and dynamic loading are nearly identical. Thus, it is possible to retrieve important information on the global dynamic response of structures from simple static testing of scaled models.
(6) Bending stiffness is not affected by size for unidirectional, cross-ply, and quasi-isotropic laminates; angle-ply laminates, however, exhibit greater stiffness, with decreasing size.

In addition to specific observations regarding scaled composite beams, the work by Jackson and Fasanella [88] and Jackson [89] highlights the problem of size effects: noticeable departure from the predictions of similitude methods in actual experimental tests.

4.1.2 Static Analysis. Static tests on composite beams were performed by Asl et al. [90–93]. In this work, the authors investigate composite I-beams analytically, numerically, and experimentally in the framework of model analysis for subcomponent testing; the beams are equivalent to the spar caps and shear webs of wind turbine blades. Similitude conditions are obtained by means of STAGE. The novelty of these works is in the use of partial similitude. Indeed, in theory, it is possible to obtain a complete similitude with ply-level scaling and keeping the same aspect ratio. When the laminate thickness is supposed to be scaled down below the range in which there is no integer number of lamina left in the stack up, however, ply-level scaling is no more achievable; reducing the lamina thickness is not an available option. Ply-level scaling is applicable only to specific lamination schemes but the possibility of keeping the same lay-up in the scaled models as in the prototype is limited by manufacturing constraints, since only fabrics with specific thicknesses are available in industry. Thus, a partial similitude is a likely outcome due to manufacturing issues.

Aiming for a good prediction of prototype behavior using only partial similitudes, Asl et al. [90–93] introduce a permutation algorithm that searches for the potential model having ply schemes with overall laminate thickness less than that of the prototype; an error is defined to find the layup that works best with the derived scaling laws, and this lay-up is then used for predictions. Their algorithm is known as the distorted lay-up technique (DLT) and the tests prove that it is possible to have satisfactory results with errors smaller than 6% also with such distorted models. It is important to note that the probability of finding an accurate model decreases when decreasing the number of layers in a model. There is thus a limit to the amount of scaling that can be achieved using DLT. However, the technique is applicable to other geometries and ply schemes.

In a recent work [93], DLT was used to test experimentally a prototype and nine models (three small, three medium, and three large) with different lay-ups in a four-point bending test. The results show that the strain field of the small beams is representative of those of the medium and large models; the prescribed loads described by similitude analysis work accurately across different scales. The important consequence is that a certain strain level for a composite beam geometry with specific scale and lay-up can be accurately replicated in a smaller scaled model with a different lay-up. Thus, a scaled model may facilitate and expedite the fatigue testing process of large composite structures, leading to reduced costs and times.

In another experimental campaign [92], analytical and numerical results are verified by a three-point bending test measured with digital image correlation executed on a composite beam so that flapwise bending is reproduced and measured with digital image correlation. The results of the test confirm the observations previously made by Jackson and Fasanella [88] and Jackson [89] about the absence of size effects: bending stiffness of particular lay-ups is not affected by scaling. The predictions are very good also because the study is conducted in the elastic range, before yielding or failure has appeared.

4.1.3 Frequency Response. More insights on stiffness behavior with size were obtained in the experimental investigation by Asl et al. [94], of the response of three models (small, medium, and large) of a free-free beam to excitation with an impact hammer. Comparison among the models show that the FRFs agree despite a certain decorrelation, especially at higher modes. In fact, at low frequencies, effects associated with the flexural stiffness dominate over those associated with shear. The first two peaks thus exhibit a good correlation because bending stiffness is not affected by scaling [89,92]. At higher modes, shear effects become dominant. Because the FRFs decorrelation increases in this case, it is possible to conclude that shear stiffness is affected by scaling Fig. 9. Similarly, rotary inertia has an influence, shifting the frequencies of larger models to lower values.

The advantages of ASMA in studying structural dynamic behavior are shown in Refs. [55] and [95]; in the first work, the test article is a set of six in-line rods; in the second, two flexural aluminum beams and two sets of, respectively, two and four in-line rods. ASMA proves to be a valuable tool with respect to both SEA and classic modal analysis. Comparisons with classic modal analysis show that ASMA provides good matches only at high frequencies, since it captures an average energetic behavior. Nevertheless, its advantage is that it allows to deal with a scaled domain or with the same number of degrees-of-freedom across a larger frequency range [55]. ASMA can also be used to evaluate coupling loss factors providing acceptable results in regions of low, intermediate, and high modal overlap factors [95].

4.1.4 Impact Response. A particular type of dynamic behavior is that due to impacts. As previously highlighted, it is challenging to approach impact problems within a rigorous theoretical framework. There are a large number of relevant physical properties to characterize that necessitate analytical models with an

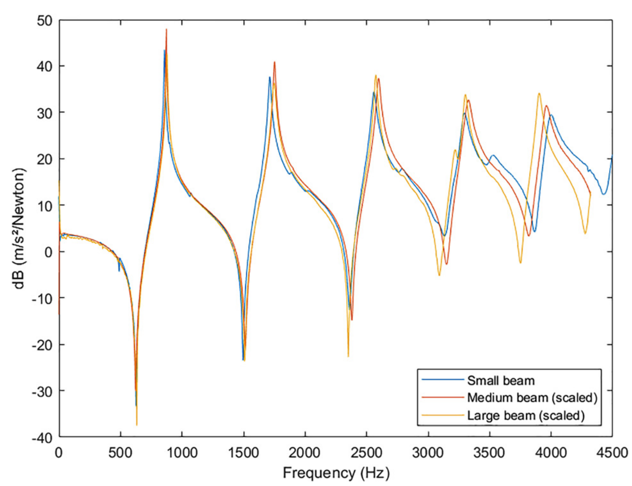

Fig. 9 Comparison of the FRF of the small beam with the scaled FRFs of the medium and large beams. (Reproduced with permission from Asl et al. [94]. Copyright by Springer.)

equally large number of parameters. The need to reduce them to a smaller, more manageable set and, more importantly, to introduce quantities that would allow comparison of results obtained for systems with similar geometries, boundary conditions, and loads, has been the main focus of several works in the literature.

Size effects similar to those found in Refs. [88] and [89] were already described in a previous work of Morton [34], which considered the experimental impact analysis of a composite beam struck at the center by a free-falling mass. There, small specimens were found to be stronger than larger ones and thus able to carry larger postdamage loads. Generally, the greater the specimen, the lower the impact velocity needed to cause damage.

Morton [34] also makes an interesting experimental observation: it seems, in fact, that smaller specimens also exhibit smaller impact duration than larger ones. In this case, the reason may not be a size effect but rather the fact that the articles exhibiting this behavior are made of the same material (carbon fibers in an epoxy matrix) coming from another, older batch. This shows that the results obtained with a particular experimental procedure, on the one hand, may be important and highlight hidden phenomena but, on the other hand, must be treated carefully.

Another example of results possibly polluted by improper experimental procedures is the work by McKown et al. [96] in which FML beams and plates are studied by means of dimensional analysis. Some results are consistent with those already listed, such as the good agreement with predictions of load and deflections in both static (four-point bend flexure) and dynamic (low velocity impacts) tests, or the persistence of failure mechanisms. On the other hand, the flexural yield forces of the 1/4-scale model are said to be 15% smaller than those of the other models; this may be a size effect but could, alternatively, be the consequence of the incorrect alignment of the smallest specimens on the test supports, a particularly difficult task. It is important to point out that in this investigation only geometrical scaling has been performed, thus the approach may not work when higher strain-rates are considered.

An early contribution to this effort is presented in Zhao [97], who uses dimensional analysis to find a unique, dimensionless number to describe the dynamic plastic response of bodies subject to impacts. This so-called response number is given by the product of Johnson's damage number [98] and the geometrical influence of the structure. It takes into account the three aspects: load inertia, material resistance, and structure geometry. This paper uses theoretical and experimental comparisons to show that the response number is suitable for representing the plastic response of beams and plates for many boundary and loading conditions. It also considers second-order effects such as finite deflections, transverse shear, strain-rate sensitivity, and dynamic tearing.

The fact that the response number is the product of a similitude parameter in impact dynamics and a term related to the geometry of the structure leads to different forms of this number according to the loading conditions. This kind of considerations led Zhao to formulate a generalization of the response number to cover other forms of dynamic plastic failure, e.g., bifurcation buckling problems [99]. Other authors expanded its application to more geometries, including circular and quadrilateral plates [65], and generalized the technique to different types of shells [66]. These works are the evidence that the response number is, indeed, quite useful to study the dynamic plastic response and failure of structures (beams, plates, shells, etc.) subject to large dynamic loading.

The same aim is the core of the works of Christoforou and Yigit [100,101]. These authors introduce dimensionless numbers, analytically or numerically obtainable according to the system complexity, to reduce the number of parameters characterizing impacts. Their results provide both physical insight and a tool for generalizing and correlating experimental results through the use of minimum data and model tests. Different structures (beams and plates) made from different materials, under different support conditions and under different impacts, but having the same values of such nondimensional numbers, share the same normalized responses. Thus, it is possible to scale the impact responses among different systems. Importantly, however, similitude is achievable only during the initial response or, more generally, before the mechanical waves are reflected back by the structure interfaces (after such reflection, beams and plates exhibit different dynamics). Thus, the global response scales well in terms of impact force and deflection, while the local response scales well only in terms of force. Since the transition region between global and local behavior is not captured accurately by the dimensionless number, it is not possible to generalize this among different structures.

Pintado and Morton [102] focus their work on the analysis of size effects in graphite-epoxy composite beams under three-point bending vertical impact loading. Two sources of lack of similitude are considered: constant gravitational acceleration and nonscaling of stacking sequence. The former introduces small errors in model behavior, thus it can be neglected; the latter leads to greater discrepancies. Applying Buckingham's Π theorem, the authors notice that a complete similitude is achievable only with ply-level scaling; using sublaminate-level scaling leads to a partial similitude. There is a physical reason behind these results: with ply level scaling, both in-plane and flexural moduli of the structure are kept, while sublaminate-level scaling changes the flexural stiffness of the laminate.

The distortions introduced with sublaminate scaling can be adjusted, under certain circumstances, by means of a correction factor. In order to derive this factor, Pintado and Morton use dimensional analysis based on bending stiffness. Because the predictions of such stiffness given by the composite laminate theory are inaccurate, it is evaluated with experimental tests. Using such countermeasures against distortions, the predictions provided by similitude theory replicate results already seen [34,88,89]: smaller models exhibit higher energy thresholds and fail at higher loads. In certain cases, the discrepancy in terms of failure scaled load is of 25%.

The source of size effects is not clear to the authors, who propose two possible explanations:

(1) Possibility of finding a critical defect in the material. Because the distribution of defects of any size is uniform in the volume of the structure, the probability of finding a critical defect in larger specimens is higher than in smaller ones.
(2) The size dependence of strength is driven by fracture mechanisms principles. For example, the authors refer to the fracture model of Laws and Dvorak [103] for cross-ply laminates in which the stresses necessary to produce first ply failure depend on the absolute size. Thus, larger specimens are weaker than smaller ones.

However, these explanations turn out to be incomplete. For example, Kellas and Morton [73] demonstrate that the dependence of strength on size can be inverted for certain lay-ups and loading conditions. In fact, even though in-plane moduli are equal for the specimens with both ply- and sublaminate-level scaling, the tensile strength of ply level laminates decreases as the specimen size and thickness increase. For angle-ply laminates, instead, when sublaminate level scaling is used, the tensile strength increases with the size.

Pintado and Morton [102] also emphasize the problem of results interpretability. The outcomes obtained from their tests are not easy to compare in a scaled manner because the use of dimensional analysis does not allow the derivation of a unique set of dimensionless parameters. The approach used by the authors, i.e., bending-stiffness-based dimensional analysis, leads to significant size effects; using, instead, an approach which neglects the lack of similitude in stacking sequence, a limited size effect is noticed.

An application of scaled models to terminal ballistics is discussed in Rosenberg et al. [104]. This investigation is motivated by the previous works focused on geometric scaling issues and nonscaling effects in this field. For example, Sorensen et al. [105] analyze penetration mechanics and potential benefits of high velocity for both monolithic and segmented penetrators. The two-dimensional numerical simulations performed by Anderson et al. [106] aim at demonstrating that the strain-rate sensitivity of the flow stress in the target material can cause some nonscaling effects in the penetration depths of long rods. The differences between a full- and 1/10-scaled model amount to 5%, small enough to be neglected. Magness and Farrand [107] present experimental results showing that, for both tungsten alloy (WA) and depleted uranium penetrators, simple scaling does not exist. Furthermore, penetration capabilities for both materials are significantly improved by increasing the penetrator scale. The primary aim of Magness and Farrand is to demonstrate that such size effect depends on target properties. However, because the comparison of the results between two different targets does not show differences (size effects are the same), the authors are forced to admit that the results do not single out any definite source for the scale dependency of their tests.

Rosenberg et al. [104] share the goals of Magness and Farrand [107] but their assumption is that size effects depend on the properties of the penetrator, not on those of the target. More precisely, the lack of geometric scalability is due to the failure mode: geometric scaling should hold for ductile penetrators, like copper, while semibrittle penetrators, made of WA or depleted uranium, may perform better at full scale because of their different mode of failure. The authors support their idea with some experimental observations. First, while copper penetrators exhibit a perfect scaling of penetration depth, WA penetrators lead to 10% of discrepancy. WA penetrators are more prone to early failure at their interface with the target, while copper, being a very ductile metal, creates a relatively wide crater due to the hydrodynamic nature of its penetration process. Moreover, copper penetrators create totally clean craters, while those generated by WA penetrators are full of debris. These results highlight a totally different mechanism of penetration and erosion which the authors think to be the sources of differences in scaling behavior. There is an analytical support to the authors' assumption, too. In fact, the main cause of such nonscalability is traced to the plastic zone size parameter. Its value is very large for semibrittle materials that, consequently, exhibit different failure mechanisms at different scales. For example, the larger the penetrator, the smaller the plastic zone ahead of cracks, which leads to a more brittle failure.

The application of dimensional analysis to overcome the difficulties due to strain-rate sensitivity is the subject of several works by Alves and Oshiro [108–113]. There, the authors propose a new method to overcome the distortion problems in impacts. The basis of the approach is provided in Ref. [108], which introduces a new dimensional base: from MLT to VSG (initial impact velocity, dynamic yielding stress, and impact mass). Then, and this is the real novelty of the work, the distortion due to rate-sensitivity is compensated for by defining a new model/prototype impact velocity ratio without directly taking into account the constitutive model of the material. The investigated structures are a clamped beam subject to an impulsive velocity and a Calladine model (two plates clamped together) under axial impact. The results show that the technique is robust, it scales different types of structures having different behaviors and undergoing different phases of motion with errors below 1%. A possible source of discrepancy is due to the strain-rate choice: constant through the whole motion for beams, but only during the final phase of motion for plates. This means that it is not possible to correct all the motion stages at the same time.

The apparent success of the method in Ref. [108] led the authors to expand the approach to demonstrate the VSG base versatility and to overcome some experimental constraints. In Ref. [109], they considered a scaling based on the impact mass rather than the initial impact velocity. Very good results are obtained, achieving even effectively zero error. In Ref. [110], the authors successively changed the scale factor for the initial impact velocity in order to take into account the models made of different materials. The reason behind this study is that material properties change when models are very small or very large with respect to the prototype (i.e., size effects can occur, as shown in Refs. [34], [88], and [89] and discussed previously). Because the constitutive curve changes, inaccurate predictions result when inferring prototype behavior from that of a model. The proposed method is able to recover the response of the prototype, made of mild steel, from that of a model made of aluminum, with an error smaller than 3%. The authors, however, underline that the method works under the particular assumption that the wave speed is the same in both prototype and model. If this were not so, there would be changes in the model response when elastic effects are important. In Ref. [110], such effects were ignored.

A common problem for all the previous approaches is the choice of representative strain-rate; typically, an average value was used but it is not always easy to accurately estimate this average. Based on this consideration, the approach was further expanded in Ref. [111] in which the choice of constitutive law changes. Instead of a Cowper–Symonds law, the authors used a Norton–Hoff law. Although they describe the strain-rate of the material in the same way as before, the new law allows an exact scaling without a priori knowledge of the structural response. Using this idea, the already small errors obtained with the previous approach were now totally removed.

Geometric distortion is considered in Ref. [113] in addition to strain-rate effects, in order to address the complexity of manufacturing models whose dimensions are flawlessly scaled. As argued by the authors, the geometric and strain-rate distortions can be dealt with separately. Here, the authors use an exponential scaling law for the geometry, but since the exponent is difficult to determine experimentally, some residual errors appear inevitable.

The VSG-based method is used also in an experimental test on a *T*-cross section beam made of low carbon steel 1006 subject to a quasi-static loading [112]; a comparison with the results obtained with the MLT-based method still demonstrates the robustness and accuracy of the VSG technique.

4.2 Plates. The wide range of practical applications and the extensive literature have made plates one of the most investigated structural elements. Plates are used as upper and lower skins in wing boxes or as spar caps of a wind turbine blade near to its maximum chord; engine blades can be regarded as cantilever plates. Coated plates are used as aircraft panel covered with a damping material that can reduce the flutter caused by airflow [114] and on ocean platforms. They are also used as propeller blades, vibrations adaptors, and to achieve anti-scour performance [115,116].

The works of Simitses and coworkers [1,33,74–77,82–86,117] made a significant contribution to the study of laminated plates in similitude, thanks to the several applications and the fundamental results obtained. The investigations cover a wide range of loading conditions and structural configurations: bending of laminated, cross-ply orthotropic beamplates [1,82,117], buckling and free vibrations of laminated cross-ply orthotropic beamplates [1,77], symmetric laminated angle-ply plates [74–77], delaminated beamplates [83] and sandwich plates [33], flutter of symmetric angle-ply [84], antisymmetric cross-ply [85], and delaminated cross-ply and quasi-isotropic laminated plates [86]. The purpose of these works is to analyze complete similitudes and, above all, to find the scaling conditions leading to the best predictions if partial similitudes are considered. The authors apply STAGE to the solutions of governing equations and boundary conditions.

Consistent with observations in the Secs. 4 and 4.1, the work of Simitses and coworkers shows that in order to obtain a true model, scaling of a composite material must satisfy at least two conditions, namely the conservation of both stacking sequence and material properties. Such conditions are satisfied, respectively, by applying ply level scaling and designing the model with the same material of the prototype. For certain applications, additional conditions apply; for example, mode shapes must be retained for cross-ply [77,85] and delaminated [83] laminates.

When partial similitudes are considered, it is not feasible to deduce a general behavior because each system, with its own geometry, loading, and boundary conditions, is sensitive in its own way to a particular set of design parameters. This obligates the analyzer to investigate each system separately. However, some commonalities can be identified. In Refs. [1], [82], and [117], it is shown that a distortion in the number of plies still leads to good predictions of maximum deflection and stress provided that the right scaling law is chosen. Experimental validations are obtained in Ref. [117], which also show that STAGE fails in predicting any type of damage.

The estimation of buckling load is very sensitive to the number of plies (thus, the thickness) and aspect ratio [1,74–76]. It is still possible to obtain good predictions by changing the number of plies of the model along as this is not too low [1] or by modulating the aspect ratio [74–76].

Distortions in material properties make more difficult achieving good matches with the prototype behavior. Depending on the chosen scaling law, discrepancies vary between 5% and 30% if the model is made of isotropic material (like metal and plastic) and between 15% and 20% if it is made of fiber-reinforced material [1]. If the stacking sequence and the number of plies are conserved, choosing a proper fiber-reinforced material for the model allows a good prediction of the buckling load without modulating the aspect ratio. When the prototype material is a Kevlar/epoxy composite, for example, good accuracy is achieved when the model is made of boron/epoxies, boron/polymider, and most of the graphite/epoxies materials. On the contrary, glass/epoxy is not a good choice. When the model material is isotropic, it is still possible to accurately predict the buckling load by modulating the aspect ratio [74–76].

When determining the flutter speed in aerodynamic applications, distortions in thickness, fiber orientation, and aspect ratio still allow good predictions. In contrast, increasing the Mach number increases the discrepancies. A possible explanation may not be related to scaling but to the aerodynamic theory used. In fact, in Refs. [84] and [85], the authors apply the quasi-steady aerodynamic theory valid for $M < \sqrt{5}$, thus a loss of accuracy at higher Mach numbers is expected.

Complete similitude for delaminated plates is achievable by fulfilling two new conditions: the conservation of the buckling modes (local for both thin and large delaminations) and of the delamination position. When the delamination length is too low or the delamination position is too close to the plate midplane, there is a loss of accuracy because the modes are no more local but global or mixed, thus the conservation of modes is no more observed [83,86].

Until now, STAGE has been applied to the solutions of the governing equations. In similar investigations [50,118–122], STAGE is applied no more to the solutions but directly to the governing equations. In this way, the scaling conditions and laws are more general because they do not depend on the boundary conditions. These investigations can be seen as a natural continuation of the previous works of Simitses, Rezaeepazhand, and their collaborators [1,33,74–77,82–86,117].

Several test articles and loading are considered: buckling of symmetric cross-ply [50], antisymmetric cross- and angle-ply laminated plates [119] subject to biaxial loading, symmetric plates under normal in-plane loading [120], polar orthotropic clamped annular plate under compression and torsional load, and free vibrations of antisymmetric cross- and angle-ply laminated plates [118].

The results of the listed works confirm many of the results already seen, e.g., that ply level scaling is necessary for complete similitude. Physically, this means that the flexural stiffness of the structure must be retained when scaling plates. By limiting the distortions of flexural stiffness, good results can be obtained. This is why, by changing the model material from Kevlar/epoxy to E-glass/epoxy, prediction accuracy decreases, while the discrepancies are very low when switching from a stainless steel material to aluminum, because their flexural stiffnesses are very close [76,121]. This justification is further confirmed when distortions in extensional, bending, and bending-extension stiffnesses are considered: the discrepancies are always higher when the flexural stiffness is changed [118].

In Ref. [122], experimental tests are performed on vibrating thin plates. This paper underlines, as already seen in Refs. [34] and [96], the difficulties of experimental testing. The results of the tests made on plates with different boundary conditions highlight inconsistencies between the theoretical and the experimental predictions. However, such outcomes are, likely, related to imperfections in reproducing the boundary conditions. In fact, analyses on free plates exhibit good theoretical/experimental matches.

4.2.1 Frequency Response. The advantages of ASMA are illustrated in two works. In the first work, De Rosa et al. [54] analyzed a two plates assembly joined at right angle by means of ASMA, no more justified with SEA but with EDA. The experiments were conducted by exciting one plate and acquiring the response on the other. ASMA always predicts well the response of the excited system because it is dominated by the input power, well represented by the scaling procedure. Instead, the predictions of the receiving system exhibit some approximations but the response is still acceptable. ASMA is successively applied to study the dynamic behavior of plates [57,123], two-plates [57,95], and three-plates [95,124] assemblies.

In Ref. [125], a panel excited by turbulent boundary layer (TBL) is investigated. Typically, to well estimate the dynamic response above the structural/aerodynamic coincidence frequency, the structure and the fluid should be discretized with meshes of different scales, then these meshes should be linked with an interpolation matrix. This procedure is time expensive. By using ASMA, a mesh with a scaled size can be used for both structural and aerodynamic operators, recovering the global response with an acceptable approximation. The local response, of course, is not well reproduced. A direct comparison with finite element method results show how finite element (FE) analysis diverges above the coincidence region due to the spatial aliasing of the TBL correlation lengths, while ASMA remains accurate since the minimum scaled flexural wavelength is still smaller than TBL correlation length.

Li provides two extensions of the ASMA method [126,127]. In Ref. [126], the scaling laws are determined by using random process theory with the Gaussian orthogonal ensemble assumption. A plate under harmonic excitation is analyzed and the method allows a good estimation of ensemble statistics (mean and variance) of the mean squared velocities of a model which retains the ensemble size of the original system. In Ref. [127], SEA is combined with Skudrzyk's mean-value theorem to derive, first, a general scaling law, then specific laws for a flexural plate. A control factor, representative of the modal density scaling, is introduced to simulate high-frequency dynamics with coarse finite element models. The results show that both local and global responses are accurately estimated when the control factor is closer to one, which means that the modal density of the model is closer to the modal density of the prototype. Although the method has been developed for global responses, it works well for local responses, too.

Similitude and asymptotic models for structural-acoustic research applications were applied for the first time by De Rosa et al. [58] to investigate the response of an elastic homogeneous plate in contact with an acoustic cavity. For the sake of simplicity, the global modes are represented by the uncoupled structural and acoustic modal bases. However, the system under analysis is still a coupled one. In order to keep the relative distribution of natural frequencies, the ratio structural to acoustic frequencies must not change. This assumption leads to the important condition that plate thickness and area must not change. A complete similitude is investigated. After the remodulation process, this allows a perfect reconstruction of the prototype behavior.

In Ref. [59], both replica and proportional sides models allow a good reconstruction of the dynamic response. Thus, to accurately predict the prototype behavior, there is no need to scale all the structural dimensions (i.e., to perform a complete geometrical scaling). It is simply necessary to satisfy the similitude conditions. Avatars are analyzed for the first time in this paper. The tests prove that the response estimation is acceptable until the distortion is limited. Furthermore, the authors introduce the modal density as similitude index. The comparisons among avatars seem promising because the degree of distortion increases with the value of modal density. However, it turns out that the replica and the proportional sides model, similar among them, differ significantly in density (0.33 and 8.0, respectively). Thus, the modal density is not a good measure of similitude degree.

New insights into model behavior are obtained in the application of SAMSARA to cantilever plates in Meriuane et al. [128]. Numerical/experimental comparisons exhibit good matches also when avatars are used. In all cases, however, inconsistencies occur in the high frequency range. It is found that the source of such decorrelations is the damping. In fact, the numerical models assume a constant damping for the prototype and all the models. Comparing the experimental results with those obtained with numerical simulations at different values of damping ratios, it is shown that the prototype response is closer to the numerical results obtained with lower damping ratio, while the model response is closer to the numerical results obtained with higher damping ratio. Thus, the assumption that the damping is constant among models is not fulfilled. An augmented loss at the constraints may be the source of such behavior.

While complete similitudes allow a perfect reconstruction of prototype behavior, Meruane et al. [128] show that avatars also allow acceptable predictions of structural response from experimental data. However, in all the cases, there are significant discrepancies at high frequencies. These errors are due to the article sizes. In fact, the response of the scaled-up models scales well in all the frequency range, while this is not true for the scaled-down models, for which the response scales well only at low frequencies. The reason is the modal density, i.e., the number of modes in a certain frequency range. The prototype and the models are analyzed in the same frequency range; thus, the scaled-up model has a sufficient number of poles (modes) in such a range to suitably reconstruct the prototype response. The scaled-down model is characterized, instead, by a smaller number of poles, moved to higher frequencies and insufficient in number in the considered experimental frequency range. This result is in line with the results of Li [127] and underlines the importance of keeping the modal density as unchanged as possible.

In Refs. [59] and [128], the role of the modal density in the similitude is highlighted. In fact, in Ref. [59], it is concluded that the modal density does not allow an acceptable interpretation of replica and proportional sides, thus the applicability of modal density as a similarity index cannot be generalized to all the types of similitude. In contrast, in Ref. [128], it is remarked that modal density must be kept in order to reconstruct the prototype response. This seems contradictory, because the values of modal density for replica and proportional sides are different, but both of them perfectly predict the full-scale structure behavior. A further apparent contradiction arises from the observation that, by definition, the replica model can act as a prototype for the proportional sides model. Actually, both the conclusions are true and in accordance between them. The modal density represents the number of resonating modes in a given frequency range (that can be changed according to the model considered), thus it is a quantitative information. Two models of the same prototype may have the same modal density, i.e., the same number of modes in a certain frequency range, but one may be a replica, the other an avatar. In fact, distortions can change the succession of modes, that is a qualitative information, and the response is no longer reconstructed although the modal density is the same. The quantitative condition allows the redistribution of the energy in the right number of poles, while the qualitative condition ensures that the succession of such poles is kept.

Similitude and asymptotic models for structural-acoustic research applications has been used to evaluate not only the dynamic response, but also the radiated acoustic power [129] of a plate. In this case, the introduction of the radiation function entails the definition of a new scaling condition for the frequency. The experimental results prove that both the response and the acoustic power can be predicted by an avatar only beyond a certain frequency value.

Xiaojian et al. [130] study the dynamic response of a plate subjected to TBL. While ASMA and SAMSARA scaled only the structural properties, here the aerodynamic and material properties are also considered. Furthermore, a method to determine the frequency offset between low and high frequency region is provided. The scale derivation of scaling conditions is very similar to SAMSARA. Numerical and experimental predictions prove to be good, although some slight discrepancies between them. It is not known if such errors are due to the approximated experimental fixing conditions or to the thickness effect that strongly affects the vibration response.

An innovative approach in dealing with partial similitudes was proposed by Luo et al. [131]. In this work, the authors first apply STAGE to derive the scale factors, then evaluate the applicable structure size interval to determine accurate distorted scaling laws. The procedure consists in fixing the discrepancy value that must be returned by the partial similitudes, designed by changing the structural parameters. The method is applied to simply supported plates numerically [131] and experimentally [132], and to coated thin plates in Ref. [133]. Sensitivity analysis is then introduced to support STAGE in Ref. [133] to determine accurate distorted scaling laws. The operating principles are summarized in four points (listed in Sec. 3.6) relating the design scale factors to the sensitivities of the system. The method is used to investigate thin walled plates [133] and annular thin plates [62].

Sensitivity analysis does not just support already existing similitude methods [62,133], but can also be used to find scaling laws independently. This is the approach used by Adams et al. [63], who use GSA to derive sensitivity-based scaling laws. GSA considers the design parameter space as a whole and allows to evaluate the effect of each parameter as well as their interactions. In Ref. [63], the test article is a simply supported aluminum plate and both natural frequencies and mean squared transfer admittance (MSTA) are the response parameters observed. To derive the sensitivity-based scaling laws, design of experiment is first used to determine the effects of the design parameters, successively with multiple quadratic regression. Thus, an implicit assumption is made: that both natural frequencies and MSTA are modeled quadratically. When considering a complete geometrical scaling, the SA approach returns satisfactory agreements, while changing the thickness leads to significant error in the MSTA prediction, ranging from 21% to 85%. This means that a second-order model is no more sufficient; in fact, a fourth order model would be more suitable.

In Adams et al. [64], LSA is applied to similitude theory. This method relies on differentiating the system under investigation at a particular point in the parameter space by performing a first-order sensitivity analysis. This procedure leads to the definition of power-law sensitivity-based scaling laws. In this work, three cases are presented: an analytical study of a simply supported plate described by Kirchhoff theory, a numerical, finite element analysis of the same test article described with Mindlin–Reissner theory, and the investigation of a generic car undercarriage. The second case is the most interesting, because it highlights the pitfalls of sensitivity-based scaling laws, namely their mathematical origin. In fact, while similitude-based laws are based on the physical properties of the phenomenon under analysis, sensitivity-based scaling laws are instead obtained by means of a mathematical procedure, which lacks any link to the physical behavior of the system. For this reason, when analyzing the Mindlin–Reissner plate, SA tends to overestimate both natural frequencies and MSTA, because it does not take into account the influence of thickness. At high frequency, the mode shapes also change.

An interesting variation of STAGE method is proposed by Coutinho et al. [48]. The authors introduce a modular approach to STAGE that would lead to scaling relationships as general and structured as possible because of their organization into modules. These modules are derived by applying STAGE to the most basic equations: the governing equations derived from elasticity theory, force and moments resultants written as integrals of stress fields, stress–strain and strain–displacements relations, and displacement field. In this way, it is possible to obtain flexible groups of scaling laws that can be efficiently re-used in a multilevel methodology. Using basic, general equations, no simplifying assumption is made, thus the scaling relationships obtained are as general as possible and applicable also to complex systems that lack of governing equations. The approach is a big step forward in similitude methods, because all the previous methods considered just specific cases and the similitude conditions were derived for each one of them, with great effort of the analyzer. Instead, the method proposed by Coutinho et al. derives the modular scaling laws just once and shows how they can be assembled to solve more complex problems (e.g., acoustic and thermal). The modular approach is applied to analyze a stiffened aluminum plate with pinned edges and the predictions provided are very good.

4.2.2 Impact Response. When dimensional analysis is used, the simplest scaling procedure is the geometrical one. However, geometric scaling along is not always sufficient to describe the response to a loading condition; for example, it is not sufficient to accurately scale impact phenomena. In fact, impact may produce fracture and effects on strain rate that do not scale with geometry. The limits of geometrical scaling with dimensional analysis are highlighted by a series of works aimed to study the impact response of plates [134–138].

Nettles et al. [134] execute an experimental campaign of tests on composite plates subject to a transverse load. The results confirm some behaviors already encountered in the previous works [34,88,89], e.g., the increased scaled load of small models with respect to the prototype. Others highlight new phenomena. For example, the dents due to impacts do not scale well and the scaled delamination area of the models is always smaller than that of the prototype (passing from 32 to 16 plies, there is a change of 71%). Furthermore, a longer matrix splitting induces a change into the delamination shape when the number of stacks increases (the shape changes from circular to a more elongated shape).

The effects of delamination and fiber failures are described by Ambur et al. [135], which execute impact experimental tests on six flat and curved composite panels, with two geometrically scaled sizes. The tests show significant size effects. The results suggest that the impact energy absorption appears to depend on the approach used to scale the laminate. In fact, flat panels, subjected to low damage impacts and scaled with the ply level procedure, are less resistant than the sublaminate-level scaled panels. Instead, when subjected to high damage impacts, the ply level scaled panels are more damage resistant than the sublaminate-level scaled ones (which absorb more energy through local fiber failure). When the panels are curved, sublaminate-level scaling induces less damage resistance than ply level scaling. Furthermore, damage mode and extent are influenced and, as expected, scaled-up models exhibit more damage with respect to the prototype.

Sutherland and Guedes Soares [136] investigate an orthotropic plate made of a marine composite material and struck by a mass. Buckingham's Π theorem is used to derive the similitude conditions. The derived geometrical scaling laws work only in the elastic range. In fact, deviations are observed due to size effects: in larger specimens, the fiber failure occurs at relatively lower load and displacements (as already seen in Refs. [134] and [135]); the effects of stiffening are limited for larger plates. When the specimens have thinner woven ravings, higher strain-rate results.

The limits of geometrical scaling and the general smaller resistance to damage of large test articles are underlined also by Viot et al. [137] and Xu et al. [138].

Shokrieh and Askari [139] propose the *sequential* similitude method, introduced to scale buckling problems of structures previously impacted. Because of this impact, the test article is already damaged before the buckling load. The main principle of sequential similitude is to define the scaling laws in two consecutive steps:

(1) Step one: The similitude method is first applied in the case of impact loading to produce similar damaged areas in all the plates.
(2) Step two: The similitude is developed between plates under buckling loading without considering the effect of initial damages on buckling equations. The damaged plates are introduced in the buckling problem by setting the initial condition of the structure to the ultimate situation of the corresponding impacted plate.

Similitude theory applied to governing equations is the similitude method used in the abovementioned steps and the structures investigated are three carbon/epoxy composite plates. The predictions from models are accurate even for impacts in the inelastic region: all the plates have damaged regions and the damage patterns are similar. The buckling loads and the mode shapes are predicted with small errors.

Some studies [140–144] focus on the scaling of blasts that can be regarded as a particular type of impact problem. The blast is a destructive wave of highly compressed air, typically produced by an explosion. Blasts are characterized by high accelerations, which allow to neglect other types of accelerations, for example, that of gravity. The latter assumption simplifies the derivation of scaling laws, since gravitational acceleration is one of the phenomena that are not geometrically scalable. However, a structure undergoing blasts also exhibits other types of nongeometrically scalable phenomena, like fracture failure and rate-sensitivity.

Neuberger et al. apply dimensional analysis in order to investigate the response of plates subjected to explosions in free air [141], due to buried charges [142] and the springback of a circular plate under TNT blast [143]. The blasts are scaled with the Hopkinson method, also known as "cube root" method [24]. This is based on the assumption that self-similar blast waves are produced at identical scaled distances when two explosive charges of similar geometries and explosive, but different weight, are detonated in the same atmosphere. Thus, a scaled distance, a characteristic time of the blast, and an impulse are introduced.

In Ref. [141], a circular plate is subject to close-range large blasts. The models are geometrically scaled. The normalized midpoint deflections and stresses scale well as a function of scaled time when using both a rate-insensitive bilinear and a rate-sensitive material model. To emulate possible manufacturing problems, changes in material properties due to changes in material thickness are introduced. In this case, there is a certain discrepancy in the predictions of both midpoint deflection and stresses, reaching values of 7% for the peak values. The matches between experimental and numerical tests prove that a nonlinear phenomenon such as plasticity scales well. The result should not be surprising, because, as already reviewed in Rosenberg et al. [104], geometric scaling holds for ductile penetrators and any deviation from this scaling should be attributed to the failure mechanism at the penetrator's head, not to the target properties as suggested by Magness and Farrand [107].

In the second part of their investigation [142], Neuberger et al. investigate the case in which a clamped circular plate is subject to blasts due to large buried spherical charges. Also in this study, changes in thickness lead to discrepancies in the numerical results. Moreover, the experimental/numerical comparisons show slight disagreements when the scaled distance decreases; the source may be the change of material properties because of thickness variation. These works prove that the problem of determining the dynamic response of a structure subject to blasts is well scaled.

Noam et al. [144] highlight, however, that the method used by Neuberger et al. [141–143] works just for the structural response without addressing potential fracture failure. Furthermore, Jones [145] states that it is not possible to scale failure in blast loaded structures when using fracture-mechanics based (fracture toughness) considerations. Thus, Noam et al. [144] aim to provide an alternative approach based on two scalable competitive fracture failure criteria so that the blast scaling approach can be fully treated. Their similitude method is based on the dimensional analysis and it is coupled with the following failure criteria:

(1) Strain energy density criterion: This describes adiabatic shear and is derived from the considerations of Rittel et al. [146], according to which the dynamic failure energy can be viewed as a failure criterion when adiabatic shear is considered (adiabatic shear banding failure, or ASB failure).
(2) Maximum principal stress criterion: This is introduced because the authors do not know if the blasts induce ASB failure. The criterion states that failure occurs when a maximum principal stress, developed in an element, is greater than the ultimate tensile stress of the material. It is a typical brittle fracture criterion, but the authors are not interested in describing the differences of various types of fracture (cf., Rosenberg et al. [104]), they just want to represent the fragmentation, i.e., the creation of new surfaces.

Both criteria undergo complete scaling under the condition of rate-insensitive material. This is proved by numerical results of air plates under air blasts due to spherical charge. For fine and medium meshes, the normalized dimensions of the cracks and the von Mises stresses are comparable; some slight differences appear but they are negligible. Because the fracture is triggered when the maximum stress criterion is satisfied, it is possible to consider it as a good alternative to fracture-mechanics based criteria when the problem has to be scaled.

The extensive experimental campaign by Jacob et al. [140] is worthy of mention. There, quadrangular plates are subjected to impacts and both charge (diameter and height) and plate (thickness and aspect ratio) geometries are changed. Different combinations of charge and plate properties return a multitude of responses and interactions. To simplify such complexity, the authors introduce a parameter for localized loading of quadrangular plates. In fact, by reviewing many previous works on the topic [65,97,98,145,147–149], it is noticed that such parameter was not introduced yet. It is a modification of a dimensionless parameter previously introduced by Nurick and Martin [149] and it is useful to evaluate the midpoint deflection for many loading conditions and plate geometries. Its introduction allows a good estimation of such deflection, also confirmed by numerical and experimental tests.

4.3 Cylinders. Cylinders are another type of widely used structural element widely used. They are useful to model tubes, aeronautical structures like fuselages (especially when the cylinder is stiffened), or other types as containers and tanks. They are also used as casks for the storage, transportation, or final disposal of irradiated nuclear reactor fuel [36], gasholder barrels [150], and riser tube for fluid in drilling operations [151,152].

4.3.1 Buckling and Frequency Response. As was done for composite plates, STAGE is applied to composite cylinders in Refs. [78–81,87], and [153–155]. The conditions for complete similitude are those already obtained for plates, plus the conservation of the curvature parameter (squared length over the product between thickness and radius). Thus, a great sensitivity is expected when varying the length, the radius or the thickness of the cylinder. Of course, complete similitude allows for perfect reconstruction of the prototype behavior.

Rezaeepazhand et al. investigate the predictive capabilities of STAGE in free vibration problems of symmetric cross-ply laminated cylindrical shells with single [78] and double [81] curvature. It is possible to introduce distortions in the stacking sequence only if the number of plies of the cylinder is an odd number; the accuracy improves by increasing the number of plies of the prototype. When the length or the radius changes, the nondimensional frequency is still predictable with sufficient accuracy only if the mode shapes are retained. In contrast, a distortion in length returns errors up to 20% when flutter boundaries are investigated [87]. The response is more sensitive to variations in radius than in length [78]; the Gaussian curvature also affects considerably the estimations [81]. It should be underlined that retaining a mode shape is a simple matter only from the theoretical point of view, because it is enough to impose and respect the similitude condition. The condition fulfillment in an experimental test is not so easy to achieve.

The investigation by Rezaeepazhand et al. also seeks to determine the buckling load of cross-ply laminated cylindrical shell under axial compression [79] and lateral [81] loading. Again, distortions in stacking sequence still allow good predictions of the buckling load, while the sensitivity to variations in radius leads to high discrepancies, even if the distortions are small. Instead, changing the length returns good results, even if the mode shapes are not retained. In Ref. [80], it is noted that more accurate predictions result from an increase in length than from a decrease; yet, when the length reaches very low values, even if the mode shapes change, the buckling load is well estimated.

A variation on STAGE is proposed by Tabiei et al. [156]. This work can be regarded as a continuation of the investigation made in Ref. [81] on the buckling behavior of cross-ply laminated cylindrical shells under lateral pressure. The proposed variation consists in a curve fitting technique involving scale factors as a function of other scale factors. The considered factors do not need to be derived from equations, it is enough to consider those that bring to the sought distorted model. With respect to the classical scaling laws, the fitted model captures higher-order terms that reduce the inaccuracies.

Ungbhakorn et al. investigated the buckling and free vibrations of antisymmetric angle-ply [153], symmetric cross-ply [154], and antisymmetric cross-ply [155] laminated circular cylindrical shells. Their results show that neglecting the bending-extension coupling effects leads to small errors, typically smaller than 1%, while neglecting the extensional and flexural effects leads to higher errors, from 33% for the buckling load up to 100% and 200% for the natural frequencies.

From these works, it is possible to infer some information that confirm the results already obtained by scaling composite plates. The distortions in stacking sequence are the only one allowed. It is not necessary to fulfill the conditions related to the coupled extensional-bending stiffness, while it is important to fulfill those related to the flexural stiffness. This means that the response of the system is sensitive to changes in the number of plies, i.e., thickness. However, the varying sensitivity with, for example, length in different systems proves that it is not easy to deduce a general behavior.

Yu and Li [150] analyzed prestressed, stiffened cylindrical panels and shells using an approach similar to the energy-based method described in Ref. [53]. Specifically, the authors relate the total energy of prototype and model by means of a functional relationship between transformation parameters. When the similitude is complete, buckling loads are perfectly predicted and are unaffected by changes in aspect ratio and curvature; the natural frequencies and modes are also accurately predicted as long as the wavenumbers are retained. Changing the stiffener material leads to design equivalent stiffeners that support a very good prediction of both buckling load and natural frequencies. The error is smaller than 3%. Changes in material are acceptable as long as Poisson's ratio does not vary excessively: if the model deviates too much from the prototype, the discrepancies become significant.

Similitude and asymptotic models for structural-acoustic research applications are applied to investigate an infinite cylinder filled with air in Ref. [58]. According to the scaling laws, variations of thickness and the area of the cylinder lead to a modification of both structural and acoustic natural frequencies distributions; thus, for these acoustic-elastic systems, the structural and acoustic poles scale with different laws. Damping must be kept if a complete similitude is desired; by changing it, only the mean response can be replicated. The similitude conditions are violated on purpose in Ref. [157] so that avatars of thin aluminum cylindrical shells can be investigated. According to the scaling laws, length, radius, and thickness should vary in the same way. In this work, instead, length and radius vary according to scaling laws different from that of the thickness. Such a choice seems to affect only the first axial-radial modes. However, the distortions alter not only the natural frequencies but also their distribution, so a partial reconstruction of the response is feasible only in particular frequency ranges. As also proved in Ref. [158], the smaller the distortion, the higher the prediction accuracy.

In Ref. [158], orthogonally stiffened cylinders are also investigated. The adopted structural model is the smeared stiffness approach, i.e., the rigidity properties of the stiffeners are spread along an equivalent continuous cylinder, with the same geometrical properties as the prototype. The stiffeners decrease the modal density. Thus, for the same reason previously illustrated in Ref. [128], there is an improvement in the agreement between prototype and avatar. The number and the area of the stiffeners are also changed, which lead to good local results when the modal overlap factor is low, and good results only in the average sense when the modal overlap factor is high.

In Petrone et al. [60], the authors perform a numerical analysis of longitudinally and orthogonally stiffened cylinders using SAMSARA. The results for replicas and avatars follow those of the previous works [58,157,158], but in this work it is proposed to use several scaling laws to describe the behavior of avatars. Thus, two different frequency scaling laws are derived *a posteriori* and are used to define the frequency ranges of validity of the laws. The results exhibit an error lower than the case in which just one scaling law is used. The identification of a confidence band shows that the low frequency range dictates the confidence interval, because the greater errors (maximum 35%) are placed in the low frequency range. Thus, it is hard to reconstruct the local response.

Orthogonally stiffened cylinders are also investigated by Torkamani et al. [51,159], who apply STAGE to the nondimensional solutions of the governing equations. The stiffened structure is replaced by a smeared one also in this work. Thus, until the wavelength is greater than the distance between stiffeners, accurate predictions can be obtained.

Scaling of stiffened cylinders is not a trivial matter because manufacturing constraints may limit the production of stiffening elements or shell thicknesses that fulfill the scaling conditions. Torkamani et al. propose some approaches to bypass the problem. Equivalent stiffeners can be designed so that the same mode shapes are kept. Only the cross section is changed; shell material and geometry, stiffener material and distribution, boundary conditions and loading are kept. The conditions show that the equivalent stiffener is obtained by conserving the cross-sectional area, the moment of inertia, the polar moment of inertia, and the eccentricity. The simpler equivalent stiffener has a T-shaped cross section. To circumvent the thickness limitations, both shell and stiffeners can be designed with different materials having better formability. The thickness of the stiffeners can also be changed without varying the cross section shape. Another approach to scaling the thickness is to modify the number of stiffeners. However, since smearing theory is used, lowering the number of stiffeners too much leads to inaccurate predictions. To verify the numerical predictions, an experimental test was performed by Torkamani et al. The prototype is made of aluminum and presents Z-shaped ribs and Ω-shaped stringers; a one-third model is made of steel alloy and has equivalent T-shaped ribs and stringers. The cylinders are free on both the edges. The predictions are very good: the response peaks coincide although some small errors were attributed to the nonlinearities of the model.

4.3.2 Impact Response. Until now, test articles made of isotropic and composite materials have been reviewed. The analysis of Sato et al. [36] involves concrete cylinders, so it provides an interesting insight into the behavior of material not commonly tested. Experimental tests on four thick-walled concrete cylinders with circumferential and tie reinforcements made of steel were performed. The aim was to investigate the damage modes and extent generated by impacts on three scaled-down models. These are expected to be the same for the prototype and models. Indeed, the damage modes are similar, as the models exhibit the formation of a shear plug at the impact point, crushing of the concrete of the inner surface, flexural cracking of the outer surface, and cracking of both surfaces. In contrast, the damage extent differs between the models and the prototype. The main results can be summarized as follows:

(1) The end cover spalling decreases when the model size decreases. The source of this phenomenon has found difficulties in modeling the micro-aspects of concrete that governs fracture toughness; very high strain-rate is observed in the smaller models resulting in high tensile strength and lower-than-expected deceleration forces in smaller models.
(2) Smaller models exhibit a reduced extent of concrete crushing damage, because strain rate increases the concrete compressive strength and, maybe, also enhances the properties of the steel reinforcements.
(3) Deceleration peak and strain rate are consistent with the scaling laws.
(4) The increase of compressive strength in models leads to underpredicted footprint widths; cracks are sometimes overpredicted, sometimes underpredicted. Although these slight differences, the predictions are good.
(5) Outside cracking spacing is overpredicted, while the inside spacing is underpredicted.

Therefore, the models are more severely cracked. The results exhibit different behaviors: crack data, generally, agrees with the scaling laws but is susceptible to impact randomness of concrete scaling. Because of such randomness, the study of scaled models should involve more specimens so that a good statistical response can be obtained.

Size effect in cylinders are also experimentally investigated by Jiang et al. [160]. The authors perform quasi-static compression and impact tests on thin walled mild steel circular tubes that are geometrically scaled, but without scaling impact velocities and mass. Strain rate affects both quasi-static and impact tests and its influence is stronger in the smaller models. Other experimental tests were conducted by Tarfaoui et al. [161]. These tests focused on low velocity impact to simulate the dynamics of underwater impacts. In this case, the observed damage consists in local crushing of the resin at the point of contact with the projectile, without fiber failure. The scaling laws, obtained with dimensional analysis, can predict the dynamic response but underestimate the error. Larger tubes are more damaged.

4.4 Summary of Similitude Theory Applications. The reviewed articles demonstrate the wide applicability of similitude theory. Many engineering fields, loading conditions, and materials are involved.

Dimensional analysis has proven to be the most suitable similitude method to scale impact problems. In fact, geometrical scaling allows good predictions of the prototype behavior until the plastic threshold, and even beyond if the damages are not too accentuated and the material has a limited rate-sensitivity. However, when failure occurs and damages and rate-sensitivity are not negligible, such scaling fails in predicting the prototype response. For these cases, DA exhibits a strong versatility; for example, the VSG-based method [108] and other applications [97,100] prove that, with a suitable choice of the dimensional parameters that constitute the dimensionless groups, some limits of geometrical scaling can be circumvented. This again underlines the need for an experienced analyzer of the subject under examination. The knowledge of the theory underlying the phenomenon is also important for distinguishing inaccuracies due to the limits of such a theory from those of the adopted similitude method. The works [84,85] are a perfect example, as the discrepancies in the predictions of prototype behavior may come from the application of quasi-steady aerodynamic theory outside its validity boundaries.

As demonstrated in the literature, however similitude methods do not allow one to bypass all of these limits at the same time. In fact, on the one hand, the work by Neuberger et al. [141,142] scales plasticity accurately when not considering fracture. On the other hand, Noam et al. [144] are able to scale fracture in terms of failure criteria that scale well only under the assumption of rate-insensitive material. Furthermore, the fact that dimensional analysis does not provide a unique set of nondimensional parameters leads to interpretability problems, as Pintado and Morton [102] highlight. Thus, the versatility of DA is not always an advantage.

Similitude theory applied to governing equations is less versatile than DA, but the scaling laws have more physical meaning because they derive from the governing equations. However, it is necessary to point out some inconveniences when STAGE is used. First, prototype static and dynamic behavior may often be predicted by means of partial similitude in an acceptable way when an accurate set of governing equations is provided. However, since a certain scale factor may take different alternative forms, when partial similitudes are considered, it is a good practice to investigate all of them, because while some may give good predictions, others may not. For example, the laws obtained in Ref. [92] of the transverse deflection of a beam have two forms, one of which underpredicts the prototype behavior, while the other overpredicts it. Typically, the chosen equation is valid in a limited range of values of the design parameters. This consideration highlights the usefulness of the applicable size interval determination [131–133].

Similitude theory applied to governing equations and SAMSARA share a common point in such limited validity of the scaling laws. While the conditions found with STAGE are valid in intervals of the design parameters, the conditions provided by SAMSARA are valid in frequency intervals. Indeed, it has also been demonstrated that different laws allow good estimation of the dynamic response in particular frequency ranges [60].

Whereas DA has proven to be versatile, STAGE has been shown to support some interesting variations, such as the modular approach [48], the determination of size applicable intervals [131–133], and the support of sensitivity analysis [62,133].

Until now, the aim of similitude methods has been the reconstruction of the response characteristics in order to save costs and time in the experimental procedures. It is interesting to note that ASMA introduces a new point of view, namely to use a scaled-down model to save computational time in numerical simulations in those frequency ranges that make finite element method unusable. The method cannot substitute SEA, whose prediction capabilities are better, but it is useful for those cases in which analytical solutions are not available and FE models still represent the best tools. ASMA has also proven to be an efficient method to fulfill the meshing requirements in fluid-structure interaction problems thereby avoiding a prohibitive computational time [125].

Sensitivity analysis has shown to be an approach that can support already existing methods like STAGE [62,133] or derive sensitivity-based scaling laws [63,64] independently from the classical similitude procedures. The global approach is useful to obtain the effects of the parameters and their combinations on the structural response, even for complex systems. LSA represents a first order derivative, which means that the system is linearized in the vicinity of the current design point. A certain accuracy is thus expected in a limited range, typically $\pm 5\%$. Similitude-based laws allow, instead, an application in a wider range; assuming a complete similitude, the range over which the field equations are valid.

Suitable sensitivity-based laws can always provide fitting prediction but their origin is mathematical, so they totally lose sight of the physical aspects of the problem. However, the method proposed by Adams et al. [63,64] is a step forward in the automation of the scaling procedure. Comparing the similitude-based laws with those sensitivity-based, it is possible to conclude that each method has its own advantages and disadvantages so that they are balanced.

A common problem of many similitude methods is the inability to predict size effects, i.e., the change of strength properties of specimens when their size changes. Usually, the smaller the structure, the more resistant it is, but this is not a general rule; the results in Refs. [36] and [73] are evidence of an exception. Something similar happens in frequency and is highlighted, for example, in Refs. [127] and [128]. The size decrease of the model moves the modes to higher frequencies, so analyzing their structural response in the same frequency range of the prototype would lead to inaccurate predictions. The reason lies in the modal density: it must be retained as much as possible in order to reconstruct an acceptable response.

Size effects are not predictable with similitude methods but they can be observed by means of experimental procedures. The matter is not so simple, because an improper setup may pollute the results [34] to the point that it is not possible to distinguish if the error originates from an improper experimental procedure or a physical phenomenon not taken into account by the scaling laws [130]. Experimental tests also are useful to investigate the validity of theoretical assumptions, as in Ref. [128], where the constant damping assumption among models is shown to not be exactly fulfilled.

In conclusion, all the listed applications of similitude methods have dealt with partial similitudes. All the authors, in fact, unanimously agree that complete similitude at some point becomes unfeasible from the manufacturing point of view. As long as the distortion is limited, that is an acceptable, or even mandatory, assumption in the manufacturing error framework, since the predictions have an acceptable accuracy. Nevertheless, the study of partial similitudes is still important.

5 Complex Structures and Other Fields of Application

The Secs. 3 and 4 have concerned the definition of similitude methods and their application to simple structures such as beams, plates, and cylinders. Their accuracy and limits, especially when phenomena like size effects or distortions are considered, were studied and analyzed.

Similitude theory has also been applied to study more complex structures, often made of several subcomponents, such as satellites, launch vehicles, spacecraft, aircraft, ships, and buildings. This section has a double purpose: to review the main applications in industrial engineering and, by doing so, to demonstrate the actual usefulness of similitude theory. The section is divided into the following subsections:

(1) *Aerospace engineering*: Investigations on static and dynamic behavior of structures such as spacecraft, aircraft, satellites, and their components. Beyond some typical applications of similitude theory, two branches stand out for their peculiar characteristics: aeroelastic and thermal similitudes, treated in two distinct subsections.
(2) *Civil engineering*: Applications to investigate the dynamic response of buildings and physical infrastructure, especially when subject to seismic phenomena.
(3) *Impact engineering*: Investigations of short-lasting events caused by collision between two bodies, characterized by rapid induced motion and deformation, release of high

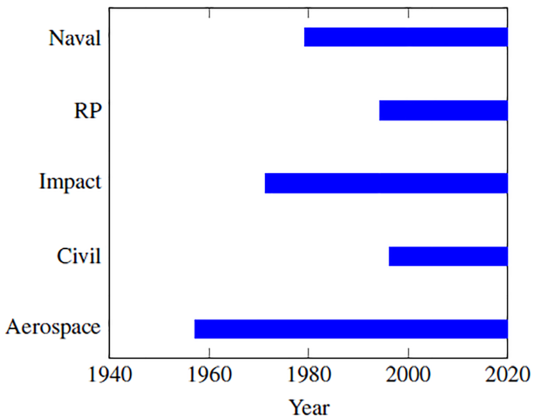

Fig. 10 Time overview of engineering fields

kinetic energy and, often, damage of the impacted structure.

(4) *Rapid prototyping (RP)*: Applications to quick fabrication techniques supported by computer aided design.

(5) *Naval and marine engineering*: Applications to study naval structures and marine installations.

In the following Secs. 5.1–5.5, the most relevant works are discussed; a complete reference list is provided in Table 5, while Fig. 10 illustrates the application of similitude methods over the years (on the horizontal axis) to complex structures in the listed engineering fields (on the vertical axis).

5.1 Aerospace Engineering. Similitude methods have been widely used in the aerospace field. From the early 1960s, NASA Langley Research Center (LaRC) investigated the structural behavior of space vehicle, e.g., landers, launchers, spacecrafts, and their subcomponents. These structures had large dimensions. Considering the limitations of ground facilities, many tests were feasible only using scaled models. A comprehensive review of relevant LaRC technical reports is provided by Horta and Kvaternik [162].

These works were not based on a complete similitude theory and its limits; neither were differences between prototype and model behavior analyzed. Similitude methods were used as a tool to investigate (theoretically and experimentally) the static and dynamic behavior of structures, sloshing phenomena into fuel tanks, and to understand the most suitable analyses and the most convenient construction philosophy. Experimental tests were often used to validate new analytical models or structural simulation software (for example, NASTRAN). Different scale sizes were used, from 1/5 to 1/10 or more. Sometimes, hybrid scaling was used (for example, scaling geometrical and dynamic parameters with different factors). However, all models were perfect replicas. Thus, all structural elements were scaled-down: hat-section stringers, corrugated intertank sections, joints, etc. In certain cases, different gravity conditions were emulated and tested, so shock-chord suspension systems were created on purpose. This kind of work required a substantial improvement of fabrication procedures: machining and chemical milling tolerances, curvature forming techniques, aluminum forgings, machining of complex ring frames, etc.

Some works were dedicated to test early stage spacecraft and landers. Indeed, before encountering the hazardous space environment, a spacecraft is subjected to extreme vibrations during the launch and the boost phases. It is not feasible to design a spacecraft so that its natural frequencies are such that the structure does not respond to the booster inputs. Considering also that instrumentation and payloads are damaged by vibration conditions less severe than those expected during the flight plan, it is necessary to investigate suitable procedures to reduce the severity of many resonant conditions. Different lander designs were also tested, considering several multilegged designs with different suspension systems. These vehicles, in fact, must land on irregular surfaces of unknown topology and must not overturn after landing. These are some of the reasons that led NASA engineers to test spacecraft, such as the Nimbus [163], and landers, such as the lunar module [164,165] or the Viking spacecraft lander [166,167].

Launch vehicles require a high operational reliability due to high costs and payload preservations, so a reliable structural design is necessary for the launch vehicle to survive the shock and vibration environment encountered during the transportation to the launch site, construction on the launch pad, launch, and flight. In particular, during the launch and the flight phases, there are several phenomena to take into account, for example, the fuel consumption and the resulting change in weight condition and sloshing. All these environments contain many sources of transient and quasi-steady-state excitations that may produce undesirable vibration response levels in the vehicle structure. Therefore, it is also important to investigate the feasibility of using replica models in order to obtain vibration data necessary for the design of complex launch vehicle structures, control systems, clustered tank configurations, etc. Many works were dedicated to test launch vehicles, including a generic launch vehicle [4]; Saturn SA-1 [168–170]; Titan III in A [171], B [172], and C [173] configurations; and Apollo-Saturn V [174–180].

Large structures such as spacecraft, space stations, and deployable systems (as antennas or solar sails) defy conventional testing because of their size and flexibility. Furthermore, the static preloads and deflections due to gravity are greater than those developed in orbit. Scaled models were used also to overcome these problems, for example, testing Space Shuttle subcomponents [181–190]. NASA established a dedicated program, the dynamic scale model technology project, aimed at the development of model technology for space structures too large to be tested on ground in full scale. The space station freedom [191–196], large antennas [197,198], and Pathfinder [199] are the structures tested under this program.

In another NASA program, the in-space propulsion project, tests were performed on models of solar sails. Solar sails are thrust devices consisting of a membrane-based structure, lightweight and large, made of gossamer. They convert solar pressure into thrust of a spacecraft. On the one hand, solar sails can potentially provide low-cost propulsion and operate without the use of propellant allowing access to non-Keplerian orbits through a constant thrust; on the other hand, solar pressure is small, so the sails must have a significant size and, at the same time, a small enough system mass to achieve reasonable accelerations. Solar sails can reach dimensions ranging from 200 to 10^4 m^2. For obvious reasons, ground demonstrations must be conducted at significantly smaller sizes. Therefore, the limitations of ground facilities and costs force the use of scaled models in order to test numerically and experimentally [200–205] solar sails coupled with booms.

Solar sail-boom systems are an example of deployable structures, i.e., structures folded into several tight bundles for stowage that are propelled in specific directions in space at the beginning of the deployment phase. Again, testing difficulties and costs require the use of scaled models. Because of manufacturing limits (e.g., thickness control and accuracy), standard geometrical scaling cannot be used. Instead, Greschik et al. [206] propose a constant thickness scaling, which entails the uniform scaling of the global dimensions while keeping the thickness constant. The work of Greshcik et al. [206] is continued by Holland et al. [207], who explore the computational and experimental issues (FE model complexity, accuracy, and differences between analytical and experimental results) arising in the modeling and testing of scale models of inflatable structures.

Fuselages crashworthiness is the aim of Jackson and Fasanella [208,209], who subject a 1/5-scale model to drop tower tests. The results highlight some events characteristic of size effects. In fact, both prototype and model subfloor sections exhibit the same damage modes, but the amount of relative damage and accelerations are greater in the prototype.

All these works prove that scaled models are useful to overcome experimental problems due to size, facility limits, and costs. Selecting with care the scale factors and the methods of manufacture, with a judicious evaluation of deviations from direct scaling duplications, replica models turn out to be technically and economically feasible to study complex structures.

5.1.1 Aeroelastic Similitude. Aeroelastic testing has the purpose of verifying the numerically predicted aeroelastic characteristics of an entire vehicle or a part of it. In general, the scaled model must represent exactly the prototype dynamics matching, basically, mass and stiffness distributions [210–214]. Examples of structures that need aeroelastic validation, in terms of flutter clearance, gust response, and so on, are flexible wing rotors, high and low aspect ratio wings, and new designs of aircraft.

Typically, the selected similitude method is based on dimensional analysis; aeroelastic similitude is achieved matching the nondimensional parameters governing aerodynamics, the structural response, and their coupling. According to Bisplinghoff et al. [210], these nondimensional parameters are scale factors relating the static deflections and the modal behavior of the model with those of the prototype. Typically, wind tunnel limitations dictate the length scale as the ratio of the allowable model span in the wind tunnel to the real wing span [215].

More details on the constraints of aeroelastic scaling are provided by Molyneux [211], who identifies two types of similitudes to establish:

1. *Aerodynamic similitude*: Mach and Reynolds numbers must be retained and the bodies must be geometrically similar at the surface, i.e., same shape, same incidences to the flow, and same static elastic deformations.
2. *Structural similitude*: By analyzing the force-deflection, vibration, and equilibrium equations, the following quantities must be maintained: ratio between stiffness and aerodynamic forces, stiffness distribution, reduced frequency, mass ratio, and Froude number.

The above types of similitude lead to many conditions to be fulfilled. In some cases, such as studies of static aeroelasticity [216], some terms can be neglected because they are relevant only for dynamic phenomena (e.g., mass ratio). In other cases, for example, the study made by Hunt [212] on flexible lifting rotors when thermal effects are neglected, some compromises must be accepted. In fact, the author states that in his analysis, the requirements on Mach and Froude numbers cannot be fulfilled at the same time. Thus, the scaling procedure can be applied only if one of these two conditions is relaxed.

The flow conditions (subsonic, transonic, etc.) deserve some attention in the similitude approaches.

If the full-scale flow is not wholly subsonic, the full-scale Mach number is retained, leading to a structural model having same mass density and same modulus of elasticity. The full-scale Froude number is retained when the dynamic phenomenon is characterized by a significant weight dependence or when high-speed flight is performed in low-speed facilities. In this case, the mass density is kept the same while the modulus of elasticity is lower, so that an arbitrary structure or a replica can be used.

It can be noticed that the structural aspect is mainly addressed in terms of material properties such as mass density and modulus of elasticity. Considering also the aerodynamic requirements, an alternative manner to define the conditions for aeroelastic scaling is to keep mass and stiffness distributions and, at the same time, the aerodynamic envelope unchanged, as discussed in Refs. [210] and [213]. Consequently, the model must not necessarily resemble the internal structure of the full-scale prototype, allowing one to fabricate simpler structures, with noticeable money saving. In the same investigation, Reynolds number conservation cannot be achieved at all, i.e., the model cannot be tested at full-scale Reynolds number. Nevertheless, this number must be high enough to ensure the right type of viscous effects. In the work of Hunt [212], an important remark is also made on some experimental aspects. The dimensional tolerances are scaled with the same scale of linear dimensions, thus the quality of manufacture of the model is fundamental: spurious dynamic effects may arise due to errors in manufacturing.

A significant number of works in the aeroelastic field rely on the coupling between scaling procedures and optimization techniques [213,214,217–220]. In fact, keeping in mind the requirements for aeroelastic scaling, the function to minimize may be the structural mass distribution, while the design requirements of the model (limits on deflections under static loading, natural frequencies, flutter speed, etc.) may be used as constraints.

The first work in which optimization procedures are used is French [213], aimed at designing a scaled model of a low aspect ratio wing made of anisotropic material. The usual simplifying assumptions made in aeroelasticity, such as chordwise rigid wing and consequent beam-like response, are not applicable because they apply only for high aspect ratio wings made of metal. To overcome such difficulties, French proposed an approach based on optimization techniques. In a successive work, French and Eastep [214] break the optimization process into two steps: first to size the structural stiffness and second to size the mass distribution. The approach leads to good results; it is suitable for every structure that can be discretized with an FE approach. Furthermore, it saves a lot of time otherwise required for the correct sizing of the model and provides an interesting perspective on automatic procedures when only structural influence coefficients are known.

A variation of the method introduced by French is provided by Richards et al. [217]. The authors propose two scaling methodologies. One matches directly the modal response by updating mass and stiffness distributions simultaneously in a single optimization routine. In the second approach, mass and stiffness are updated in two separate optimization loops. Both the methods converge to an acceptable result but the single loop method performs poorly when a gradient-based technique is used; the authors underline how it would be more effective if another search method, such as genetic algorithms, is used. In contrast, the two-loop method proves to be computationally more efficient and more robust. However, this technique has the disadvantage that additional information, namely displacement sets under given loads, is required.

The method proposed by Richards et al. [217] is expanded by Ricciardi et al. [218], who also include the match with nonlinear static deflections in the stiffness optimization loop. The implementation is successful, leading to a good estimation of aeroelastic frequency, damping, and nonlinear static responses; however, some issues are highlighted due to the decoupling of mass and stiffness. The procedure is further expanded in Ref. [219] in which the vehicle elastic stiffness, geometric stiffness, and nonstructural mass are simultaneously designed. The work is based on the results obtained in Ref. [218] and in a successive work [221] in which the authors develop an aeroelastic interface that loosely couples a custom vortex-lattice code with MSC-NASTRAN. Spada et al. [220] propose a nonlinear scaling methodology similar to the one of Ricciardi et al. [219]. The main difference is that the scaling of stiffness and mass is achieved in two different optimization loops.

Several works are dedicated to aeroservoelastic applications [114,222–226]. They show that the classical aeroelastic scaling relations, typically developed for flutter, need to be extended when dealing with modern aeroelasticity, i.e., active control of aeroelastic stability, response problems, and extensive use of computer simulations [24]. For example, Friedmann and coworkers [114,222–225] aim to obtain scaling laws for aeroservoelastic problems emphasizing scaling requirements for actuator forces, hinge moments, and actuation power. These purposes are pursued under different flow conditions and for different control devices: subsonic flow [222,223], compressible flow [224], trailing edge flap [222,223], and piezoelectric induced actuation [224]. In particular, in Refs. [114], [224], and [225], a two-pronged approach is introduced that perfectly fits in the framework of modern aeroelasticity. In fact, the classical approach is supported by parallel computer simulations playing the role of numerically derived "similarity solutions". These solutions are applied where innovative scaling laws are required (e.g., control power, control surfaces, and shock wave motion in transonic flows), so that an expanded or refined set of scaling laws is obtained.

5.1.2 Thermal Similitude. Coutinho et al. [5] refer to thermal similitude as an independent or complementary branch of structural similitude. It has been used extensively in space structures modeling. As already mentioned, small-scale model testing has proven to be important due to the high costs of space structure testing with full-scale hardware. At the same time, it is important to obtain an experimental validation of the mathematical methods used for predicting the thermal performance of aircraft and spacecraft. In fact, aircraft must be capable of withstanding the adverse effects of aerodynamic heating (high temperatures and rates of change) during their mission. Spacecraft must keep temperature values in fairly narrow limits because of complex electronic equipment and instrumentations. This is not a trivial matter because the space environment is hazardous, exhibiting high temperatures and significant gradients, especially when space vehicles pass from sunlight to shadow and vice versa. Thermal control is acquired through proper design of the conductive and radiative heat-transfer paths between components in the vehicle, in conjunction with the control of the exterior radiative exchange of the vehicle with its environment. The thermal scaling can be easily derived by applying dimensional analysis, in an additional demonstration of its versatility.

Environmental simulations are typically executed in suitable structures known as "space chambers." Because small test chambers appear to offer better environmental control and reliability, small models are required for the experimental tests. Therefore, on the one hand, a structural scaling must be executed; on the other hand, because of the characteristic problem under observation, thermal characteristics must also be scaled. Dictating a similitude in thermal terms means to have similar temperatures, temperature distribution, heat content, and heat flow.

Two works are of relevant importance. Vickers [227] identifies two possible procedures to perform thermal scaling: temperature preservation and material preservation. The former considers prototype and model with the same absolute temperature, the latter considers prototype and model made of the same materials. Watkins [228] derives and provides all possible sets of independent similitude ratios for thermal modeling in a simulated space environment. The ratios are defined by a computer program which applies dimensional analysis on the physical quantities of interest (e.g., energy transfer from and to a single, elemental, and isothermal volume). In particular, the algorithm uses a matrix formulation of Buckingham's Π theorem.

According to O'Sullivan [229], in an analysis of aerodynamic heating of aircraft, geometrical similitude coupled with material preservation ensures a thermal similitude in terms of heat flow, while, keeping the temperature, thermal stresses, and deformations are similar. Katzoff [230] shows that all conditions for thermal similitudes cannot be satisfied simultaneously because of their complexity. This is the case, for example, of thermal conductivity and heat capacity scaling. Rolling [231] underlines that the temperature preservation method is a better choice because it allows material change, thus the choice of a material suitable to comply with the similitude conditions. Furthermore, Gabron [232] states that temperature preservation requires the conservation of thermal paths; to satisfy this requirement, material and geometric distortions (of the minor dimensions as the thickness of plates, shells, etc.) can be effectively used. Thermal conduction and radiation under transient conditions are the research subject of Maples and Scogin [233], who prove that thermal similitude can be applied also to transient systems with internal generation. Shannon [234] takes into account not only radiation and conduction but also convection, demonstrating that it can be considered with both the preservation methods achieving adequate thermal similitudes.

These works also highlight some difficulties encountered during thermal scaling. The constraints on temperature or material introduce limits on the properties and the possible length ratios for models. More generally, the pure adherence to thermal modeling laws is often experimentally unfeasible, because of the limited choice of materials, fabrication difficulties, and high costs. An example is provided by Gabron [232], who shows why a 1/5-scale model of a Voyager-type spacecraft is impractical due to the difficulties in fabricating small elements. In the same work, there are also some examples of scaled-up spacecraft appendages. However, the results in terms of measured temperature are not very accurate.

5.2 Civil Engineering. Limitations in testing equipment open the way to small-scale testing also for investigations on seismic response and performances of civil structures. Kumar et al. [235] and Usami and Kumar [236] discuss the aspects to consider in selecting a suitable set of scaling factors, procedure often complicated due to the great number of possible sets. They show that the whole procedure can be divided into two distinct types depending on whether the scale factor is chosen for mass or time.

A relevant work on the topic has been performed by Kim et al. [237]. Because the scaling laws are derived for the elastic range, the inelastic response of small scale models exhibits some discrepancies. The authors apply and compare three scaling laws, based on mass, time, or acceleration, according to the importance of gravity; they are derived by means of dimensional analysis. The authors conclude that, when using the same scale factors for length and force, the comparisons of pseudodynamic tests with the three similitude laws lead to inelastic responses which are practically coincident. Pseudodynamic tests on steel columns prove that these laws work well also in the inelastic domain. Furthermore, they propose a modified similitude law which considers both a scale factor for length and a stiffness ratio; it can effectively simulate the seismic response of prototype structures.

When dealing with the inelastic range, conventional similitude requirements based on geometry may not be suitable. To overcome some problems related to the scale factor reduction, Kim et al. [238] propose models with dissimilar materials to those of the prototype. For this reason, the authors modify the acceleration-based law, introduced in the previous article, into an equivalent multiphase similitude law which takes into account the material nonlinearities. The key parameters of the model are the equivalent modulus ratio and the peak strain ratio. Then, the law is implemented in a numerical algorithm reproducing a pseudodynamic test; the results prove that such a modified law is applicable to the seismic simulation tests. The investigation is completed with experimental tests of a 1/5 scale reinforced concrete model and its prototype. Results prove that a variable modulus ratio produces similar responses, while a constant one produces large errors because the strain level of the small scale model is not considered.

5.3 Impact Engineering. This subsection is dedicated to investigations of impact phenomena by means of similitude theory. An important suggestion for how to deal with nonscaling phenomena occurring in scaled problems of mechanical impact and fracture was provided by Atkins [239]. According to his energy analysis, when the problem presents a mixture of surface and volume effects, a perfect replica scaling is unfeasible. Such a mixture is present in the majority of problems.

Through a rigorous analysis of the governing equations and a detailed comparison between theory and test results, Atkins defines a nondimensional parameter as the ratio between the energy involved in volume deformation and the energy involved into forming the crack surfaces. Thus, it is a function of both material properties and the absolute size of the prototype. The scaling laws derived consider the classical scaling factors and the dimensionless parameter and explain why geometric scaling of energy fails in problems of combined flow and fracture.

Me-Bar [240] proceeds in the same direction as Atkins [239], dividing the impactor energy, lost during the penetration into two contributions: energy expended in surface and volume effects, respectively. The normalized impact energy involved in volume effects is the same in all scales, while the fraction of normalized energy involved in surface effects increases when the scale factors decrease. Thus, a smaller structure absorbs more energy, a clear size effect. In this way, the method explains why scaling does not hold in ballistic configurations when surface effects are significant. Furthermore, it can be used in complex configurations without knowledge of the constitutive relations of various materials involved. Actually, for simple configurations and when just one material is present, nonscaling due to strain-rate effects can be considered. Instead, the method proposed by Atkins [239] allows to evaluate the energy transfer interaction for a given material at any given scale, only if its constitutive relations and fracture toughness are known.

Other theoretical studies involving, more generally, scaling of material failure are provided for linear elastic range in Refs. [241] and [242], plastic fracture in Ref. [239], nonlinear elastic range in Ref. [243], elastoplastic materials in Refs. [244] and [245], and epoxy and polyether ether ketone composites in Ref. [246]. Bažant et al. also provide an extensive treatise of failure scaling [247–253], while the failure of quasi-brittle materials is experimentally investigated by van Vliet and van Mier [254].

Westine and Mullin [255] study experimentally hypervelocity impacts into semi-infinite, shielded targets. In this case, beyond the typical phenomena expected when impacts are involved, such as plastic flow, fragmentation, and spalling, other mechanical and thermal phenomena must also be taken into account, e.g., melting and vaporization. The authors derive scaling laws suitable for both semi-infinite and complex, finite size targets. Hypervelocity impacts are found to scale well for both replica and dissimilar materials models.

Going beyond purely theoretical investigations, impact analysis has been applied to tests on scaled models of casks, for shipping radioactive waste [256] or spent fuel elements [257]. Scaled models are useful in the automotive field, too [2,258–260]. In fact, the response of an automobile in high speed crashes is complex: the intricate structure of an automobile undergoes large deformations, buckling, fracture, tearing, and joints deformation. The response also depends on other elements, such as impact velocity, angle of incidence, and the type of obstacle impacted by the car. Crashworthiness problems have analytical solutions limited to simple cases and depend on empirically derived data, thus relying strongly on experiments. Scaled-down models allow one to perform an acceptable number of experiments reducing the financial and temporal costs.

5.4 Naval and Marine Engineering. Similitude methods in naval and marine engineering are addressed toward two main applications: ocean structures, that can be studied in model basins, as well as the behavior of ships, typically due to collisions.

Kure [261] gives an interesting perspective on several problems with scaling in marine environment. For example, when dealing with offshore structures, habitability is a factor not to underestimate. These structures are subjected to loads that are easy to model as long as still water is considered. However, complex phenomena such as wave loads and drifting forces may also need to be considered. Oceanic environment is also characterized by wind, waves, currents and, in particular applications, ice flows, continuous winter sea ice, and icebergs.

Ships behavior in a collision scenario is the topic of the review by Calle and Alves [262]. Ship collisions and grounding represent the majority of ship accidents and are caused, mainly, by human errors, ship failure, and harsh environment. Considering that the global fleet has increased significantly in the number of ships in recent years, the risk of a collision has increased in parallel. About 48% of the world fleet consists of tankers, thus the risk of oil leakage is high. Furthermore, ship collisions lead to other serious damages, e.g., the degradation of the marine environment, explosions, human losses, blocking of ship traffic, and permanent damage to ships. While this is a sensitive topic, ship sizes are too large to permit experimental testing of prototypes. Calle and Alves [262] underline the necessity of more tests on models taking into account the structural aspects.

There are many works on experimental testing of colliding ships [263–270]. In all of them, the ships are scaled-down, sometimes significantly (1/45 [263], 1/35 [267], and 1/100 [268] scaled models). What really jumps out from these works is the difficulty in realizing the experimental tests. For example, in order to estimate the energy involved in low energy collisions, Hagiwara et al. [264] simplify the model manufacturing by omitting some structural members, which invalidates the experimental results. Also, nonsimilarities in material failure appear. The manufacturing difficulties are remarked upon also by Ohtsubo et al. [265] and Calle et al. [268]. For example, interior welding is limited by restricted accesses. To fabricate, all the components would lead to an enormous complexity, disproportionate cost, and long times for assembly. Therefore, simplified geometries are a necessity: only the main plates and stiffeners are typically considered. To reproduce the striker body, Lehmann and Peschmann [266] and Tabri et al. [267] use a rigid, bulbous bow as striker (instead of making a second, scaled-down ship model).

5.5 Rapid Prototyping. Rapid prototyping is a group of industrial techniques used in many engineering fields. This section reviews the use of similitude methods to rapid prototyping techniques, independent of the final application.

Cho and Wood [61] report that, between the 1980s and 1990s, various rapid prototyping techniques emerged and advanced, so that at least twenty companies already commercialized diverse rapid prototyping systems; such diffusion can be explained with the dramatic reduction of fabrication cost and time that RP provides. Cho et al. [271] underline that, in the late 1990s, there was only limited literature about similitude methods applied to rapid prototyping, generally works based on dimensional analysis, such as Refs. [272] and [273], that just examine experimentally the test results. In Ref. [274], the prediction of aluminum prototypes was performed by means of impacted stereolithography (SL) models.

Coutinho et al. [5] list other studies concerning rapid prototyping, many of them related to wind tunnel testing: Springer [275] obtains models with fused deposition method (FDM) using ABS plastic or polyether ether ketone, SL, selective laser sintering, and laminated object manufacturing; Nadooshan et al. [276] employ FDM with polycarbonate; Chuk and Thomson [277] compare times and costs of ten rapid prototyping techniques in making wind tunnel models. However, these authors agree on the fact that such technologies are applicable for models as long as the loads are kept sufficiently low, because those parts made of plastic materials or metal powders do not provide enough structural integrity for testing.

In order to improve the structural integrity of RP models and reduce the manufacturing period and cost, in Refs. [278] and [279], a preliminary design and manufacturing technique is introduced. This technique is applied to hybrid high-speed wind-tunnel models with an internal frame and an outer resin, fabricated, respectively, with a conventional method and stereolithography. A similar method is already applied by Fujino et al. [280] to experimentally investigate the flutter characteristics of an over-the-wing engine mount configuration by using different scale models at different flow conditions.

Ziemian et al. [281] present a different case of study. They investigate the correlation between the dynamic behavior of a full-scale steel prototype and a small-scale plastic model fabricated using FDM, in order to obtain baseline information on the dynamic response on the dynamic behavior on FDM plastic parts. By means of a shake-table test, the feasibility of the small-scale FDM models is assessed comparing the experimental results with those of a full prototype study and with computational models.

In Ref. [282], a novel method to design and fabricate aeroelastic wing models for wind tunnel tests is presented. It is based on SL and derives the model through a sequential design procedure of dimensional scaling, and stiffness and mass optimization. It is applied to an aluminum wing box, scaled down to obtain the desired dynamic behavior data.

As reported in Ref. [5], all these researches do not propose innovations and do not try to overcome the typical problems of RP testing by changing the method. To address this, Cho and Wood [61] propose the ESM methodology, claiming that their method is more suitable in solving distortion problems. In this paper, ESM is first used to predict the deflection of an aluminum beam in two locations with a certain distance from the clamping point, then to investigate a thermostructural problem in which some of the dimensionless parameters are not kept identical. Applications on an aluminum/nylon rod and to study temperature transition of an aluminum/nylon mold are considered in Ref. [271], and on a numerical slotted rod and a mold in Ref. [283]. Error estimation of both dimensional analysis and ESM results is performed in Ref. [284], with a numerical application to the study of thermal behavior of turbine blades. In Ref. [285], three approaches to construct the transformation matrix are extensively proposed: a pseudo-inverse approach, diagonal matrix approach, and circulant matrix approach. Then, a numerical analysis of the deflection of a cantilever beam is exposed; the same application is repeated after introducing an advanced ESM, proposed to overcome the problems of specimen distortion. The novel method is applied also to the control of steady-state temperature of central processing unit surfaces. The advanced ESM technique is applied in Ref. [286] to investigate the deflection of a cantilever beam with five holes subjected to a concentrated load at the tip. In Ref. [287], a lumped ESM is introduced to link distorted systems made of more than one part. A numerical study is performed of an archery bow, then an experimental one on a heat sink (to control the steady-state temperature of a central processing unit).

6 Future Research and Conclusions

Similitude theory has proven to be an interesting and useful tool, especially in structural design and testing. It is applied to study many kinds of problem, such as free and forced vibrations, buckling, and impact response, in several engineering fields (e.g., aerospace, civil, and naval engineering).

Historical methods, such as those based on dimensional analysis and governing equations, are still widely used, but it is clear that the possibilities they offer are limited due to, for example, the efforts to derive appropriate similitude conditions. Some of the new methodologies show how the scientific community is trying to go beyond such limitations. Considering the constantly increasing computational resources, a general trend can be intuitively read. On the one hand, new methods try to face the resolution of more complex problems, such as applications to acoustic-elastic systems or structures made of several components. On the other hand, a procedure that can be implemented in an algorithm is searched, to reduce the effort needed to the analyst in deriving the similitude conditions and transforming the problem of spent time in a problem of computational time, i.e., machine capabilities.

The analytical and numerical implications must not distract the attention from the main purpose of similitude theory: to reduce the problems concerning full-scale testing. In fact, experimental tests are fundamental because they allow to investigate real structures without the simplifications of analytical and numerical models (such as absence of noise and perfect boundary conditions). More in general, experimental tests are useful to validate theoretical models.

Almost in all applications of similitude methods, partial similitude may be the best one can hope for: it is not only an analytical matter but also a result of manufacturing constraints (methods limitations, errors, etc.). Nonscaling phenomena, such as size effects, must also be taken into account, because they affect important properties of the specimens, especially in terms of strength and load-bearing. The problem cannot be generalized, since each system is sensitive to different parameters: aspect ratio for panels, radius or length for cylinders, damping in modal approaches, and strain-rate effects for impact problems (without taking into account more general data, such as material and excitation source).

It may be interesting trying to understand if it is possible to use distorted models in order to take more advantages from their response. Distortions may be viewed as manufacturing variabilities, or perturbations of a system with respect to a reference state that lead to differences in response (to get a better idea, refer to the works [288,289]). Because these events may happen in reality, the ability to predict the impact of parameter variation on a system would allow one to identify the perturbed parameter and to locate the manufacturing error, without resorting to several experimental and numerical tests, with a remarkable saving of time and resources.

In this context, the path opened by sensitivity analysis is very interesting. In already existing works, the evolution of a system when design parameters change has been studied; another way may be to perform sensitivity analysis directly on the structural eigensolutions, i.e., natural frequencies and mode shapes, to be related, then, to the system response.

The improvement of computer capabilities may be exploited by employing numerical procedures belonging to the wide spectrum of data-driven analysis methods, such as machine learning. On the one hand, clustering algorithms may help to identify the response of distorted models in parameters space, in order to identify, if possible, the closest replica. On the other hand, neural networks training may help to predict the behavior of systems when design parameters change, by submitting for the learning process data obtained from experimental and numerical tests.

In conclusion, the purpose of this paper has been to give an updated review on applications of similitude methods in structural mechanics classifying them by test articles, with a brief insight on historical developments and a deeper focus on the applied methodologies, providing a comprehensive list of references for those who are interested in this topic. Similitude theory is well assessed until partial similitudes are taken into account. Until now, such partial similitudes have been treated as a problem: a consequence of similitude methods that are not able to provide the wanted results. Some ideas on how partial similitudes can be exploited have been provided, but goals and guidelines need a careful definition, which can be the next step of actual investigations.

Acknowledgment

The authors would like to thank the reviewers, the Associate editors, and the Editor of the journal for their precious advices, who helped to improve the quality of this paper.

Appendix: Reference Tables

Three reference tables will follow in order to provide a useful synopsis to the interested readers. They report the methods, Table 3, and the test articles, Table 4, respectively. The last one, Table 5, presents the references for complex structures and other application fields.

Table 3 Reference table of similitude methods

	References
DA	[2,4,9,10,12,14–21,23–31,34,37,38,65,88,89,96,97,99–102,104,106–114,135,136,138,141,142,144,147,163–193,199–201,206–209, 212–214,216–220,222–226,228–230,232–238,246,255–260,272,273,290–327]
STAGE	[1,3,6,21,22,29,33,50–52,62,74–87,90–94,118–122,131–133,139,151–156,159,328–340]
EM	[53,340,341]
ASMA	[54,55,95,123–127,129,342]
SAMSARA	[57–60,128,157,158,343]
ESM	[61,271,283–287]
SA	[62–64,133,328]

Table 4 Reference table of test articles

	References
Beam	[34,53,55,88–97,99–102,104–113,137, 290–292,307,329–332,341,342,344,345]
Unstiffened plate	[1,14,50,52–54,57,59,62–65,74–77,82–86,95–97,100,101,108–111,113,115,117–128,130–144, 290,293–295,297,298, 304,308,330,332–334,336–338,345–350]
Stiffened plate	[32,48]
Sandwich plate	[33,296,335]
Unstiffened cylinder	[35,78–81,87,151–158,160,161,299,300,305,306,328,339,349–351]
Stiffened cylinder	[36,60,150,158,352]

Table 5 Reference table of other application fields

	References
Aerospace engineering	[4,114,162–210,212–214,216–220,222–226,228–230,232–234,301,302,309–323]
Civil engineering	[235–238,353]
Impact engineering	[2,35,239,240,255–260,303,345]
Naval engineering	[8,261–270,354,355]
Rapid prototyping	[61,271–287]

References

[1] Simitses, G. J., and Rezaeepazhand, J., 1993, "Structural Similitude for Laminated Structures," Compos. Eng., **3**(7–8), pp. 751–765.

[2] Holmes, B. S., and Sliter, G., 1974, "Scale Modeling of Vehicle Crashes—Techniques, Applicability, and Accuracy; Cost Effectiveness," SAE Paper No. 740586.

[3] Simitses, G. J., Starnes, J. H., Jr., and Rezaeepazhand, J., 2000, "Structural Similitude and Scaling Laws for Plates and Shells: A Review," AIAA Paper No. AIAA-2000-1383.

[4] Wissmann, J. W., 1968, "Dynamic Stability of Space Vehicles-Structural Dynamics Model Testing," National Aeronautics and Space Administration, Washington, DC, Report No. NASA CR–1195.

[5] Coutinho, C. P., Baptista, A. J., and Rodrigues, J. D., 2016, "Reduced Scale Models Based on Similitude Theory: A Review up to 2015," Eng. Struct., **119**, pp. 81–94.

[6] Zhu, Y., Wang, Y., Luo, Z., Han, Q., and Wang, D., 2017, "Similitude Design for the Vibration Problems of Plates and Shells: A Review," Front. Mech. Eng., **12**(2), pp. 253–264.

[7] Rosen, R., 1989, "Similitude, Similarity and Scaling," Landscape Ecol., **3**(3–4), pp. 207–216.

[8] Vassalos, D., 1998, "Physical Modelling and Similitude of Marine Structures," Ocean Eng., **26**(2), pp. 111–1232.

[9] Cagliostro, D. J., Florence, A. L., and Abrahamson, G. R., 1979, "Scale Modelling in LMFBR Safety," Nucl. Eng. Des., **55**(2), pp. 235–247.

[10] Saito, K., and Kuwana, K., 2017, "Scale Modeling Vibro-Acoustics," Acoust. Sci. Tech., **38**(3), pp. 113–119.

[11] Galilei, G., and Weston, J., 1730, *Mathematical Discourses Concerning Two New Sciences Relating to Mechanics and Local Motion: In Four Dialogues*, John Hooke, London.

[12] Rayleigh, L., 1915, "The Principle of Similitude," Nature, **95**, pp. 66–68.

[13] Macagno, E. O., 1971, "Historico-Critical Review of Dimensional Analysis," J. Franklin Inst., **292**(6), pp. 391–402.

[14] Goodier, J. N., and Thomson, W. T., 1944, "Applicability of Similarity Principles to Structural Models," National Advisory Committee for Aeronautics, Washington, DC, Report No. CR-4068.

[15] Goodier, J. N., 1950, *Dimensional Analysis*, Wiley, New York.

[16] Murphy, G., 1950, *Similitude in Engineering*, Ronald Press, New York.

[17] Langhaar, H. L., 1951, *Dimensionless Analysis and Theory of Models*, Wiley, New York.

[18] Charlton, T. M., 1954, *Model Analysis of Structures*, Wiley, New York.

[19] Pankhurst, R. C., 1964, *Dimensional Analysis and Scale Factors*, Chapman and Hall, London.

[20] Gukhman, A. A., 1965, *Introduction to the Theory of Similarity*, Academic Press, New York.

[21] Kline, S. J., 1965, *Similitude and Approximation Theory*, McGraw-Hill, New York.

[22] Szucs, E., 1980, *Similitude and Modelling*, Elsevier, New York.

[23] Singer, J., Arbocz, I., and Weller, T., 1997, *Buckling Experiments*, Wiley, Chickester, UK.

[24] Baker, W. E., Westine, P. S., and Dodge, F. T., 1991, *Similarity Methods in Engineering Dynamics: Theory and Practice of Scale Modeling*, Revised ed., Elsevier, Amsterdam, The Netherlands.

[25] Sonin, A. A., 2001, *The Physical Basis of Dimensional Analysis*, Department of Mechanical Engineering, MIT, Cambridge, MA.

[26] Harris, H. G., and Sabnis, G. M., 1999, *Structural Modeling and Experimental Techniques*, CRC Press, Boca Raton, FL.

[27] Szirtes, T., 2007, *Applied Dimensional Analysis and Modeling*, 2nd ed., Elsevier and Butterworth-Heinemann, Oxford, UK.

[28] Tan, Q. M., 2011, *Dimensional Analysis With Case Studies in Mechanics*, Springer-Verlag, Berlin.

[29] Kuneš, J., 2012, *Similarity and Modeling in Science and Engineering*, Springer, Cambridge International Science Publishing Ltd. and Springer, Cambridge, UK.

[30] Zohuri, B., 2012, *Dimensional Analysis and Self-Similarity Methods for Engineers and Scientists*, Springer International Publishing, Cham, Switzerland.

[31] Zohuri, B., 2017, *Dimensional Analysis Beyond the Pi Theorem*, Springer International Publishing, Cham, Switzerland.

[32] Mazzariol, L. M., Calle, M. A. G., Oshiro, R. E., and Alves, M., "Scaling of Stiffened Panels Subjected to Impact Loading," Mecánica Computational, Vol. XXIX, E. Dvorkin, M. Goldscmit, and M. Storti, eds., Asociación Argentina de Mecánica Computacional, Buenos Aires, Argentina, pp. 1275–1289.

[33] Frostig, Y., and Simitses, G. J., 2004, "Similitude of Sandwich Panels With a 'Soft' Core in Buckling," Compos. Part B, **35**(6–8), pp. 599–608.

[34] Morton, J., 1988, "Scaling of Impact-Loaded Carbon-Fiber Composites," AIAA J., **26**(8), pp. 989–994.
[35] Hamada, H., and Ramakrishna, S., 1995, "Scaling Effects in the Energy Absorption of Carbon-Fiber/PEEK Composite Tubes," Compos. Sci. Technol., **55**(3), pp. 211–221.
[36] Sato, J. A., Vecchio, F. J., and Andre, H. M., 1989, "Scale-Model Testing of Reinforced Concrete Under Impact Loading Conditions," Can. J. Civ. Eng., **16**(4), pp. 459–466.
[37] Ezra, A. A., 1962, "Similitude Requirements for Scale Model Determination of Shell Buckling Under Impulsive Pressures," National Aeronautics and Space Administration, Washington, DC, Report No. NASA-TN-D-1510.
[38] Soedel, W., 1971, "Similitude Approximations for Vibrating Thin Shells," J. Acoust. Soc. Am., **49**(5 Pt. 2), pp. 1535–1541.
[39] Sterrett, S. G., 2002, "Physical Model and Fundamental Laws: Using One Piece of the World to Tell About Another," Mind Soc., **3**(1), pp. 51–66.
[40] Sterrett, S. G., 2009, "Similarity and Dimensional Analysis," *Philosophy of Technology and the Engineering Sciences* (Handbook of the Philosophy of Science, Vol. 9), A. Meijers, ed., Elsevier, Amsterdam, The Netherlands, pp. 799–824.
[41] Sterrett, S. G., 2015, "Experimentation on Analogue Models," *Springer Handbook of Model-Based Science*, L. Magnani and T. Bertolotti, eds., Springer International Publishing, Berlin.
[42] Sterrett, S., 2006, "Models of Machines and Models of Phenomena," Int. Stud. Philos. Sci., **20**(1), pp. 69–80.
[43] Sterrett, S. G., 2014, "The Morals of Model-Making," Stud. Hist. Philos. Sci., **46**, pp. 31–45.
[44] Sterrett, S. G., 2015, "Physically Similar Systems: A History of the Concept," *Springer Handbook of Model-Based Science*, L. Magnani and T. Bertolotti, eds., Springer International Publishing, Berlin.
[45] Polsinelli, J., and Levent Kavvas, M., 2016, "A Comparison of the Modern Lie Scaling Method to Classical Scaling Techniques," Hydrol. Earth Syst. Sci., **20**(7), pp. 2669–2678.
[46] Bluman, G. W., and Cole, J. D., 1974, *Similarity Methods for Differential Equations*, Springer-Verlag, New York.
[47] Jackson, K. E., 1993, "Workshop on Scaling Effects in Composite Materials and Structures," Workshop Sponsored by the National Aeronautics and Space Administration, Hampton, VA, Nov. 15–16, Paper No. 3271.
[48] Coutinho, C. P., Baptista, A. J., and Dias Rodriges, J., 2018, "Modular Approach to Structural Similitude," Int. J. Mech. Sci., **135**, pp. 294–312.
[49] Buckingham, E., 1914, "On Physically Similar Systems, Illustrations of the Use of Dimensional Equations," Phys. Rev., **4**(4), pp. 345–376.
[50] Ungbhakorn, V., 2001, "A New Approach for Establishing Structural Similitude for Buckling of Symmetric Cross-Ply Laminated Plates Subjected to Combined Load," Thammasat. Int. J. Sci. Technol., **6**(3), pp. 55–60.
[51] Torkamani, S., Jafari, A. A., and Navazi, H. M., 2008, "Scaled Down Models for Free Vibration Analysis of Orthogonally Stiffened Cylindrical Shells Using Similitude Theory," 26th International Congress of the Aeronautical Sciences (ICAS), Anchorage, AL, Sept. 14–19, pp. 3458–3469.
[52] Wu, J. J., 2003, "The Complete-Similitude Scale Models for Predicting the Vibration Characteristics of the Elastically Restrained Flat Plates Subjected to Dynamic Loads," J. Sound Vib., **268**(5), pp. 1041–1053.
[53] Kasivitamnuay, J., and Singhatanadgid, P., 2005, "Application of an Energy Theorem to Derive a Scaling Law for Structural Behaviors," Thammasat. Int. J. Sc. Tech., **10**(4), pp. 33–40.
[54] De Rosa, S., Franco, F., and Mace, B. R., 2005, "The Asymptotic Scaled Modal Analysis for the Response of a 2-Plate Assembly," XVIII AIDAA National Congress, Volterra, Italy, Sept. 19–22.
[55] De Rosa, S., Franco, F., Ricci, F., and Marulo, F., 1997, "First Assessment of the Scaling Procedure for the Evaluation of the Damped Structural Response," J. Sound Vib., **204**(3), pp. 540–548.
[56] Mace, B., 2003, "Statistical Energy Analysis, Energy Distribution Models and System Modes," J. Sound Vib., **264**(2), pp. 391–409.
[57] De Rosa, S., Franco, F., and Polito, T., 2011, "Structural Similitudes for the Dynamic Response of Plates and Assemblies of Plates," Mech. Syst. Signal Process., **25**(3), pp. 969–980.
[58] De Rosa, S., Franco, F., Li, X., and Polito, T., 2012, "A Similitude for Structural Acoustic Enclosures," Mech. Syst. Signal Process., **30**, pp. 330–342.
[59] De Rosa, S., Franco, F., and Meruane, V., 2015, "Similitudes for Structural Response of Flexural Plates," Proc. Inst. Mech. Eng., Part C, **230**(3), pp. 174–188.
[60] Petrone, G., Manfredonia, M., De Rosa, S., and Franco, F., 2017, "Structural Similitudes of Stiffened Cylinders," Math. Mech. Solids, **24**(3), pp. 527–541.
[61] Cho, U., and Wood, K., 1997, "Empirical Similitude Method for the Functional Test With Rapid Prototypes," Symposium for Solid Freeform Fabrication, The University of Texas at Austin, Austin, TX.
[62] Luo, Z., Wang, Y., Zhu, Y., Zhao, X., and Wang, D., 2015, "The Similitude Design Method of Thin-Walled Annular Plates and Determination of Structural Size Intervals," Proc. Inst. Mech. Eng., Part C, **230**(13), pp. 2158–2168.
[63] Adams, C., Bös, J., and Melz, T., 2016, "A Scaling Method for Vibrating Structures Using Global Sensitivity Analysis," 45th International Congress and Exposition on Noise Control Engineering: Towards a Quieter Future, INTER-NOISE 2016, Hamburg, Germany, Aug. 21–24, pp. 5411–5420.
[64] Adams, C., Bös, J., Slomski, E. M., and Melz, T., 2018, "Scaling Laws Obtained From a Sensitivity Analysis and Applied to Thin Vibrating Structures," Mech. Syst. Signal Process., **110**, pp. 590–610.
[65] Hu, Y. Q., 2000, "Application of Response Number for Dynamic Plastic Response of Plates Subjected to Impulsive Loading," Int. J. Pressure Vessels Piping, **77**(12), pp. 711–714.
[66] Shi, X. H., and Gao, Y. G., 2001, "Generalization of Response Number for Dynamic Plastic Response of Shells Subjected to Impulsive Loading," Int. J. Pressure Vessels Piping, **78**(6), pp. 453–459.
[67] Vlot, A., 2001, *Fiber Metal Laminates: An Introduction*, Kluwer Academia, Dordrecht, The Netherlands.
[68] Carrillo, J. G., and Cantwell, W. J., 2007, "A Comparison of Ply-Level and Sublaminate-Level Scaling of Fibre-Metal Laminates With In-Plane Dimensions," Adv. Compos. Lett., **16**(6), pp. 233–236.
[69] Carrillo, J. G., and Cantwell, W. J., 2007, "Scaling Effects in the Tensile Behavior of Fiber-Metal Laminates," Compos. Sci. Technol., **67**(7–8), pp. 1684–1693.
[70] Wisnom, M. R., and Atkinson, J. W., 1997, "Reduction in Tensile and Flexural Strength of Unidirectional Glass Fibre-Epoxy With Increasing Specimen Size," Compos. Struct., **38**(1–4), pp. 405–411.
[71] Johnson, D. P., Morton, J., Kellas, S., and Jackson, K., 1998, "Scaling Effects in Sublaminate-Level Scaled Composite Laminates," AIAA J., **36**(3), pp. 441–446.
[72] Johnson, D. P., Morton, J., Kellas, S., and Jackson, K. E., 2000, "Size Effects in Scald Fiber Composites Under Four-Point Flexure Loading," AIAA J., **38**(6), pp. 1047–1054.
[73] Kellas, S., and Morton, J., 1992, "Strength Scaling in Fiber Composites," AIAA J., **30**(4), pp. 1074–1080.
[74] Rezaeepazhand, J., and Simitses, G. J., 1993, "Design of Scaled Down Models for Stability and Vibration Studies," National Aeronautics and Space Administration, Washington, DC, Technical Report No. 194687.
[75] Rezaeepazhand, J., Simitses, G. J., and Starnes, J. H., Jr., 1995, "Design of Scaled Down Models for Stability of Laminated Plates," AIAA J., **33**(3), pp. 515–519.
[76] Simitses, G. J., and Rezaeepazhand, J., 1995, "Structural Similitude and Scaling Laws for Buckling of Cross-Ply Laminated Plates," J. Thermoplast. Compos. Mater., **8**, pp. 240–251.
[77] Rezaeepazhand, J., Simitses, G. J., Rezaeepazhand, J., and Simitses, G. J., 1995, "Use of Scaled-Down Models for Predicting Vibration Response of Laminated Plates," Compos. Struct., **30**(4), pp. 419–426.
[78] Rezaeepazhand, J., Simitses, G. J., and Starnes, J. H., Jr., 1996, "Design of Scaled Down Models for Predicting Shell Vibration Response," J. Sound Vib., **195**(2), pp. 301–311.
[79] Rezaeepazhand, J., Simitses, G. J., and Starnes, J. H., Jr., 1996, "Scale Models for Laminated Cylindrical Shells Subjected to Axial Compression," Compos. Struct., **34**(4), pp. 371–379.
[80] Simitses, G. J., Rezaeepazhand, J., and Sierakowski, R. L., 1997, "Scaled Models for Laminated Cylindrical Shells Subjected to External Pressure," Mech. Compos. Mater. Struct., **4**(3), pp. 267–280.
[81] Rezaeepazhand, J., and Simitses, G. J., 1997, "Structural Similitude for Vibration Response of Laminated Cylindrical Shells With Double Curvature," Compos. Part B, **28B**(3), pp. 195–200.
[82] Simitses, G. J., 2001, "Structural Similitude for Flat Laminated Surfaces," Compos. Struct., **51**(2), pp. 191–194.
[83] Rezaeepazhand, J., and Wisnom, M. R., 2009, "Scaled Models for Predicting Buckling of Delaminated Orthotropic Beam-Plates," Compos. Struct., **90**(1), pp. 87–91.
[84] Rezaeepazhand, J., and Yazdi, A. A., 2011, "Similitude Requirements and Scaling Laws for Flutter Prediction of Angle-Ply Composite Plates," Compos. Part B, **42**(1), pp. 51–56.
[85] Yazdi, A. A., and Rezaeepazhand, J., 2011, "Accuracy of Scale Models for Flutter Prediction of Cross-Ply Laminated Plates," J. Reinf. Plast. Compos., **30**(1), pp. 45–52.
[86] Yazdi, A. A., and Rezaeepazhand, J., 2013, "Applicability of Small-Scale Models in Prediction Flutter Pressure of Delaminated Composite Beam-Plates," Int. J. Damage Mech., **22**(4), pp. 590–601.
[87] Yazdi, A. A., 2013, "Prediction Flutter Boundaries of Laminated Cylindrical Shells Using Scaling Laws," J. Aerosp. Eng., **27**(1).
[88] Jackson, K. E., and Fasanella, E. L., 1989, "Scaling Effects in the Static Large Deflection Response of Graphite-Epoxy Composite Beams," National Aeronautics and Space Administration, Washington, DC, Report No. NASA-TM-101619.
[89] Jackson, K. E., 1990, "Scaling Effects in the Static and Dynamic Response of Graphite-Epoxy Beam-Columns," National Aeronautics and Space Administration, Washington, DC, Report No. NASA-TM-102697.
[90] Asl, M. E., Niezrecki, C., Sherwood, J., and Avitabile, P., 2016, "Similitude Analysis of Composite I–Beams With Application to Subcomponent Testing of Wind Turbine Blades," *Experimental and Applied Mechanics* (Proceedings of the Society for Experimental Mechanics Series, Vol. 4), C. Sciammarella, J. Considine, and P. Gloeckner, eds., Springer, Cham, Switzerland.
[91] Asl, M. E., Niezrecki, C., Sherwood, J., and Avitabile, P., 2017, "Similitude Analysis of Thin-Walled Composite I–Beams for Subcomponent Testing of Wind Turbine Blades," Wind Eng., **41**(5), pp. 297–312.
[92] Asl, M. E., Niezrecki, C., Sherwood, J., and Avitabile, P., 2017, "Experimental and Theoretical Similitude Analysis for Flexural Bending of Scaled-Down Laminated I–Beams," Compos. Struct., **176**, pp. 812–822.
[93] Asl, M. E., Niezrecki, C., Sherwood, J., and Avitabile, P., 2018, "Scaled Composites I–Beams for Subcomponent Testing of Wind Turbine Blades: An Experimental Study," *Mechanics of Composite and Multi-Functional Materials* (Conference Proceedings of the Society for Experimental Mechanics

Series, Vol. 6), P. Thakre, R. Singh, and G. Slipher, eds., Springer, Cham, Switzerland.
[94] Asl, M. E., Niezrecki, C., Sherwood, J., and Avitabile, P., 2017, "Similitude Analysis of the Frequency Response Function for Scaled Structures," *Model Validation and Uncertainty Quantification* (Conference Proceedings of the Society for Experimental Mechanics Series, Vol. 3), R. Barthorpe, R. Platz, I. Lopez, B. Moaveni, and C. Papadimitriou, eds., Springer, Cham, Switzerland.
[95] De Rosa, S., and Franco, F., 2010, "On the Use of the Asymptotic Scaled Modal Analysis for the Time-Harmonic Structural Analysis and for the Prediction of Coupling Loss Factors for Similar Systems," Mech. Syst. Signal Process., **24**(2), pp. 455–480.
[96] McKown, S., Cantwell, W. J., and Jones, N., 2008, "Investigation of Scaling Effects in Fiber-Metal Laminates," J. Compos. Mater., **42**(9), pp. 821–829.
[97] Zhao, Y. P., 1998, "Suggestion of a New Dimensionless Number for Dynamic Plastic Response of Beams and Plates," Archive Appl. Mech., **68**(7–8), pp. 524–538.
[98] Johnson, W., 1972, *Impact Strength of Materials*, Edward Arnold (Publishers), London.
[99] Zhao, Y. P., 1999, "Similarity Consideration of Structural Bifurcation Buckling," Forschung Ingenieurwesen, **65**(4), pp. 107–112.
[100] Christoforou, A. P., and Yigit, A. S., 1998, "Effect of Flexibility on Low Velocity Impact Response," J. Sound Vib., **217**(3), pp. 563–578.
[101] Christoforou, A. P., and Yigit, A. S., 2009, "Scaling of Low-Velocity Impact Response in Composite Structures," Compos. Struct., **91**(3), pp. 358–365.
[102] Pintado, P., and Morton, A., 1994, "On the Scaling of Impact Loaded Composite Beams," Compos. Struct., **27**(4), pp. 357–365.
[103] Laws, N., and Dvorak, G. J., 1988, "Progressive Transverse Cracking in Composite Laminates," J. Compos. Mater., **22**(10), pp. 1563–1568.
[104] Rosenberg, Z., Kreif, R., and Dekel, E., 1997, "A Note on the Geometric Scaling of Long-Rod Penetration," Int. J. Impact Eng., **19**(3), pp. 277–283.
[105] Sorensen, B. R., Kimsey, K. D., Silsby, G. F., Scheffler, D. R., Sherrick, T. M., and De Rosset, W. S., 1991, "High Velocity Penetration of Steel Targets," Int. J. Impact Eng., **11**(1), pp. 107–119.
[106] Anderson, C., Jr., Mullin, S., and Kuhlman, C., 1993, "Computer Simulations of Strain-Rate Effects in Replica Scale Model Penetration Experiments," Int. J. Impact Eng., **13**(1), pp. 35–52.
[107] Magness, L., and Farrand, T., 1990, "Deformation Behavior and Its Relationship to the Penetration Performance of High Density KE Penetrator Materials," Army Science Conference, Durham, NC, June 12–15.
[108] Oshiro, R. E., and Alves, M., 2004, "Scaling Impacted Structures," Archive Appl. Mech., **74**(1–2), pp. 130–145.
[109] Alves, M., and Oshiro, R. E., 2006, "Scaling the Impact of a Mass on a Structure," Int. J. Impact Eng., **32**(7), pp. 1158–1173.
[110] Alves, M., and Oshiro, R. E., 2006, "Scaling Impacted Structures When the Prototype and the Model Are Made of Different Materials," Int. J. Solids Struct., **43**(9), pp. 2744–2760.
[111] Oshiro, R. E., and Alves, M., 2009, "Scaling Structures Subject to Impact Loads When Using a Power Law Constitutive Equation," Int. J. Solids Struct., **46**(18–19), pp. 3412–3421.
[112] Oshiro, R. E., Calle, M. A. G., Mazzariol, L. M., and Alves, M., 2011, "Experimental Study of Scaled T Cross–Section Beams Subjected to Impact Load," 21st Brazilian Congress of Mechanical Engineering, Natal (RN), Brazil, Oct. 24–28.
[113] Oshiro, R. E., and Alves, M., 2012, "Predicting the Behaviour of Structures Under Impact Loads Using Geometrically Distorted Scaled Models," J. Mech. Phys. Solids, **60**(7), pp. 1330–1349.
[114] Friedmann, P. P., 2004, "Aeroelastic Scaling for Rotary-Wing Aircraft With Applications," J. Fluids Struct., **19**(5), pp. 635–650.
[115] Bachynski, E. E., Motley, M. R., and Young, Y. L., 2012, "Dynamic Hydroelastic Scaling of the Underwater Shock Response of Composite Marine Structures," ASME J. Appl. Mech., **79**(1), p. 014501.
[116] Young, Y. L., 2010, "Dynamic Hydroelastic Scaling of Self-Adaptive Composite Marine Rotors," Compos. Struct., **92**(1), pp. 97–106.
[117] Simitses, G. J., and Rezaeepazhand, J., 1992, "Structural Similitude and Scaling Laws for Laminated Beam-Plates," National Aeronautics and Space Administration, Washington, DC, Report No. NAG–1–1280.
[118] Singhatanadgid, P., and Ungbhakorn, V., 2002, "Scaling Laws for Vibration Response of Anti-Symmetrically Laminated Plates," Struct. Eng. Mech., **14**(3), pp. 1–20.
[119] Ungbhakorn, V., and Singhatanadgid, P., 2003, "Similitude Invariants and Scaling Laws for Buckling Experiments on Anti-Symmetrically Laminated Plates Subjected to Biaxial Loading," Compos. Struct., **59**(4), pp. 455–465.
[120] Singhatanadgid, P., and Ungbhakorn, V., 2003, "Buckling Similitude Invariants of Symmetrically Laminated Plates Subjected to Biaxial Loading," Compos. Struct., **59**(4), pp. 455–465.
[121] Singhatanadgid, P., and Ungbhakorn, V., 2005, "Scaling Laws for Buckling of Polar Orthotropic Annular Plates Subjected to Compressive and Torsional Loading," Thin-Walled Struct., **43**(7), pp. 1115–1129.
[122] Singhatanadgid, P., and Na Songkhla, A., 2008, "Experimental Investigation Into the Use of Scaling Laws for Predicting Vibration Responses of Rectangular Thin Plates," J. Sound Vib., **311**(1–2), pp. 314–327.
[123] De Rosa, S., and Franco, F., 2008, "A Scaling Procedure for the Response of an Isolated System With High Modal Overlap Factor," Mech. Syst. Signal Process., **22**(7), pp. 1549–1565.
[124] Martini, L., D., Rosa, S., and Franco, F., 2004, "The Structural Response of a Three Plate Assembly by Scaled Finite Element Method," ISMA, Leuven, Belgium, Sept. 20–22, pp. 1539–1554.
[125] De Rosa, S., and Franco, F., 2008, "Exact and Numerical Responses of a Plate Under a Turbulent Boundary Layer Excitation," J. Fluids Struct., **24**(2), pp. 212–230.
[126] Li, X., 2010, "Scaling for the Ensemble Statistics Prediction of a Random System Subjected to Harmonic Excitations," J. Acoust. Soc. Am., **127**(5), p. EL203.
[127] Li, X., 2010, "A Scaling Approach for the Prediction of the High-Frequency Mean Responses of Vibrating Systems," J. Acoust. Soc. Am., **127**(5), p. EL209.
[128] Meruane, V., De Rosa, S., and Franco, F., 2015, "Numerical and Experimental Results for the Frequency Response of Plates in Similitude," Proc. Inst. Mech. Eng., Part C, **230**(18), pp. 3212–3221.
[129] Robin, O., De Rosa, S., and Berry, A., 2016, "Similitudes for the Structural Response and Radiated Power From Plates," 45th International Congress and Exposition on Noise Control Engineering: Towards a Quieter Future (INTER-NOISE), Hamburg, Germany, Aug. 21–24, pp. 5421–5430.
[130] Xiaojian, Z., Bangcheng, A., Ziqiang, L., and Dun, L., 2016, "A Scaling Procedure for Panel Vibro-Acoustic Response Induced by Turbulent Boundary Layer," J. Sound Vib., **380**, pp. 165–179.
[131] Luo, Z., Zhu, Y., Wang, Y., and Zhao, X., 2013, "Study of the Structure Size Interval of Incomplete Geometrically Similitude Model of the Elastic Thin Plates," J. Meas. Eng., **1**(4), pp. 207–218.
[132] Luo, Z., Zhu, Y., Chen, X., and Zhao, X., 2014, "Determination Method of the Structure Size Intervals of Dynamic Distorted Model of Elastic Cantilever Thin Plate," Adv. Mech. Eng., **2014**, pp. 1–10.
[133] Luo, Z., Wang, Y., Zhu, Y., and Wang, D., 2016, "The Dynamic Similitude Design Method of Thin Walled Structures and Experimental Validation," Shock Vib., **2016**, p. 6836183.
[134] Nettles, A. T., Douglas, M. J., and Estes, E. E., 1999, "Scaling Effects in Carbon/Epoxy Laminates Under Transverse Quasi-Static Loading," National Aeronautics and Space Administration, Washington, DC, Report No. NASA/TM–1999–209103.
[135] Ambur, D. R., Chunchu, P. B., Rose, C. A., Feraboli, P., and Jackson, W. C., 2005, "Scaling the Non-Linear Impact Response of Flat and Curved Composite Panels," AIAA Paper No. 2005-2224.
[136] Sutherland, L. S., and Guedes Soares, C., 2007, "Scaling of Impact on Low Fibre-Volume Glass-Polyester Laminates," Compos. Part A, **38**(2), pp. 307–317.
[137] Viot, P., Ballére, L., Guillaumat, L., and Lataillade, J. L., 2008, "Scale Effects on the Response of Composite Structures Under Impact Loading," Eng. Fract. Mech., **75**(9), pp. 2725–2736.
[138] Xu, Z., Yang, F., Guan, Z. W., and Cantwell, W. J., 2016, "An Experimental and Numerical Study on Scaling Effects in the Low Velocity Impact Response of CFRP Laminates," Compos. Struct., **154**, pp. 69–78.
[139] Shokrieh, M. M., and Askari, A., 2013, "Similitude Study of Impacted Composite Under Buckling Loading," J. Eng. Mech., **139**(10), pp. 1334–1340.
[140] Jacob, N., Chung Kim Yuen, S., Nurick, G. N., Bonorchis, D., Desai, S. A., and Tait, D., 2004, "Scaling Aspects of Quadrangular Plates Subjected to Localised Blast Loads—Experiments and Predictions," Int. J. Impact Eng., **30**(8–9), pp. 1179–1208.
[141] Neuberger, A., Peles, S., and Rittel, D., 2007, "Scaling the Response of Circular Plates to Large and Close Range Spherical Explosions—Part I: Air-Blast Loading," Int. J. Impact Eng., **34**(5), pp. 859–873.
[142] Neuberger, A., Peles, S., and Rittel, D., 2007, "Scaling the Response of Circular Plates to Large and Close Range Spherical Explosions—Part II: Buried Charges," Int. J. Impact Eng., **34**(5), pp. 874–882.
[143] Neuberger, A., Peles, S., and Rittel, D., 2009, "Springback of Circular Clamped Armor Steel Plates Subjected to Spherical Air-Blast Loading," Int. J. Impact Eng., **36**(1), pp. 53–60.
[144] Noam, T., Dolinski, M., and Rittel, D., 2014, "Scaling Dynamic Failure: A Numerical Study," Int. J. Impact Eng., **69**, pp. 69–79.
[145] Jones, N., 1989, *Structural Impact*, Cambridge University Press, Cambridge, UK.
[146] Rittel, D., Wang, Z., and Merzer, M., 2006, "Adiabatic Shear Failure and Dynamic Stored Energy of Cold Work," Phys. Rev. Lett., **96**, p. 075502.
[147] Li, Q. M., and Jones, N., 2000, "On Dimensionless Numbers for Dynamic Plastic Response of Structural Members," Archive Appl. Mech., **70**(4), pp. 245–254.
[148] Nurick, G. N., and Martin, J. B., 1989, "Deformation of Thin Plates Subjected to Impulsive Loading–A Review—Part I: Theoretical Considerations," Int. J. Impact Eng., **8**(2), pp. 159–170.
[149] Nurick, G. N., and Martin, J. B., 1989, "Deformation of Thin Plates Subjected to Impulsive Loading–A Review—Part II: Experimental Studies," Int. J. Impact Eng., **8**(2), pp. 171–186.
[150] Yu, W., and Li, Z. L., 2016, "Structural Similitude for Prestressed Vibration and Buckling of Eccentrically Stiffened Circular Cylindrical Panels and Shells by Energy Approach," Int. J. Struct. Stab. Dyn., **16**(10), p. 1550074.
[151] Chouchaoui, O., and Ochoa, O. O., 1999, "Similitude Study for a Laminated Cylindrical Tube Under Tensile, Torsion, Bending, Internal and External Pressure—Part I: Governing Equations," Compos. Struct., **44**(4), pp. 221–229.
[152] Chouchaoui, O., Parks, P., and Ochoa, O. O., 1999, "Similitude Study for a Laminated Cylindrical Tube Under Tensile, Torsion, Bending, Internal and External Pressure—Part II: Scale Models," Compos. Struct., **44**(4), pp. 231–236.
[153] Ungbhakorn, V., and Singhatanadgid, P., 2003, "Scaling Law and Physical Similitude for Buckling and Vibration of Antisymmetric Angle-Ply Laminated Cylindrical Shells," Int. J. Struct. Stab. Dyn., **3**(4), pp. 567–583.

[154] Ungbhakorn, V., and Singhatanadgid, P., 2003, "Similitude and Physical Modeling for Buckling and Vibration of Symmetric Cross-Ply Laminated Circular Cylindrical Shells," J. Compos. Mater., **37**(19), pp. 1697–1712.
[155] Ungbhakorn, V., and Wattanasakulpong, N., 2007, "Structural Similitude and Scaling Laws of Anti-Symmetric Cross-Ply Laminated Cylindrical Shells for Buckling and Vibration Experiments," Int. J. Struct. Stab. Dyn., **7**(4), pp. 609–627.
[156] Tabiei, A., Sun, J., and Simitses, G. J., 1997, "Scaling Laws of Cylindrical Shells Under Lateral Pressure," AIAA J., **35**(10), pp. 1669–1671.
[157] De Rosa, S., Franco, F., and Polito, T., 2012, "SAMSARA for Thin Cylindrical Shells," Noise and Vibration: Emerging Methods (NOVEM 2012), Sorrento, Italy, April 1–4, pp. 048-1–048-12.
[158] De Rosa, S., and Franco, F., 2015, "Analytical Similitudes Applied to Thin Cylindrical Shells," Adv. Aircr. Spacecr. Sci., **2**(4), pp. 403–425.
[159] Torkamani, S., Jafari, A. A., Navazi, H. M., and Bagheri, M., 2009, "Structural Similitude in Free Vibration of Orthogonally Stiffened Cylindrical Shells," Thin-Walled Struct., **47**(11), pp. 1316–1330.
[160] Jiang, P., Wang, W., and Zhang, G. J., 2006, "Size Effects in the Axial Tearing of Circular Tubes During Quasi-Static and Impact Loadings," Int. J. Impact Eng., **32**(12), pp. 2048–2056.
[161] Tarfaoui, M., Gning, P. B., Davies, P., and Collombet, F., 2007, "Scale and Size Effects on Dynamic Response and Damage of Glass/Epoxy Tubular Structures," J. Compos. Mater., **41**(5), pp. 71–84.
[162] Horta, L. G., and Kvaternik, R. G., 2000, "A Historical Perspective on Dynamics Testing at the Langley Research Center," National Aeronautics and Space Administration, Washington, DC, Report No. NASA/TM–2000–210295.
[163] Carden, H. D., and Herr, R. W., 1964, "A Study on the Effectiveness of Various Methods of Vibration Reduction on Simplified Scale Models of the Nimbus Spacecraft," National Aeronautics and Space Administration, Washington, DC, Report No. NASA TN D–2418.
[164] Herr, R., and Wayne Leonard, H., 1967, "Dynamic Model Investigation of Touchdown Stability of Lunar-Landing Vehicles," National Aeronautics and Space Administration, Washington, DC, Report No. NASA TN D–4215.
[165] Blanchard, U. J., 1968, "Evaluation of a Full-Scale Lunar-Gravity Simulator by Comparison of Landing-Impact Tests of a Full-Scale and a 1/6-Scale Model," National Aeronautics and Space Administration, Washington, DC, Report No. NASA TN D–4474.
[166] Stubbs, S. M., 1971, "Investigation of Technique for Conducting Landing-Impact Tests at Simulated Planetary Gravity," National Aeronautics and Space Administration, Washington, DC, Report No. NASA TN D–6459.
[167] McGehee, J. R., and Stubbs, S. M., 1973, "Experimental Validation of a Landing-Dynamics Computer Program for Legged Spacecraft Landers," National Aeronautics and Space Administration, Hampton, VA, Report No. TN D–7301.
[168] Mixson, J. S., and Catherine, J. J., 1964, "Comparison of Experimental Vibration Characteristics Obtained From a 1/5-Scale Model and From a Full-Scale Saturn SA-1," National Aeronautics and Space Administration, Washington, DC, Report No. NASA TN D–2214.
[169] Mixson, J. S., and Catherine, J. J., 1964, "Experimental Lateral Vibration Characteristics of a 1/5-Scale Model of Saturn SA-1 With an Eight-Cable Suspension System," National Aeronautics and Space Administration, Washington, DC, Report No. NASA TN D–2214.
[170] Catherine, J. J., 1965, "Torsional Vibration Characteristics of a 1/5-Scale Model of Saturn SA-1," National Aeronautics and Space Administration, Washington, DC, Report No. NASA TN D–2745.
[171] Thompson, W. M., Jr., 1967, "An Investigation of the Response of a Scaled Model of a Liquid-Propellant Multistage Launch Vehicle to Longitudinal Excitation," National Aeronautics and Space Administration, Washington, DC, Report No. NASA TN D–3975.
[172] Peele, E. L., Thompson, W. M., Jr., and Pusey, C. G., 1968, "A Theoretical and Experimental Investigation of the Three-Dimensional Vibration Characteristics of a Scaled Model of an Asymmetrical Launch Vehicle," National Aeronautics and Space Administration, Washington, DC, Report No. NASA TN D–4707.
[173] Morosow, G., and Jaszlics, I. J., 1966, "Titan III 20 Percent Dynamic Model Characteristics—Comparison of Theory and Experiment," Air Force Flight Dynamics Laboratory, Wright-Patterson Air Force Base, OH, Report No. AFFDL–TR–66–80.
[174] Steeves, E. C., and Catherines, J. J., 1968, "Lateral Vibration Characteristics of a 1/40-Scale Dynamic Model of Apollo-Saturn V Launch Vehicle," National Aeronautics and Space Administration, Washington, DC, Report No. NASA TN D–4872.
[175] Leadbetter, S. A., Wayne Leonard, H., and John Brock, E., Jr., 1967, "Design and Fabrication Considerations for a 1/10-Scale Replica Model of the Apollo/Saturn," National Aeronautics and Space Administration, Washington, DC, Report No. NASA TN D–4138.
[176] Pinson, L. D., and Wayne Leonard, H., 1969, "Longitudinal Vibration Characteristics of a 1/10-Scale Apollo/Saturn V Replica Model," National Aeronautics and Space Administration, Washington, DC, NASA TN D–5159.
[177] Peele, E. L., Wayne Leonard, H., and Leadbetter, S. A., 1970, "Lateral Vibration Characteristics of the 1/10-Scale Apollo/Saturn V Replica Model," National Aeronautics and Space Administration, Washington, DC, Report No. NASA TN D–5778.
[178] Leadbetter, S. A., 1970, "Application of Analysis and Models to Structural Dynamic Problems Related to the Apollo-Saturn V Launch Vehicle," National Aeronautics and Space Administration, Washington, DC, Report No. NASA TN D–5831.
[179] Catherines, J. J., 1968, "Experimental Vibration Characteristics of a 1/40-Scale Dynamic Model of the Saturn V–Launch–Umbilical-Tower Configuration," National Aeronautics and Space Administration, Washington, DC, Report No. NASA TN D–4870.
[180] Adelman, H. M., and Steeves, E. C., 1968, "Vibration Analysis of a 1/40-Scale Dynamic Model of Saturn V–Launch-Platform–Umbilical-Tower Configuration," National Aeronautics and Space Administration, Washington, DC, Report No. NASA TN D–4871.
[181] Leadbetter, S. A., Stephens, W. B., Sewall, J. L., Majka, J. K., and Barrett, J. R., 1976, "Vibration Characteristics of a 1/8-Scale Dynamic Models of the Space-Shuttle Solid-Rocket Boosters," National Aeronautics and Space Administration, Washington, DC, Report No. NASA TN D - 8158.
[182] Pinson, L. D., 1975, "Analytical and Experimental Vibration Studies of a 1/8-Scale Shuttle Orbiter," National Aeronautics and Space Administration, Washington, DC, Report No. NASA TN D–7964.
[183] Thornton, E. A., 1971, "Vibration Analysis of a 1/15 Scale Dynamic Model of a Space Shuttle Configuration," National Aeronautics and Space Administration, Washington, DC, Report No. NASA CR–111984.
[184] Mason, P. W., Harris, H. G., Zalesak, J., and Bernstein, M., 1974, "Analytical and Experimental Investigation of a 1/8-Scale Dynamic Model of the Shuttle Orbiter—Volume I: Summary Report," National Aeronautics and Space Administration, Washington, DC, Report No. NASA CR–132488.
[185] Mason, P. W., Harris, H. G., Zalesak, J., and Bernstein, M., 1974, "Analytical and Experimental Investigation of a 1/8-Scale Dynamic Model of the Shuttle Orbiter—Volume II: Technical Report," National Aeronautics and Space Administration, Washington, DC, Report No. NASA CR–132489.
[186] Bernstein, M., Coppolino, R., Zalesak, J., and Mason, P. W., 1974, "Development of Technology for Fluid-Structure Interaction Modeling of a 1/8-Scale Dynamic Model of the Shuttle External Tank (ET)—Volume I: Technical Report," National Aeronautics and Space Administration, Washington, DC, Report No. NASA CR–132549.
[187] Bernstein, M., Coppolino, R., Zalesak, J., and Mason, P. W., 1974, "Development of Technology for Fluid-Structure Interaction Modeling of a 1/8-Scale Dynamic Model of the Shuttle External Tank (ET)—Volume I: Supporting Data, Appendixes A Through B," National Aeronautics and Space Administration, Washington, DC, Report No. NASA CR–132549.
[188] Levy, A., Zalesak, J., Bernstein, M., and Mason, P. W., 1974, "Development of Technology for Modeling of a 1/8-Scale Dynamic Model of the Shuttle Solid Rocket Booster (SRB)," National Aeronautics and Space Administration, Washington, DC, Report No. NASA CR–132492.
[189] Zalesak, J., 1975, "Modal Coupling Procedures Adapted to NASTRAN Analysis of the 1/8-Scale Shuttle Structural Dynamics Model—Volume I: Technical Report," National Aeronautics and Space Administration, Washington, DC, Report No. NASA CR–132666.
[190] Blanchard, U. J., Miserentino, R., and Leadbetter, S. A., 1977, "Experimental Investigation of the Vibration Characteristics of a Model of an Asymmetric Multielement Space Shuttle," National Aeronautics and Space Administration, Washington, DC, Report No. NASA TN D–8448.
[191] McGowan, P. E., Jaeed, M., and Edighoffer, H. E., 1991, "Status of DSMT Research Program," National Aeronautics and Space Administration, Washington, DC, Report No. NASA-TM-102764.
[192] McGowan, P. E., Edighoffer, H. E., and Wallace, J. W., 1990, "Development of an Experimental Space Station Model for Structural Dynamics Research," National Aeronautics and Space Administration, Washington, DC, Report No. NASA-TM-102601.
[193] Keith Belvin, W., and Edighoffer, H. E., 1986, "Experimental and Analytical Generic Space Station Dynamic Models," National Aeronautics and Space Administration, Washington, DC, Report No. NASA-TM-87696.
[194] Shih, C. F., Chen, J. C., and Garba, J. A., 1987, "Verification of Large Beam-Type Space Structures," National Aeronautics and Space Administration, Washington, DC, Report No. NASA TM–4073.
[195] Gronet, M. J., Pinson, E. D., Voqui, H. L., Crawley, E. F., and Everman, M. R., 1987, "Preliminary Design, Analysis, and Costing of a Dynamic Scale Model of the NASA Space Station," National Aerospace and Space Administration, Washington, DC, Report No. NASA-CR-4068.
[196] Davis, D. A., Gronet, M. J., Tan, M. K., and Thorne, J., 1994, "Conceptual Design and Analysis of a Dynamic Scale Model of the Space Station Freedom," National Aeronautics and Space Administration, Washington, DC, Report No. NASA-CR-4598.
[197] Schroeder, L. C., Adams, R. R., Bailey, M. C., Keith Belvin, W., Butler, D. H., and Campbell, T. G., 1989, "Near-Field Testing of the 15-Meter Hoop-Column Antenna," National Aeronautics and Space Administration, Washington, DC, NASA Technical Memorandum 4073.
[198] Keith Belvin, W., and Edighoffer, H. E., 1986, "15 Meter Hoop-Column Antenna Dynamics: Test and Analysis," First NASA/DOD CSI Technology Conference, National Aeronautics and Space Administration, Norfolk, VA, Nov. 18–21, pp. 167–185.
[199] Letchworth, R., McGowan, P. E., and Gronet, M. J., 1988, "Space Station: A Focus for the Development of Structural Dynamic Scale Model for Large Flexible Space Structures," AIAA/ASME/ASCE/AHS 29th SDM Conference, Greenbelt, MD, pp. 1–10.
[200] Canfield, S. L., Beard, J. W., Peddieson, J., Ewing, A., Garbe, G., 2004, "Similarity Rules for Scaling Solar Sail Systems," Solar Sail Technology and Application Conference (SSTAC), Greenbelt, MD, pp. 1–10.
[201] Canfield, S. L., Peddieson, J., and Garbe, G., 2010, "Similarity Rules for Scaling Solar Sail Systems," National Aeronautics and Space Administration, Washington, DC, Report No. M10–0055.

[202] Murphy, D. M., Macy, B., and Gaspar, J. L., 2004, "Demonstration of a 10-m Solar Sail System," AIAA Paper No. 2004-1576.
[203] Gaspar, J. L., Mann, T., Behun, V., Macy, B., Barker, P., and Murphy, D. M., 2006, "Testing of a 10-Meter Quadrant Solar Sail," IMAC—XXIV Conference and Exposition on Structural Dynamics, Sant Louis, MO, Jan. 30–Feb. 2.
[204] Gaspar, J. L., Behun, V., Mann, T., Murphy, D., and Macy, B., 2005, "Testing of a 20-Meter Solar Sail System," 53rd JANNAF Propulsion Meeting, Monterey, CA, Dec. 5–8 .
[205] Laue, G., Case, D., and Moore, J., 2005, "Fabrication and Deployment Testing of Solar Sail Quadrants for a 20-Meter Solar Sail Ground Test System Demonstration," AIAA Paper No. 2005-3930.
[206] Greschik, G., Mikulas, M. M., and Freeland, R. E., 1999, "The Nodal Concept of Deployment and the Scale Model Testing of Its Application to a Membrane Antenna," AIAA Paper No. 99-1523.
[207] Holland, D. B., Virgin, L. N., Tinker, M. L., and Slade, K. N., 2002, "Geometric Scaling Properties of Inflatable Structures for Use in Space Solar Power Generation," AIAA Paper No. 2002-1264.
[208] Jackson, K. E., and Fasanella, E. L., 1999, "Crashworthy Evaluation of a 1/5-Scale Model Composite Fuselage Concept," National Aeronautics and Space Administration, Washington, DC, Report No. NASA/TM–1999–209132, ARL–MR–441.
[209] Jackson, K. E., and Fasanella, E. L., 2003, "Comparisons of the Impact Responses of a 1/5-Scale Model and a Full-Scale Crashworthy Composite Fuselage Section," American Helicopter Society 59th Annual Forum, Phoenix, AZ, May 6–8.
[210] Bisplinghoff, R., Ashley, H., and Alfman, R., 1996, *Aeroelasticity*, Dover Publications, Mineola, NY.
[211] Molyneux, W. G., 1964, "Aeroelastic Modeling," RAE, Washington, DC, Report No. 353.
[212] Hunt, G. K., 1973, "Aero-Elastic Models of Helicopter Rotors," Aeronautical Research Council, London, Report No. CP 1245.
[213] French, M., 1990, "An Application of Structural Optimization in Wind Tunnel Model Design," AIAA Paper No. 90-0956-CP.
[214] French, M., and Eastep, F. E., 1996, "Aeroelastic Model Design Using Parameter Identification," J. Aircr., **33**(1), pp. 198–202.
[215] Pereira, P., Almeida, L., Suleman, A., Bond, V., Canfield, R., and Blair, M., 2007, "Aeroelastic Scaling and Optimization of a Joined-Wing Aircraft Concept," AIAA Paper No. 2007-1889.
[216] Heeg, J., Spain, C. V., and Rivera, J. A., 2004, "Wind Tunnel to Atmospheric Mapping for Static Aeroelastic Scaling," AIAA Paper No. 2004-2044.
[217] Richards, J., Suleman, A., Canfield, R. A., and Blair, M., 2009, "Design of a Scaled RPV for Investigation of Gust Response of Joined-Wing Sensorcraft," AIAA Paper No. 2009-2218.
[218] Ricciardi, A. P., Canfield, R. A., Patil, M. J., and Lindsley, N., 2012, "Nonlinear Aeroelastic Scaling of a Joined Wing Aircraft," AIAA Paper No. 2012-1454.
[219] Ricciardi, A., Eger, C. A. G., Canfield, R. A., and Patil, M. J., 2014, "Nonlinear Aeroelastic-Scaled-Model Optimization Using Equivalent Static Loads," J. Aircr., **51**(6), pp. 1842–1851.
[220] Spada, C., Afonso, F., Lau, F., and Suleman, A., 2017, "Nonlinear Aeroelastic Scaling of High Aspect-Ratio Wings," Aerosp. Sci. Technol., **63**, pp. 363–371.
[221] Ricciardi, A. P., Eger, C. A. G., Canfield, R. A., Patil, M. J., and Lindsley, N., 2012, "High Fidelity Nonlinear Aeroelastic Analysis for Scaled Vehicle Design," AIAA Paper No. 2012-5624.
[222] Presente, E. H., and Friedmann, P. P., 1998, "Aeroservoelasticity in Subsonic Flow and Associated Scaling Laws," AIAA Paper No. 97-1079.
[223] Friedmann, P. P., Guillot, D., and Presente, E., 1997, "Adaptive Control of Aeroelastic Instabilities in Transonic Flow and Its Scaling," J. Guid. Control Dyn., **20**(6), pp. 1190–1199.
[224] Presente, E. H., and Friedmann, P. P., 1998, "Aeroservoelasticity in Compressible Flow and Its Scaling Laws," AIAA Paper No. 98-1899.
[225] Friedmann, P. P., 1999, "Rotary-Wing Aeroelastic Scaling and Its Implications for the Adaptive-Materials-Based Actuation," Symposium on Smart Structures and Materials, International Society for Optics and Photonics, International Society for Optics and Photonics, Newport Beach, CA, June 9, pp. 60–79.
[226] Pototzky, A. S., 2002, "Scaling Laws Applied to a Modal Formulation of the Aeroservoelastic Equations," AIAA Paper No. 2002-1598.
[227] Vickers, J. M. F., 1965, "Thermal Scale Modeling," Astronaut. Aeronaut., pp. 34–39.
[228] Watkins, J. R., 1966, "Sets of Similarity Ratios for Thermal Modeling," National Aeronautics and Space Administration, Huntsville, AL, Report No. NASA TN D–3452.
[229] O'Sullivan, W. J., 1957, "Theory of Aircraft Structural Models Subject to Aerodynamic Heating and External Loads," National Advisory Committee for Aeronautics, Langley Field, VA, Report No. TN-4115.
[230] Katzoff, S., 1963, "Similitude in Thermal Models of Spacecraft," National Aeronautics and Space Administration, Washington, DC, Report No. NASA TN D–1631.
[231] Rolling, R. E., 1966, "Thermal Scale Modeling in a Simulated Space Environment," Lockheed Missiles and Space Company, Palo Alto, CA, Report No. NAS 8–11152.
[232] Gabron, F., 1966, "Thermal Scale Modeling Techniques for Voyager-Type Spacecraft," Pasadena, CA, Report No. C–66326–0.
[233] Maples, D., and Scogin, J. V., 1970, "Thermal Modeling With Internal Generation," Marshall Space Flight Center, Huntsville, AL, Report No. NGR–10–001–068.
[234] Shannon, R. L., 1972, "A Thermal Scale Modeling Study for Apollo and Apollo Applications," National Aeronautics and Space Administration, Seattle, WA, Report No. D180–15048–1.
[235] Kumar, S., Itoh, Y., Saizuka, K., and Usami, T., 1997, "Pseudodynamic Testing of Scaled Models," J. Struct. Eng., **123**(4), pp. 524–526.
[236] Usami, T., and Kumar, S., 1996, "Damage Evaluation in Steel Box Columns by Pseudodynamic Tests," J. Struct. Eng., **122**(6), pp. 635–642.
[237] Kim, N. S., Kwak, Y. H., and Chang, S. P., 2004, "Pseudodynamic Tests on Small-Scale Steel Models Using the Modified Similitude Law," 13th World Conference of Earthquake Engineering, Vancouver, Canada, Aug. 1–6, Paper No. 3360.
[238] Kim, N. S., Lee, J. H., and Chang, S. P., 2009, "Equivalent Multi-Phase Similitude Law for Pseudodynamic Test on Small Scale Reinforced Concrete Models," Eng. Struct., **31**(4), pp. 834–846.
[239] Atkins, A. G., 1988, "Scaling Combined Plastic Flow and Fracture," Int. J. Mech. Sci., **30**(3–4), pp. 173–191.
[240] Me-Bar, Y., 1997, "A Method for Scaling Ballistic Penetration Phenomena," Int. J. Impact Eng., **19**(9–10), pp. 821–829.
[241] Atkins, A. G., and Caddell, R. M., 1974, "The Laws of Similitude and Crack Propagation," Int. J. Mech. Sci., **16**(8), pp. 541–548.
[242] Mai, Y. W., and Atkins, A. G., 1978, "Crack Propagation in Non-Proportionally Scaled Elastic Structures," Int. J. Mech. Sci., **20**(7), pp. 437–449.
[243] Mai, Y. W., and Atkins, A. G., 1975, "Scale Effects and Crack Propagation in Non-Linear Elastic Structures," Int. J. Mech. Sci., **17**(11–12), pp. 673–675.
[244] Atkins, A. G., Chen, Z., and Cotterell, B., 1998, "The Essential Work of Fracture and j_R Curves for the Double Cantilever Beam Specimen: An Examination of Elastoplastic Crack Propagation," Proc. R. Soc. London, **454**, pp. 815–833.
[245] Atkins, A. G., 1999, "Scaling Laws for Elastoplastic Fracture," Int. J. Fract., **95**(1/4), pp. 51–65.
[246] Kellas, S., and Morton, J., 1992, "Scaling Effects in Angle-Ply Laminates," National Aeronautics and Space Administration, Washington, DC, Report No. NASA Contractor Report No. 4423.
[247] Bažant, Z. P., 1993, "Scaling Laws in Mechanics of Failure," J. Eng. Mech., **119**(9), pp. 1828–1844.
[248] Bažant, Z. P., 1984, "Size Effect in Blunt Fracture: Concrete, Rock, Metal," J. Eng. Mech., **110**(4), pp. 518–535.
[249] Bažant, Z. P., 1985, "Fracture in Concrete and Reinforced Concrete," *Mechanics of Geomaterials*, Z. P. Bažant, ed., Wiley, Hoboken, NJ.
[250] Bažant, Z. P., and Pfeiffer, P. A., 1988, "Determination of Fracture Energy From Size Effect and Brittleness Number," ACI Mater. J., **84**(6), pp. 463–480.
[251] Bažant, Z. P., and Kazemi, M. T., 1990, "Size Effect in Fracture of Ceramics and Its Use to Determine Fracture Energy and Effective Process Zone Length," J. Am. Ceram. Soc., **73**(7), pp. 1841–1853.
[252] Bažant, Z. P., Xi, Y., and Reid, S. G., 1991, "Statistical Size Effect in Quasi-Brittle Structures—I: Is Weibull Theory Applicable?," J. Eng. Mech., **117**(11), pp. 2609–2622.
[253] Bažant, Z. P., Xi, Y., and Reid, S. G., 1991, "Statistical Size Effect in Quasi-Brittle Structures—I: Is Weibull Theory Applicable?," J. Eng. Mech., **117**(11), pp. 2623–2640.
[254] van Vliet, M. R. A., and van Mier, J. G. M., 2000, "Experimental Investigation of Size Effect in Concrete and Sandstone Under Uniaxial Tension," Eng. Fract. Mech., **65**(2–3), pp. 165–188.
[255] Westine, P. S., and Mullin, S. A., 1987, "Scale Modeling of Hypervelocity Impact," Int. J. Impact Eng., **5**(1–4), pp. 693–701.
[256] Acquaro, D., Zaccari, N., Prinzio, M. D., and Forasassi, G., 2010, "Numerical and Experimental Analysis of the Impact of a Nuclear Spent Fuel Cask," Nucl. Eng. Des., **240**(4), pp. 706–712.
[257] Quercetti, T., Müller, K., and Schubert, S., 2008, "Comparison of Experimental Results From Drop Testing of Spent Fuel Package Design Using Full Scale Prototype Model and Reduced Scale Model," Packag., Transp., Storage Secur. Radioact. Mater., **19**(4), pp. 197–202.
[258] Emori, R. I., 1973, "Scale Models of Automobile Collisions With Breakaway Obstacles," Exp. Mech., **63**(9), pp. 64–69.
[259] Lowe, W. T., Al-Hassani, S. T. S., and Johnson, W., 1972, "Impact Behaviour of Small Scale Model Motor Coaches," Proc. Inst. Mech. Eng., **186**(1), pp. 409–419.
[260] Brownfield, H. A., and Rogers, D. O., 1978, "Analysis of 30 Mph Frontal Barrier Utilizing Half-Scale Metal Models," SAE Paper No. 780366.
[261] Kure, K., 1981, "Model Tests With Ocean Structures," Appl. Ocean Res., **3**(4), pp. 171–176.
[262] Calle, M. A. G., and Alves, M., 2011, "Ship Collision: A Brief Survey," 21st Brazilian Congress of Mechanical Engineering, Natal, Brazil, Oct. 24–28.
[263] Blok, J. J., and Dekker, J. N., 1979, "On Hydrodynamic Aspects of Ship Collision With Rigid or Non-Rigid Structures," Offshore Technology Conference, Houston, TX, Apr. 30–May 3, pp. 2683–2698.
[264] Hagiwara, K., Takanabe, H., and Kawano, H., 1983, "A Proposed Method of Predicting Ship Collision Damage," Int. J. Impact Eng., **1**(3), pp. 257–279.
[265] Ohtsubo, H., Kawamoto, Y., and Kuroiwa, T., 1994, "Experimental and Numerical Research on Ship Collision and Grounding of Oil Tankers," Nucl. Eng. Des., **150**(2–3), pp. 385–396.
[266] Lehmann, E., and Peschmann, J., 2002, "Energy Absorption of the Steel Structure of Ships in the Event of Collisions," Mar. Struct., **15**(4–5), pp. 429–441.

[267] Tabri, K., Määttänen, J., and Ranta, J., 2008, "Model-Scale Experiments of Symmetric Ship Collisions," J. Mar. Technol., **13**(1), pp. 71–84.
[268] Calle, M. A. G., Oshiro, R. E., and Alves, M., 2017, "Ship Collision and Grounding: Scaled Experiments and Numerical Analysis," Int. J. Impact Eng., **103**, pp. 195–210.
[269] Oshiro, R. E., Calle, M. A. G., Mazzariol, L. M., and Alves, M., 2017, "Experimental Study of Collision in Scaled Naval Structures," Int. J. Impact Eng., **110**, pp. 149–161.
[270] Aguiar, V. S., Kirkayak, L., Suzuki, K., Ando, H., and Sueoka, H., 2012, "Experimental and Numerical Analysis of Container Stack Dynamics Using a Scaled Model Test," Ocean Eng., **39**, pp. 24–42.
[271] Cho, U., Wood, K. L., and Crawford, R. H., 1998, "Online Functional Testing With Rapid Prototypes: A Novel Empirical Similarity Method," Rapid Prototyping J., **4**(3), pp. 128–138.
[272] Dornfeld, W. H., 1994, "Direct Dynamic Testing of Stereolithographic Models," International Gas Turbine and Aeroengine Congress and Exposition, The Hague, The Netherlands, June 13–16, pp. 1–6.
[273] Steinchen, W., Kramer, B., and Kupfer, G., 2008, "Photoelastic Investigation Using New STL-Resins," Solid Freeform Fabrication Symposium, Austin, TX, Aug. 4–6, pp. 204–12.
[274] Mahn, J. P., and Bayly, P. V., 1999, "Impact Testing of Stereolithographic Models to Predict Natural Frequencies," J. Sound Vib., **224**(3), pp. 411–430.
[275] Springer, A. M., 1998, "Application of Rapid Prototyping Methods to High Speed Wind Tunnel Testing," National Aeronautics and Space Administration, Huntsville, AL, Report No. NASA TP–1998–208396.
[276] Nadooshan, A. A., Daneshmand, S., and Aghanajafi, C., 2007, "Application of RP Technology With Polycarbonate Material for Wind Tunnel Model Fabrication," Int. J. Mech. Ind. Sci. Eng., **1**(8), pp. 371–376.
[277] Chuk, R. N., and Thomson, V. J., 1998, "A Comparison of Rapid Prototyping Techniques Used for Wind Tunnel Model Fabrication," Rapid Prototyping J., **4**(4), pp. 185–96.
[278] Dang-guo, Y., Zheng-yu, Z., Yan, S., and Wei-jun, Z., 2011, "A Preliminary Design and Manufacturing Study of Hybrid Lightweight High-Speed Wind-Tunnel Models," Rapid Prototyping J., **17**, pp. 45–54.
[279] Dang-guo, Y., Yan, S., Zheng-yu, Z., Chao, W., and Wei-jun, Z., 2013, "Design and Manufacture Methods of Rapid Prototyping Wind-Tunnel Models Based on Photopolymer-Resin," Rapid Prototyping J., **17**(1), pp. 20–27.
[280] Fujino, M., Oyama, H., and Omotani, H., 2003, "Flutter Characteristics of an Over-the-Wing Engine Mount Business Jet Configuration," AIAA Paper No. 2003-1942.
[281] Ziemian, C., Ziemian, R., and Barker, E., 2010, "Shake-Table Simulation Study of Small Scale Layered Models," Rapid Prototyping J., **16**(1), pp. 4–11.
[282] Zhu, W., Li, D., Zhang, Z., Ren, K., Zhao, X., Yang, D., Zhang, W., Sun, Y., and Tang, Y., 2011, "Design and Fabrication of Stereolithography-Based Aeroelastic Wing Models," Rapid Prototyping J., **17**(4), pp. 298–307.
[283] Cho, U., Wood, K. L., and Crawford, R. H., 1998, "Novel Empirical Similarity Method for the Reliable Product Test With Rapid Prototypes," ASME Design Engineering Technical Conference, Atlanta, GE, Sept. 13–16, pp. 1–14.
[284] Cho, U., Wood, K. L., and Crawford, R. H., 1999, "Error Measures for Functional Product Testing," ASME Design Engineering Technical Conference.
[285] Dutson, A. J., and Wood, K. L., 2002, "Foundations and Applications of the Empirical Similitude Method (ESM)," ASME Design Engineering Technical Conference (DETC), Las VEgas, NE, Sept. 12–15, pp. 1–13.
[286] Dutson, A. J., Wood, K. L., Beaman, J. J., Crawford, R. H., and Bourell, D. L., 2003, "Application of Similitude Techniques to Functional Testing of Rapid Prototypes," Rapid Prototyping J., **9**(1), pp. 6–13.
[287] Cho, U., Dutson, A. J., Wood, K. L., and Crawford, R. H., 2005, "An Advanced Method to Correlate Scale Models With Distorted Configurations," ASME J. Mech. Des., **127**(1), pp. 78–85.
[288] Cunefare, K. A., and De Rosa, S., 1999, "The Sensitivity of Structural Acoustic Response to Attachment Feature Scale Representation," J. Acoust. Soc. Am., **106**(6), pp. 3384–3393.
[289] De Rosa, S., Franco, F., Cammarano, A., and Fasano, A., 2007, "Applicazione Dell'algebra Agli Intervalli Alla Risposta Strutturale," XIX Congresso Nazionale AIDAA, Forlì, Italy, Sept. 17–21.
[290] Mazzariol, L. M., Oshiro, R. E., and Alves, M., 2016, "A Method to Represent Impacted Structures Using Scaled Models Made of Different Materials," Int. J. Impact Eng., **90**, pp. 81–94.
[291] Ramu, M., Prabhu Raja, V., and Thyla, P. R., 2010, "Development of Structural Similitude and Scaling Laws for Elastic Models," Int. J. Manuf. Eng., **9**, pp. 67–69
[292] Ramu, M., Prabhu Raja, V., and Thyla, P. R., 2013, "Establishment of Structural Similitude for Elastic Models and Validation of Scaling Laws," KSCE J. Civ. Eng., **17**(1), pp. 139–144.
[293] Ciappi, E., Magionesi, F., De Rosa, S., and Franco, F., 2012, "Analysis of the Scaling Laws for the Turbulence Driven Panel Responses," J. Fluids Struct., **32**, pp. 90–103.
[294] Wen, H. M., and Jones, N., 1993, "Experimental Investigation of the Scaling Laws for Metal Plates Struck by Large Masses," Int. J. Impact Eng., **13**(3), pp. 485–505.
[295] Yulong, L., Yongkang, Z., and Pu, X., 2008, "Study of Similarity Law for Bird Impact on Structure," Chin. J. Aeronaut., **21**(6), pp. 512–517.
[296] Yang, F. J., Hassan, M. Z., Cantwell, W. J., and Jones, N., 2013, "Scaling Effects in the Low Velocity Impact Response of Sandwich Structures," Compos. Struct., **99**, pp. 97–104.
[297] Yigit, A. S., and Christoforou, A. P., 2007, "Limits of Asymptotic Solutions in Low-Velocity Impact of Composite Plates," Compos. Struct., **81**(4), pp. 568–574.
[298] Mazzariol, L. M., and Alves, M., 2014, "Scaling of the Impact of a Mass on a Plate Using Models of Different Materials," Fourth International Conference on Impact Loading of Lightweight Structures, Cape Town, South Africa, Jan. 12–16, pp. 1275–1289.
[299] Oshiro, R. E., and Alves, M., 2007, "Scaling of Cylindrical Shells Under Axial Impact," Int. J. Impact Eng., **34**(1), pp. 89–103.
[300] Mazzariol, L. M., and Alves, M., 2013, "Experimental Study on Scaling of Circular Tubes Subjected to Dynamic Axial Crushing Using Models of Different Materials," 22nd International Congress of Mechanical Engineering, (COBEM), Ribeirão Preto, Brazil, Nov. 3–7, pp. 8065–8074.
[301] Cartmell, M. P., Ziegler, S. W., and Neill, D. S., 2003, "On the Performance Prediction and Scale Modelling of a Motorised Momentum Exchange Tether," *Space Technology and Applications International Forum—STAIF 2003*, M. S. El-Genk, ed., American Institute of Physics, College Park, MD, pp. 571–579.
[302] Wolowicz, C. H., Bowman, J. S., Jr., and Gilbert, W. P., 1968, "Similitude Requirements and Scaling Relationships as Applied to Model Testing," National Aeronautics and Space Administration, Washington, DC, Report No. NASA Technical Paper 1435.
[303] Jiang, P., Tian, C. J., Xie, R. Z., and Meng, D. S., 2006, "Experimental Investigation Into Scaling Laws for Conical Shells Struck by Projectiles," Int. J. Impact Eng., **32**(8), pp. 1284–1298.
[304] Krateyrman, B., and Sabnis, G. M., 1984, "Similitude Theory: Plates and Shells Analysis," J. Eng. Mech., **110**(9), pp. 1247–1263.
[305] Swanson, S. R., Smith, N. L., and Qian, Y., 1991, "Analytical and Experimental Strain Response in Impact of Composite Cylinders," Compos. Struct., **18**(2), pp. 95–108.
[306] Moradi, B., and Parsons, I. D., 1992, "Dimensional Analysis of Buckling of Stiffened Composite Shells," J. Eng. Mech., **118**(3), pp. 557–574.
[307] Zai, B. A., Sami, S., Khan, M. A., Ahmad, F., and Park, M. K., 2015, "Prediction of Vibration Characteristics in Beam Structure Using Sub-Scale Modeling With Experimental Validation," Chin. J. Mech. Eng., **28**(5), pp. 928–933.
[308] Duffey, T. A., Cheresh, M. C., and Sutherland, S. H., 1984, "Experimental Verification of Scaling Laws for Punch-Impact-Loaded Structures," Int. J. Impact Eng., **2**(1), pp. 103–117.
[309] Bond, V., Canfield, R. A., Suleman, A., and Blair, M., 2012, "Aeroelastic Scaling of a Joined Wing for Nonlinear Geometric Stiffness," AIAA J., **50**(3), pp. 513–522.
[310] Wan, Z., and Cesnik, C. E. S., 2013, "Geometrically Nonlinear Aeroelastic Scaling for Very Flexible Aircraft," AIAA Paper No. 2013-1894.
[311] Marshall, K. N., and Foster, W. G., 1973, "Space Shuttle Thermal Scale Modeling Application Study," Lockheed Missiles and Space Company, Sunnyvale, CA, Report No. TP–3613.
[312] Sabour, M. H., and Bhat, R. B., 2010, "Thermal Scale Modeling by FEM and Test," J. Aerosp. Eng., **23**(1), pp. 24–33.
[313] Rolling, R. E., Murray, D. O., and Marshall, K. N., 1969, "Limitations in Thermal Modeling," Lockheed Missiles and Space Company, Palo Alto, CA, Report No. 6–78–69–41.
[314] Jones, B. P., 1964, "Thermal Similitude Studies," J. Spacecr. Rockets, **1**(4), pp. 364–369.
[315] Jones, B. P., and Harrison, J. K., 1965, "A Set of Experiments in Thermal Similitude," National Aeronautics and Space Administration, Huntsville, AL, Report No. NASA TM X-53346.
[316] Chao, B. T., and Wedekind, G. L., 1965, "Similarity Criteria for Thermal Modeling of Spacecraft," J. Spacecr. Rockets, **2**(2), pp. 146–152.
[317] Fowle, A. A., Gabron, F., Vickers, J. M., and Vickers, J. M. F., 1966, "Thermal Scale Modeling of Spacecraft: An Experimental Investigation," J. Spacecr. Rockets, **3**(4), pp. 577–581.
[318] Folkman, N. R., Baldwin, F. L., and Wainwright, J. B., 1965, "Tests on a Thermally Scaled Model Space Station in a Simulated Solar Environment," AIAA Paper No. 65-658.
[319] Gabron, F., and Johnson, R. W., 1965, "Thermal Scale Modeling of the Temperature Control Model of Mariner Mars 64," Jet Propulsion Laboratory, Pasadena, CA, Report No. USACR - 70178.
[320] Adkins, D. L., 1965, "Scaling of Transient Temperature Distributions of Simple Bodies in a Space Chamber," AIAA Paper No. 65–660.
[321] Shih, C., 1966, "Thermal Similitude of Manned Spacecraft," AIAA Paper No. 66–22.
[322] Wereley, N. M., and Kamath, G. M., 1997, "Bringing Relevance to Freshman Aerospace Engineering: Demonstration of Model Scale Comanche Helicopter Lag Mode Damper," Int. J. Eng. Educ., **13**(5), pp. 369–375.
[323] Tennyson, R. C., Teichman, H., Nanyaro, A. P., and Mabson, G., "Study of Crashworthiness of Light Aircraft Structures," Structural Dynamics and Materials Conference, Atlanta, GA, Apr. 6–8, pp. 276–285.
[324] Liu, J., Zhou, L., and Herrin, D. W., 2011, "Demonstration of Vibro-Acoustic Reciprocity Including Scale Modeling," SAE Paper No. 2011-01-1721.
[325] Gang, X., Wang, D., and Su, X., 2010, "A New Similitude Analysis Method for a Scale Model Test," Key Eng. Mater., **439–440**, pp. 704–709.
[326] Gauchía, A., Olmeda, E., Boada, M. J. L., Boada, B. L., and Díaz, V., 2014, "Methodology for Bus Structure Torsion Stiffness and Natural Vibration Frequency Prediction Based on a Dimensional Analysis Approach," Int. J. Automot. Technol., **15**(3), pp. 451–461.
[327] Hilburger, M. W., Rose, C. A., and Starnes, J. H., Jr., 2001, "Nonlinear Analysis and Scaling Laws for Noncircular Composite Structures Subjected to Combined Loads," AIAA Paper No. 2001-1335.
[328] Luo, Z., Zhu, Y., Zhao, X., and Wang, D., 2014, "Determination Method of Dynamic Distorted Scaling Laws and Applicable Structure Size Intervals of a

Rotating Thin-Wall Short Cylindrical Shell," Proc. Inst. Mech. Eng., Part C, **229**(5), pp. 806–817.
[329] Wu, J. J., Cartmell, M. P., and Whittaker, A. R., 2002, "Prediction of the Vibration Characteristics of a Full-Scale Structure From Those of a Scale Model," Comput. Struct., **80**(18–19), pp. 1461–1472.
[330] Wu, J. J., 2005, "Dynamic Analysis of a Rectangular Plate Under a Moving Load Using Scale Beams and Scaling Laws," Comput. Struct., **83**(19–20), pp. 1646–1658.
[331] Asl, M. E., Niezrecki, C., Sherwood, J., and Avitabile, P., 2017, "Vibration Prediction of Thin-Walled Composite I–Beams Using Scaled Models," Thin-Walled Struct., **113**, pp. 151–161.
[332] Balawi, S., Shahid, O., and Mulla, M. A., 2015, "Similitude Scaling laWs—Static and Dynamic Behaviour Beams and Plates," Procedia Eng., **114**, pp. 330–337.
[333] Yazdi, A. A., and Rezaeepazhand, J., 2011, "Structural Similitude for Flutter of Delaminated Composite Beam-Plates," Compos. Struct., **93**(7), pp. 1918–1922.
[334] Wu, J. J., 2006, "Prediction of the Dynamic Characteristics of an Elastically Supported Full-Size Flat Plate From Those of Its Complete-Similitude Scale Model," Comput. Struct., **84**(3–4), pp. 102–114.
[335] Luo, Z., Zhao, X., Zhu, Y., and Li, J., 2014, "Determination Method of the Structure Size Interval of Dynamically Similar Models for Predicting Vibration Characteristics of the Isotropic Sandwich Plates," J. Vibroeng., **16**(2), pp. 608–622.
[336] Zhu, Y., Luo, Z., Zhao, X., and Han, Q., 2014, "Determination Method of the Structure Size Intervals of Dynamically Similar Models for Predicting Vibration Characteristics of the Coated Thin Plates," Proc. Inst. Mech. Eng., Part C, **229**(1), pp. 59–68.
[337] Asl, M. E., Niezrecki, C., Sherwood, J., and Avitabile, P., 2015, "Predicting the Vibration Response in Subcomponent Testing of Wind Turbine Blades," *Special Topics in Structural Dynamics*, Vol. 6, R. Allemang, ed., Springer, Cham, Switzerland.
[338] Qian, Y., Swanson, S. R., Nuismer, R. J., and Bucinell, R. B., 1990, "An Experimental Study of Scaling Rules for Impact Damage in Fiber Composites," J. Compos. Mater., **24**(5), pp. 559–570.
[339] Luo, Z., Zhu, Y., Han, Q., and Wang, D., 2014, "The Dynamic Similitude Design of a Thin-Wall Cylindrical Shell With Sealing Teeth and Its Geometrically Distorted Model," Adv. Mech. Eng., **7**(2), pp. 1–12.
[340] Ungbhakorn, V., and Singhatanadgid, P., 2009, "A Scaling Law for Vibration Response of Laminated Curved Shallow Shells by Energy Approach," Mech. Adv. Mater. Struct., **16**(5), pp. 333–344.
[341] Kasivitamnuay, J., and Singhatanadgid, P., 2017, "Scaling Laws for Displacement of Elastic Beam by Energy Method," Int. J. Mech. Sci., **128–129**, pp. 361–367.
[342] De Rosa, S., Franco, F., and Polito, T., 2015, "Partial Scaling of Finite Element Models for the Analysis of the Coupling Between Short and Long Structural Wavelengths," Mech. Syst. Signal Process., **52–53**, pp. 722–740.
[343] De Rosa, S., Petrone, G., and Franco, F., 2016, "Similitudes for Acoustic Volumes: Analytical Model for the Response," 45th International Congress and Exposition on Noise Control Engineering: Towards a Quieter Future (INTER-NOISE), Hamburg, Germany, Aug. 21–24, pp. 3416–3424.
[344] Drazetic, P., Ravalard, Y., Dacheux, F., and Marguet, B., 1994, "Applying Non-Direct Similitude Technique to the Dynamic Bending Collapse of Rectangular Section Tubes," Int. J. Impact Eng., **15**(6), pp. 797–814.
[345] Carrillo, J. G., and Cantwell, W. J., 2008, "Scaling Effects in the Low Velocity Impact Response of Fiber-Metal Laminates," J. Reinf. Plat. Compos., **27**(9), pp. 893–907.
[346] Luo, Z., Zhu, Y., Liu, H., and Wang, D., 2016, "Dynamic Similitude Design Method of the Distorted Model on Variable Thickness Cantilever Plates," Appl. Sci., **6**(8), p. 228.
[347] Schleyer, G. K., Hsu, S. S., and White, M. D., 2004, "Scaling of Pulse Loaded Mild Steel Plates With Different Edge Restraint," Int. J. Mech. Sci., **46**(9), pp. 1267–1287.
[348] Snyman, I. M., 2010, "Impulsive Loading Events and Similarity Scaling," Eng. Struct., **32**(3), pp. 886–896.
[349] Cheng, L., and Lesueur, C., 1990, "Preliminary Study on Vibroacoustic Model Scaling of a Structure Coupled to an Acoustic Cavity," J. Acoust., **3**, pp. 349–359.
[350] Cheng, L., and Lesueur, C., 1990, "Vibroacoustic Model Scaling With Dissipation Effects," J. Phys. Colloq., **51**, pp. C2-213–C2-216.
[351] Qin, G., Duan, H., Luo, Z., and Han, Q., 2012, "Similitude Analysis on Mechanical Parameters of Thin Walled Shells," Adv. Eng. Forum, **2–3**, pp. 139–144.
[352] Hilburger, M. W., Lovejoy, A. E., and Thornburgh, R. P., 2012, "Design and Analysis of Subscale and Full-Scale Buckling-Critical Cylinders for Launch Vehicle Technology Development," AIAA Paper No. 2012-1865.
[353] Yu, H., Zhang, W., Zhang, Y., and Sun, Y., 2010, "Shaking Table Test Numerical Analysis of a 1:12 Scale Model of a Special Concentrically Braced Steel Frame With Pinned Connections," Earthquake Eng. Eng. Vib., **9**(1), pp. 51–63.
[354] Wang, S., Yang, G., and Liu, N., 2007, "Investigation of Acoustic Scale Effects and Boundary Effects for the Similitude Model of Underwater Complex Shell Structure," J. Mar. Sci. Appl., **6**(1), pp. 31–35.
[355] Brunette, H., Goldsmith, W., 1990, "Propellant-Driven Anchoring in Rock: Results From Initial Scaling Tests," Int. J. Impact Eng., **9**(1), pp. 51–69.